

TARGETED METABOLISM AND NON-TARGETED
PLASMA PROFILING IN EQUINE MODEL

THIRU SELVI D/O SELVARAJAH
(B.Sc.(Hons), University of Sydney, Australia)

FOR THE DEGREE OF MASTER OF SCIENCE
DEPARTMENT OF PHARMACY
NATIONAL UNIVERSITY OF
SINGAPORE

2011

ACKNOWLEDGMENT

There are many people who have made this journey an enjoyable and memorable one.

I would like to sincerely thank my supervisor, Associate Professor Eric Chan, for his encouragement, patience, guidance and advice throughout this project.

I am deeply indebted to Singapore Turf Club and Dr Shawn Stanley for having faith in me and funding my M.Sc. I am also grateful to my colleagues for their understanding and support.

I would also like to sincerely thank New Lee Sun, Kishore, Mainak, Saha, Phua Lee Cheng, Chng Hui Ting, Yip Lian Yee, Ching Jianhong and all those who have advised and helped in one way or another. All of them have made this journey a memorable one.

My deepest thanks to my family, especially Siva and Maya, for their sacrifices and support through this difficult time. Without them, I would not have been able to complete my M.Sc. and still stay sane at the same time. I would also like to express my heartfelt thanks to my godmother and my mother-in-law for their constant prayers, support, encouragement and endless love.

Opinions expressed in this thesis are mine and do not reflect the official policy or position of the Singapore Turf Club.

ACKNOWLEDGMENT.....	II
SUMMARY	VII
LIST OF TABLES AND FIGURES.....	X
LIST OF SYMBOLS AND ABBREVIATIONS	XIV
CHAPTER 1	1
INTRODUCTION	1
1.1 Horse racing	1
1.1.1 History.....	1
1.1.2 List of prohibited substances	2
1.1.3 Current screening methods	4
1.2 Anabolic androgenic steroids: their pathways and role in horse racing ..	6
1.2.1 Background.....	6
1.2.2 Mechanism of action.....	8
1.2.3 Challenges in detection of anabolic androgenic steroids.....	11
1.3 Metabonomics.....	16
1.3.1 Background.....	16
1.3.2 Current uses in profiling diseases and doping	19
CHAPTER 2	23
AIMS AND SIGNIFICANCE OF STUDY.....	23
2.1 Targeted approach.....	23
2.2 Non-targeted approach.....	27
2.3 Summary	29

CHAPTER 3	30
MATERIALS AND METHODS	30
3.1 Targeted approach.....	30
3.1.1 Horse liver microsome (HrLM) preparation.....	30
3.1.2 Metabolite identification (Met ID) studies	31
3.1.3 Metabolic stability studies	35
3.2 Non-targeted approach.....	39
3.2.1 Method validation	39
3.2.2 Plasma profiling	40
CHAPTER 4	43
RESULTS AND DISCUSSION	43
4.1 Targeted approach.....	43
4.1.1 Results of metabolite identification studies	43
4.1.2 Results of metabolic stability studies.....	63
4.1.3 Discussion.....	69
4.2 Non-targeted approach.....	81
4.2.1 Method validation	81
4.2.2 Chemometrics	85
4.2.3 Discussion.....	91
CHAPTER 5	96
CONCLUSION AND FUTURE WORK	96
5.1 Conclusion	96

5.1.1 Targeted approach.....	96
5.1.2 Non-targeted approach.....	97
5.2 Future work.....	98
5.2.1 Targeted approach.....	98
5.2.2 Non-targeted approach.....	99
REFERENCES	101

SUMMARY

Previous *in-vitro* studies on anabolic androgenic steroids (AAS) were performed by other horseracing clubs around the world. The studies demonstrated the extensive metabolism of hydrophobic designer steroids in the horse liver suggesting the fast elimination of the parent drug *in-vivo*. Hence, there is a potential challenge in detecting selected parent drug during targeted screening and further raises the pertinent question of whether some of the metabolites of AAS are pharmacologically active. It is therefore important to determine the appropriate analytes to monitor, like parent drug, metabolites or both. Due to ethical issues related to animal research, alternative approaches have to be used to study the metabolic stability and metabolite identification of AAS. There is also the constant challenge of detecting new AAS abuse in equine sports.

Our present study was designed to investigate both the non-targeted and targeted metabolic profiling approaches to bridge the gaps in the detection of doping agents. *In-vitro* experiments were carried out using horse liver microsomes to understand the metabolic stability and identify the metabolites of ethylestrenol, metribolone, ecdysone and 20-hydroxy ecdysone. Global profiling of equine plasma was carried out to differentiate the different gender of horses.

Ethylestrenol is a short acting AAS with progesterone-like activity and little androgenic activity. Ethylestrenol has been studied *in-vivo* in equine studies. In addition, *in-vitro* models in cattle and rats have also been investigated. From the small-scale synthesis experiment, it is clear that the unknown metabolite generated in horse liver microsomes is possibly associated with 17α -ethyl- 5α -estrane- $3\beta,17\beta$ diol. With the possible structure of the metabolite, large-scale synthesis experiments could be conducted and the product can be characterized. This metabolite could be explored as an analyte to be monitored in ethylestrenol abuse.

Metribolone is a potent synthetic AAS reported since the late 1960s. Androgen binding assays were done on metribolone and it was found to have high affinity for androgen receptors. However it was never marketed as an AAS due to its high liver toxicity. Information on metribolone metabolism is limited. Our data showed that metribolone metabolizes in horse liver microsomes to produce multiple metabolites. The major metabolite was elucidated to be 16-hydroxy metribolone. 16-hydroxy metribolone could be explored as an analyte to be monitored in metribolone abuse.

Ecdysone and 20-hydroxyecdysone are ecdysteroids which are insect-molting hormones present in various arthropods and plants. Their structures are related to cholesterol. They are known to increase protein synthesis upon administration. In addition, studies on 20-hydroxyecdysone have shown that it is capable of enhancing muscle growth without the negative effects of

synthetic AAS. Ecdysteroid metabolism was previously studied in humans. Our data showed that there is no significant metabolism of ecdysone and 20-hydroxy ecdysone in horse liver microsomes and suggested that it might be more appropriate to monitor the parent drug in dope testing.

Global profiling of equine plasma obtained from horses of different genders was performed in the current study. As the chemometric models were not sufficiently robust, the results were not conclusive in differentiating the different genders of the horses. Nevertheless, the broad classification trends suggested that there might be unique metabotype associated with each gender. Further studies need to be performed to determine the baseline metabotype of each gender of the horses before the metabonomic approach can be tested in dope testing.

LIST OF TABLES AND FIGURES

Table 1: Summary of the specific aims of this study.....	29
Table 2: Accurate mass measurement of metribolone and metabolite B, 16-hydroxy metribolone	62
Table 3: Summary of the met ID and metabolic stability studies.....	80
Figure 1: Schematic for SRM.	5
Figure 2: Biological pathway of steroid.....	9
Figure 3: Structures of (1) boldenone and (2) stanazolol.....	10
Figure 4: Chemical structure of AAS.....	12
Figure 5: Structures of (1) THG, (2) gestrinone and (3) norbolethone.....	14
Figure 6: Structures of (1) ecdysone, (2) 20-hydroxy ecdysone and (3) cholesterol.	15
Figure 7: Structures of (1) ethylestrenol and (2) metribolone respectively.	16
Figure 8: Turinabol and its metabolites. Φ - <i>in-vitro</i> metabolites and \surd - urinary metabolites.	24
Figure 9: Mesterolone and its metabolites. Φ - <i>in-vitro</i> metabolites and \surd - urinary metabolites.....	25
Figure 10: Chromatograms of ethylestrenol incubated with (A) HrLM at 0 min, (B) HrLM at 60 min, (C) HrLM mixture without cofactor at 0 min, (D) HrLM mixture without cofactor at 60 min, (E) HrLM mixture without substrate at 0 min and (F) HrLM mixture without substrate at 60 min. The analytes were derivatized with their respective derivatizing agents.	45
Figure 11: Chromatograms of standards and HrLM mixture. (A) norethandrolone standard (B) 17 α -ethyl-5 α -estrane-3 α ,17 β -diol standard (C) 17 α -ethyl-5 β -estrane-3 α ,17 β -diol standard (D) ethylestrenol standard (E) HrLM mixture at 0 min and (F) HrLM mixture at 60 min. The analytes were derivatized with their respective derivatizing agents.	46
Figure 12: Chromatograms of standards and HrLM mixture. (A) 17 α -ethyl-5 β -estrane-3 α ,17 β -diol standard, (B) 17 α -ethyl-5 α -estrane-3 α ,17 β -diol standard	

and (C) HrLM mixture at 60 min. The analytes were derivatized with their respective derivatizing agents.	47
Figure 13: Mass spectra of (A) 17 α -ethyl-5 α -estrane-3 α ,17 β -diol standard (B) 17 α -ethyl-5 β -estrane-3 α ,17 β -diol standard and (C) unknown metabolite (peak at 6.47 min) in HrLM mixture at 60 min.	48
Figure 14: Chromatograms of HrLM mixture with synthesized standards. (A) 17 α -ethyl-5 β -estrane-3 β ,17 β -diol (putative) standard (B) 17 α -ethyl-5 α -estrane-3 β ,17 β -diol (putative) standard and (C) unknown metabolite (peak at 6.47 min) in HrLM mixture at 60 min. The analytes were derivatized with their respective derivatizing agents.	49
Figure 15: Mass spectra of (A) 17 α -ethyl-5 α -estrane-3 β ,17 β -diol (putative) standard and (B) unknown metabolite (peak at 6.47 min) in HrLM mixture at 60 min.	50
Figure 16: Ecdysone and its metabolites in <i>Pieris</i> larvae.	51
Figure 17: Chromatograms of (A) 20-hydroxy ecdysone standard, (B) ecdysone standard, (C) HrLM mixture at 0 min, (D) HrLM mixture at 60 min, (E) HrLM mixture without cofactor at 0 min, (F) HrLM mixture without cofactor at 60 min, (G) HrLM mixture without substrate at 0 min and (H) HrLM mixture without substrate at 60 min. The analytes were derivatized with their respective derivatizing agents.	52
Figure 18: Mass spectra of (A) derivatized ecdysone standard and (B) derivatized ecdysone (peak at 19.20 min) in HrLM mixture at 60 min.	53
Figure 19: 20-hydroxy ecdysone and its metabolites in humans.	54
Figure 20: Chromatograms of (A) 20-hydroxy ecdysone standard, (B) HrLM mixture at 0 min, (C) HrLM mixture at 60 min, (D) HrLM mixture without cofactor at 0 min, (E) HrLM mixture without cofactor at 60 min, (F) HrLM mixture without substrate at 0 min and (G) HrLM mixture without substrate at 60 min. The analytes were derivatized with their respective derivatizing agents.	55
Figure 21: Mass spectra of (A) 20-hydroxy ecdysone standard and (B) parent drug (peak at 21.96 min) in HrLM mixture at 60 min.	56
Figure 22: Chromatograms of (A) metribolone standard, (B) HrLM mixture at 0 min, (C) HrLM mixture at 60 min, (D) HrLM mixture without cofactor at 0 min, (E) HrLM mixture without cofactor at 60 min, (F) HrLM mixture without substrate at 0 min and (G) HrLM mixture without substrate at 60 min. The analytes were derivatized with their respective derivatizing agents.	58

Figure 23: Expanded view of the chromatograms (A) metribolone standard, (B) HrLM mixture at 0 min, (C) HrLM mixture at 60 min, (D) HrLM mixture without cofactor at 0 min, (E) HrLM mixture without cofactor at 60 min, (F) HrLM mixture without substrate at 0 min and (G) HrLM mixture without substrate at 60 min.	59
Figure 24: Mass spectra of (A) metribolone and (B) parent drug (peak at 6.98 min) in HrLM mixture at 60 min.	60
Figure 25: (A) Chromatogram of possible metribolone metabolites (B) mass spectrum of unknown compound at RT 4.24 min and (C) expanded mass spectrum (m/z 160 to 230) of unknown compound at RT 4.24 min. The analytes were derivatized with their respective derivatizing agents.	61
Figure 26: Phase I metabolic profile of testosterone (positive control).	63
Figure 27: Phase II metabolic profile of testosterone (positive control).	64
Figure 28: Phase I metabolic stability profile of ecdysone.	65
Figure 29: Phase II metabolic stability profile of ecdysone.	66
Figure 30: Phase I metabolic stability profile of 20-hydroxy ecdysone.	67
Figure 31: Phase II metabolic stability profile of 20-hydroxy ecdysone.	68
Figure 32: Phase I metabolic stability profile of metribolone.	69
Figure 33: Ethylestrenol and its metabolites.	70
Figure 34: Schematic flow of synthesis.	72
Figure 35: Mass spectra of ethylestrenol metabolite in (A) cattle and (B) rat [27, 28].	74
Figure 36: Structures of metribolone and its possible metabolites. (A) 18-hydroxy metribolone (B) 16-hydroxy metribolone (C) 6-hydroxy metribolone and (D) 2,16-dihydroxy metribolone.	77
Figure 37: Relative standard deviation of intra-day precision of ISTD and six endogenous metabolites in equine plasma.	82
Figure 38: Relative standard deviation of inter-day precision of ISTD and six endogenous metabolites in equine plasma.	82
Figure 39: Relative standard deviation of autosampler stability of ISTD and six endogenous metabolites in equine plasma.	83

Figure 40: Stability of ISTD and six endogenous metabolites over two weeks stored at 4 ⁰ C with respect to day 0.	84
Figure 41: Stability of ISTD and six endogenous metabolites over six months stored at -80 ⁰ C with respect to week 0.	85
Figure 42: PCA plot obtained from equine plasma samples of different genders of horses with QC samples. H = horse, G = gelding, M = mare, R = rig, F = filly, C = colt and QC = quality control samples.	86
Figure 43: PCA plot obtained from all equine plasma samples, without QC samples and outlier. H = horse, G = gelding, M = mare, R = rig, F = filly and C = colt.	87
Figure 44: OPLS-DA plot obtained from male horses and female horses. H = horse, M = mare, R = rig, F = filly and C = colt.	87
Figure 45: OPLS-DA plot obtained from male horses and gelding horses. H = horse, G = gelding, R = rig and C = colt.	88
Figure 46: OPLS-DA plot obtained from female horses and gelding horses. G = gelding, M = mare and F = filly.	89
Figure 47: Validation plot of OPLS plots. A = OPLS for male horses and female horses, B = OPLS for male horses and gelding horses and C = OPLS for female horses and gelding horses.	90
Figure 48: An overlay of GC/MS chromatograms of the six QC samples.	95
Figure 49: An overlay of GC/MS extracted chromatograms of caffeine (ISTD at RT = 8.67 min) in the six QC samples.	95

LIST OF SYMBOLS AND ABBREVIATIONS

AAS	Anabolic androgenic steroids
ADMA	Asymmetrical dimethylarginine
amu	Atomic mass unit
C	Colt
CE/MS	Capillary electrophoresis
cm	Centimetre
CZE	Capillary-zone electrophoresis
EDTA	Ethylenediaminetetraacetic acid
EI	Electron ionization
ESI	Electrospray ionisation
eV	Electron volt
F	Filly
FT-IR	Fourier transform infrared
G	Gelding
g	Earth's gravitational force
GC/MS	Gas chromatography coupled to mass spectrometry
H	Horse
HrLM	Horse liver microsomes
IRMS	Isotopic ratio mass spectrometry
ISTD	Internal standard
K	Elimination rate constant

kV	Kilovolts
LC-ESI-HRMS	Liquid chromatography-electrospray-high resolution mass spectrometry
LC/MS/MS	Liquid chromatography coupled to tandem mass spectrometry
LDA	Linear discriminant analysis
LiAlH ₄	Lithium aluminium hydride
LIF	Laser induced fluorescence
M	Mare
MAB	Pyrolysis/metastable atom bombardment
Met ID	Metabolite identification
mg	Milligram
min	Minute
mL	Millilitre
mM	Millimolar
mm	Millimetre
MOX	Methoxyamine hydrochloride
MRM	Multiple reaction monitoring
MSTFA	N-methyl-N-trimethylsilyltrifluoroacetamide
<i>m/z</i>	mass-to-charge ratio
NADPH	Nicotinamide adenine dinucleotide phosphate-oxidase
nm	Nanometre
NMR	Nuclear magnetic resonance

OPLS-DA	Orthogonal partial least-squares discriminant analysis
PCA	Principal component analysis
PCC	Pyridinium chlorochromate
PLS	Partial least-squares
PLS-DA	Partial-least squares-discriminant analysis
Q1	First quadrupole
Q2	Collision cell
Q3	Third quadrupole
QC	Quality control
R	Rig
reGH	Recombinant equine growth hormone
rhEPO	Recombinant human erythropoietin
RSD	Relative standard deviation
RT	Retention time
SDMA	Symmetrical dimethylarginine
sec	Second
SIM	Selected ion monitoring
SPE	Solid-phase extraction
SRM	Selected reaction monitoring
t[1]	First intent variable
t[2]	Second componenet
TCM	Traditional Chinese medicine
THE	Tetrahyrofuran

THG	Tetrahydrogestrinone
TMSI	Trimethylsilyl imidazole
TOF	Time-of-flight
Tris	Trimethylol aminomethane
UGT	Uridinediphosphate-glucuronosyltransferase
U.S.A.	United States of America
UV	Univariate
V	Volts
v/v	Volume/Volume
WADA	World anti-doping agency
°C	Degrees Celsius
α	Alpha
β	Beta
μL	Microlitre
μm	Micrometre

CHAPTER 1

INTRODUCTION

1.1 Horse racing

1.1.1 History

Horse racing was first introduced in the Olympics in 680 BC in the form of chariot racing [1]. Even as early as the Roman times (10th century BC), humans embarked on the quest to improve the performance of race horses [2]. The Romans used an innocuous mix of water and honey called “hydromel” which was believed to rejuvenate race horses. The quest for good stamina and speed of the race horses led to the breeding of the Thoroughbreds in the 1700s [2]. Thoroughbreds are a distinct breed of horses that are derived from a single breed line. They are also known as purebreds and the intense selection criteria make the Thoroughbreds highly adapted athletes, known for their agility and speed. Today, horse racing is a billion-dollar industry where trainers and owners are motivated by the prize-money to overcome obstacles to win races. This has led to trainers and owners using unorthodox methods such as prohibited substances to give their horses an unfair advantage in racing.

There are generally four scenarios of doping horses with prohibited substances. The first scenario is the administration of stimulants to increase

the speed of horses in racing. The second scenario is the administration of tranquilizers or depressant drugs to suppress the performance of competitors' horses. This class of drugs is also called "stoppers". The third scenario is the restoration of the normal performance of horses post-trauma such as surgery. The fourth scenario is accidental doping of horses with food, plant or contaminants that give rise to a positive result.

1.1.2 List of prohibited substances

The prohibited substance list is a guideline that stipulates forbidden drugs in horse racing competition. The list of prohibited substances varies according to different horse racing nations. For example, in United States of America (U.S.A.), phenylbutazone and furosemide are allowed in many states but they are banned in British racing [3]. The list consists of different classes of prohibited substances like stimulants, anti-pyretics, analgesics, diuretics, anti-inflammatory substances, antihistamines, local anaesthetics, muscle relaxants, respiratory stimulants, sex hormones, anabolic agents, corticosteroids and substances affecting blood coagulation. Stimulants like amphetamine, methamphetamine, caffeine, ephedrine and methylphenidate are known to have neurological effect on the race horses thereby increasing their running ability [2]. This is primarily due to the pharmacological effects of the stimulants in increasing the alertness and decreasing fatigue of horses. Aspirin, an anti-pyretic, helps to reduce fever and pain. Diuretics like

theobromine make a good compliment for aspirin. The increased rate of urination can eliminate aspirin from the system at a faster rate than in the absence of a diuretic [2]. This would evade the detection of aspirin. Cocaine is another drug of abuse because of its stimulant and local anesthetic effects. Narcotic analgesics like fentanyl and morphine depress pain and increase the running pace of horses but lead to respiratory depression. Cimetidine, a H₂ antagonist, is used for treatment of stomach ulcers and acid reflux, common amongst race horses. The overall aim in using the prohibited substances is to improve the performance of the race horses during competition.

Doping involves good knowledge of each horse and its response when the drug is administered. Therefore doping of horses is usually secretly performed by trainers or employers. The dose of the drug is critical as too little would not elicit the desired effect while too much could kill the horse. Another important consideration is the timing of the dosing, too early could render the horse uncontrollable in the parade ring and lead to disqualification from the race. A dose administration given too late could lead to a delayed effect and minimal impact on the race outcome.

The use of prohibited substances discourages clean athletes, disillusion punters, causes unjust monetary loss to horse owners and affects the equine breeding industry. In the breeding industry, selection of horses is based on their racing ability. The inherently poor racing ability of a horse can be

masked by the use of performance enhancing substances therefore affecting the new breed.

The aim of the Singapore Turf Club is therefore to create a level playing field and discourage doping in equine racing. This is achieved through extensive pre-race and post-race testing of doped substances using both equine plasma and urine samples.

1.1.3 Current screening methods

The first case of doping was reported in England in 1666. Racing analyst at that time did not have analytical techniques to identify the exact dopant. In 1910, Russian chemist, Bukowski demonstrated that drugs could be detected in horse saliva but the analytical method was not revealed [2]. Even now, with modern analytical technologies, dope testing in equine racing is still closely guided and not publicly published.

The science of dope testing needs to be specific, sensitive and highly accurate in order to generate reliable data to differentiate between doped and un-doped horses. Analytical instruments used for this purpose usually consist of chromatographic separation techniques coupled to mass analyzers such as liquid chromatography coupled to tandem mass spectrometry (LC/MS/MS) and gas chromatography coupled to mass spectrometry (GC/MS). Selected ion

monitoring (SIM) and selected reaction monitoring (SRM) are the common scanning modes used in these analytical techniques. Modern ion monitoring was introduced by Sweeley *et al.* They developed a technique where multiple selected ions are monitored through the MS [4]. In SIM scan mode, a single, most abundant (base ion), ion of a specific compound is selected and monitored. This increases the sensitivity of the specific selected ion. SRM, also known as multiple reaction monitoring (MRM), is usually applicable with triple quadrupole mass spectrometer (Figure 1). In SRM mode, parent ions are selected in the first quadrupole (Q1) and fragmented by the collision cell (Q2 in Figure 1). This generates product ions which are analyzed via the third quadrupole (Q3) [5].

The main advantage of these scanning modes over full scan experiments is the enhanced sensitivity and selectivity as the parent-product ion pair is typically unique with regards to the chemical structure of each prohibited substance.

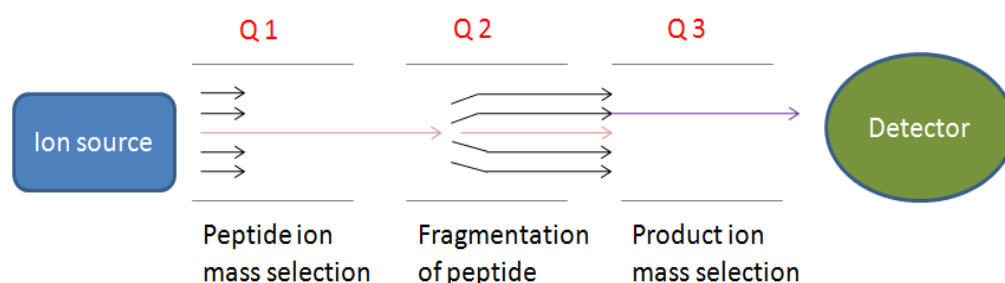


Figure 1: Schematic for SRM [6].

For example, screening, quantification and confirmation of boldenone, nandrolone, stanozolol, normethanrolone, testosterone and trenbolone were performed in the SRM mode using the triple quadrupole mass analyzer where both parent and product ions were monitored sequentially [7]. Another example is capillary-zone electrophoresis (CZE) used in the separation and identification of β -adrenoceptor agents by monitoring parent ions in the SIM mode [8]. In GC/MS, fluoxymesterone metabolite in equine urine was quantitated in SIM mode [9]. Doping control analysis of recombinant human erythropoietin (rhEPO) and its synthetic analogues in equine plasma were analyzed using nano-LC/MS/MS [10]. The main disadvantage of utilizing these selective scanning modes is that the targeted monitoring of analytes leaves a void in the testing of unknown analytes.

1.2 Anabolic androgenic steroids: their pathways and role in horse racing

1.2.1 Background

Steroids belong to an important class of prohibited substances. The first androgenic steroid, androsterone, was isolated in male bovine urine by Butenandt in the 1930s [11]. Later, Kochakian et al. demonstrated that the androgen extract from urine has anabolic effect [12]. Anabolic androgenic

steroids (AAS) are synthetic derivatives of testosterone. Testosterone is a male hormone known to promote muscle growth and was isolated by Laqueur in 1935 [13]. Testosterone is ten times more potent than androsterone. After the isolation of testosterone, research groups produced numerous analogs of testosterone in the next decade. In 1958, Dr Munson concluded that 5 α -androstanes and 3-ketosteroids were more active than 5 β -isomers and 3 β -hydroxysteroids respectively. The introduction of a methyl functional group in the 17 α -position also increased androgenic potency [13].

Although AAS have therapeutic values like treatment of cancer and AIDS, they are also used as illicit drugs in human and animal sports. For example, the synthetic AAS, stanozolol, effectively reduces the frequency of hereditary angioedema attacks [14]. Stanozolol is known to increase muscle mass in animals and can be used in human as well. Thus, the use of AAS is prohibited in human and animal sports.

The androgen part of AAS contributes to the masculinity factor and the anabolic part contributes to cell growth. The abuse of AAS is primarily due to the anabolic effect. Thus new illicit AAS are usually of higher anabolic activity but relatively weaker androgenic activities. The effects of AAS are produced by their binding to specific biological receptors where the binding affinity varies according to their chemical structures (Figure 2).

1.2.2 Mechanism of action

Each AAS binds to receptors within the cytoplasm of muscle cells of skeletal muscle tissue. Consequently, it reduces fat by increasing basal metabolic rate thereby increasing muscle mass. The process of protein synthesis within the muscle cells begins with the steroid/receptor complex entering the muscle cell nucleus. This stimulates protein synthesis resulting in muscle growth. Combination of athletic and weight training alone is deemed insufficient, so prolonged protein synthesis is induced for enhanced muscle mass, strength, stamina and endurance. Each AAS also stimulates muscle growth and increases muscle strength through reduction of protein catabolism, production of cytokines like IGF-1 and increase in androgen receptors. Administration of AAS should, theoretically, restore the balance between anabolic and catabolic hormones, therefore influencing recovery post-exercise [15].

In the bone tissue, the osteoblast is stimulated when the steroid binds to its receptors. This stimulation incorporates calcium and other proteins to form new bone tissue which increases bone mineral density and strength of bones. In the red blood cells, the binding of steroid to receptor results in an elevated haemoglobin concentration. The steroid/receptor complex together with EPO increases red blood cell formation and total blood volume [16].

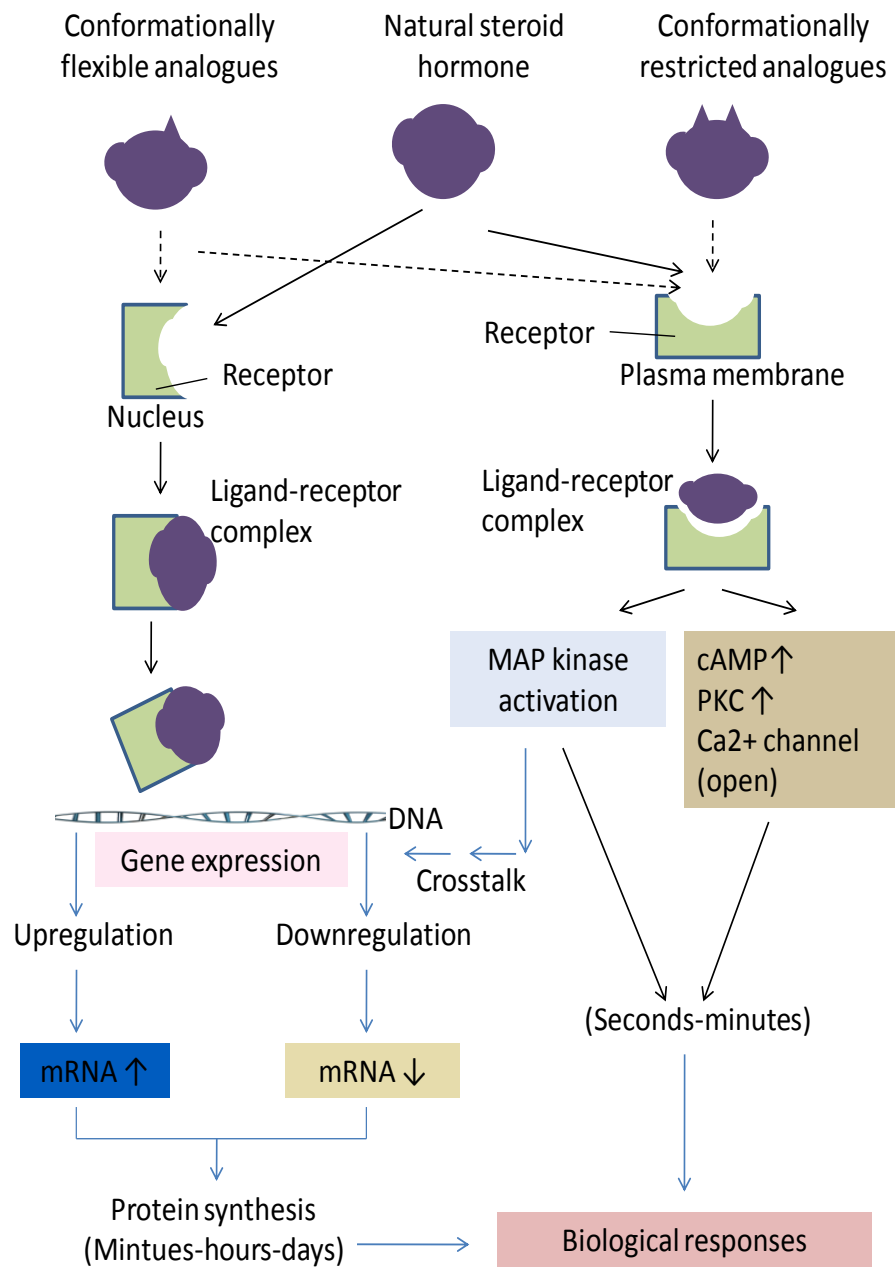


Figure 2: Biological pathway of steroid [17].

In human sports, AAS are proven to be effective, combined with exercise and proper diet [18]. In equine sports, AAS gives the horse an overall feeling of well-being, confidence, alertness, aggression and good appetite. It was demonstrated that AAS exert significant effects on mares, female horses, geldings and castrated horses [15]. However, AAS, when used extensively, have adverse effects like liver damage [15]. The use of AAS can also outstrip the strength of tendons and lead to its rupture in steroid users [19].

The two most commonly used steroids in equine sports are boldenone and stanazolol (Figure 3). These two steroids are known to increase protein synthesis in the body, as such leading to muscle and weight gain. The overall concern of integrity and safety in equine racing has forced some states, Iowa and Indiana, in the United States of America (U.S.A) to ban the use of steroids [20].

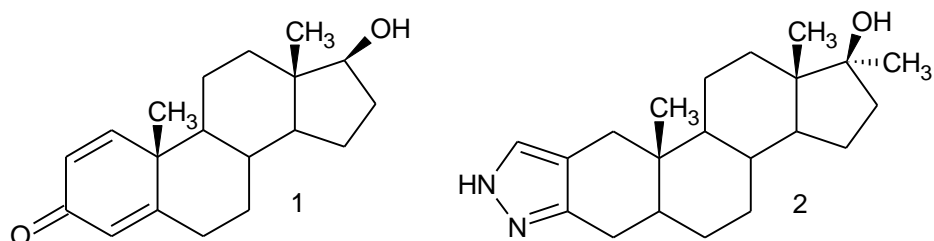


Figure 3: Structures of (1) boldenone and (2) stanazolol.

Hence it is paramount to discourage doping of AAS in horses by developing sensitive and reliable analytical methods for their detection.

One area that is currently of concern in equine and human anti-doping control is the use of so-called “designer drugs”. These compounds are synthesized to circumvent current analytical screening methods by introducing small structural changes that will render commonly used mass spectrometry-based screening methods ineffective.

Majority of designer drugs were once in the drug development pipeline of pharmaceutical companies but were not progressed to late development stage due to toxicological issues or poor pharmacokinetic characteristics. The other source of designer AAS is the black market where they are produced illicitly and their identity and purity cannot be determined. Almost always, the designer drugs are channelled from human to equine sports.

1.2.3 Challenges in detection of anabolic androgenic steroids

Anabolic steroids share a core structure (Figure 4), and minor chemical modification to one of the four rings of a known androgen can be used to produce a novel compound. This potential for structural modifications renders AAS a good designer drug scaffold. However, to be effective, the derivative must still retain the important pharmacological properties of the anabolic agents and this means that the binding to the androgen receptor must not be compromised by the structural modification. This limits the amount of modification that can be introduced into the steroid before it becomes

pharmacologically inactive. If organic chemists successfully synthesize designer AAS, it would be undetectable with present libraries due to their structural changes.

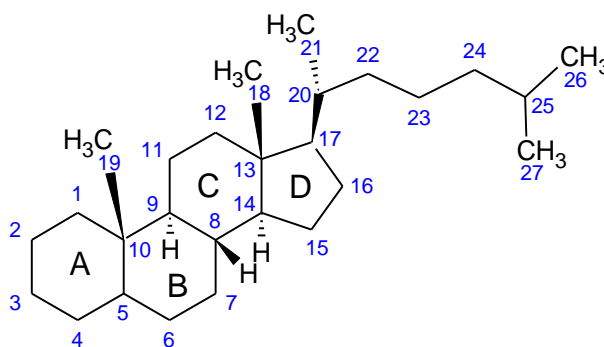


Figure 4: Chemical structure of AAS.

An example of a designer AAS is tetrahydrogestrinone (THG) which was first reported in 2003 [21]. THG is an illicit steroid that has potent androgenic and anabolic effects. THG is structurally similar to gestrinone, which is a prohibited steroid (Figure 5). The detection of this AAS was hindered by its poor behaviour under GC/MS conditions. Its poor behaviour was attributed to the production of multiple isomeric trimethylsilyl derivatives and its presence in trace amounts in urine samples. Therefore, it was found to be more suitable for LC-MS conditions [21]. This case is an example of the difficulty in detecting designer AAS using routine screening methods.

Current detection methods employed a targeted approach, using SIM and SRM, to scout for only compounds in the prohibited substance list or compounds that are well characterized. These are the limitations of the current detection methods. As such, designer drugs would escape detection by the available analytical methods due to their chemical modifications. For example, norbolethone, a designer steroid (Figure 5), could not be detected using the current detection methods. However, analytical chemists observed no detectable level of endogenous steroids in urine from female athletes. It was eventually demonstrated that norbolethone was suppressing the steroid profile [22]. Norbolethone was developed by Wyeth Pharmaceuticals in the early 1950s but was never brought to the market because it was more anabolic than its methyl isomer.

Since there is an unknown difference in metabolism between human and horse, the direct extrapolation of the human data to horse is unrealistic. Hence to understand AAS metabolism, studies need to be carried out in horse liver microsomes.

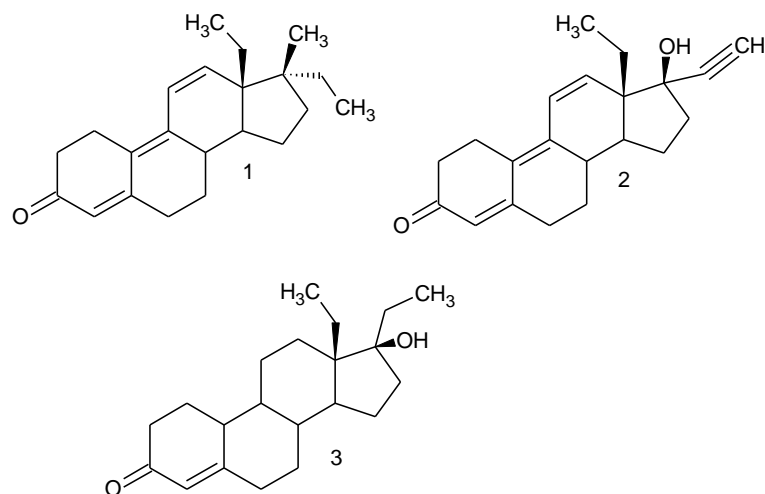


Figure 5: Structures of (1) THG, (2) gestrinone and (3) norbolethone.

With the ever-increasing list of designer AAS being synthesized and abused, testing laboratories have to constantly develop new analytical methods and strategies to detect dopers. Steroids such as ecdysone and 20-hydroxyecdysone are ecdysteroids which are insect-molting hormones present in various arthropods and plants. Their structures are related to cholesterol (Figure 6). They are known to increase protein synthesis upon administration [23, 24]. In addition, studies on 20-hydroxyecdysone have shown that it is capable of enhancing muscle growth without the negative effects of synthetic AAS [24]. Ecdysteroid metabolism was previously studied in humans [24].

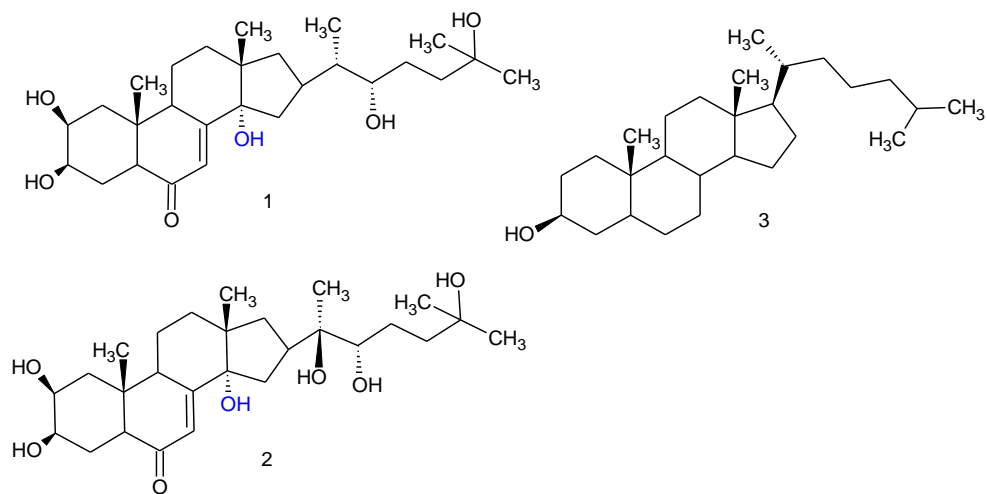


Figure 6: Structures of (1) ecdysone, (2) 20-hydroxy ecdysone and (3) cholesterol.

Ethylestrenol (Figure 7) is a short acting AAS with progesterone-like activity and little androgenic activity. Ethylestrenol have been studied in equine via *in-vivo* studies [25, 26]. In addition, *in-vitro* models (liver microsomes) of cattle and rats have also been investigated [27, 28].

Metribolone (Figure 7) is a potent synthetic AAS which was reported in the late 1960s. Androgen binding assays were done on metribolone and it was found to have high affinity for androgen receptors [29, 30]. However it was never marketed as an AAS due to its high liver toxicity [31]. Information on metribolone metabolism is limited.

These steroids have potential for abuse in equine racing. To date, only limited pharmacokinetics studies have been done in equine model. Previous works on AAS in *in-vitro* studies have been done by other horseracing clubs around the

world [32-34]. The studies demonstrated the extensive metabolism of hydrophobic designer steroids in the horse liver suggesting the fast elimination of the parent drug *in-vivo*. Hence, there is a challenge in detecting the parent drug during targeted screening and further raises the pertinent question of whether some of the metabolites of AAS are pharmacologically active. It is therefore important to determine the appropriate analytes to monitor, such as parent drug, metabolites or both.

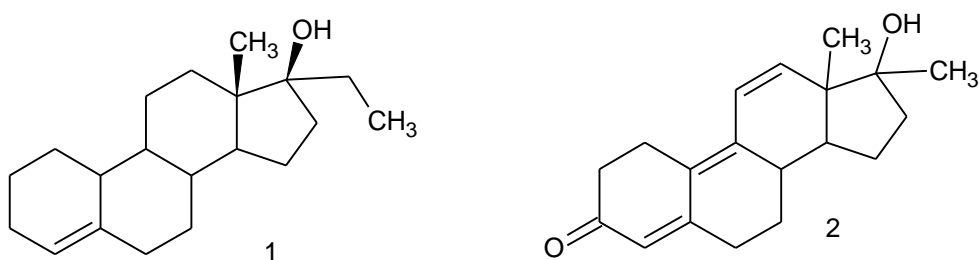


Figure 7: Structures of (1) ethylestrenol and (2) metribolone respectively.

1.3 Metabonomics

1.3.1 Background

Metabonomics is the quantitative measurement of the dynamic multiparametric metabolic response of living systems to pathophysiological stimuli, genetic modification and pharmacological intervention [35]. This was achieved through the study of biofluids and tissues with the data interpreted

using chemometrics techniques. The term metabonomics was coined in the 1990s but the technique was already in use since the 1980s [35]. Metabonomics have been used in the study of drug toxicity, animal models and description mechanisms [36, 37]. It was also used to study organisms and plants, diagnose diseases and elucidate gene function [37-40]. Metabonomics has also been used to study traditional Chinese medicine (TCM) safety studies and drug metabolism [41, 42]. The human diseases involve interaction between multiple gene processes and environmental factors. To better understand such disease mechanism, advanced analytical techniques are used to generate new molecular information to complement information from genomics and transcriptomics. Transcripts and proteins can be identified from their genomic information but the molecular identity of molecules need sophisticated instrumentation like GC/MS, LC/MS, capillary electrophoresis (CE/MS), nuclear magnetic resonance (NMR) spectroscopy, laser induced fluorescence (LIF) detection and Raman and Fourier transform infrared (FT-IR) approaches [35, 43, 44]. The large amount of data generated by these techniques make it difficult to interpret the information. Genomics and proteomics do not reflect the "final outcomes" of the phenotypes whereas metabonomics is the direct reflection of the organism's phenotypes [45, 46]. This unique advantage of metabonomics compared to proteomics and genomics.

The high quality of data shows the temporal state of the organism through their endogenous metabolites. These data can be interpreted in two ways, metabolic fingerprinting and metabolic profiling [44]. In metabolic fingerprinting, the data is a numerical representation of the biological systems without any identity of the actual metabolites. For example the acquisitions of NMR or MS spectra act as a fingerprint of the metabolites of the investigated biological system. This is done in the absence of the metabolites' identities [45]. Such data can be analyzed through multivariate statistical analysis. Global metabolic profiling is also known as metabonomics or metabolomics depending on the nature and scope of scientific investigation. Metabolic profiling provides mechanistic information on perturbed metabolic pathways and the associated biomarkers. This is targeted and usually quantitative analysis of a specific group of metabolites like amino acids [45]. Data analysis in metabolic profiling involves supervised and unsupervised multivariate chemometrics statistics. The unsupervised principal component analysis (PCA) is used to study the classification trends associated with the test groups (e.g. different types of race horses) and identify outliers (e.g. horse suffering from an unknown disease). Supervised partial-least squares-discriminant analysis (PLS-DA) generates a predictive model that identifies the marker metabolites characterizing each test groups.

1.3.2 Current uses in profiling diseases and doping

Metabonomics, a global non-targeted metabolic profiling approach, has been explored to study different biological systems. For example, stress in rat models have been studied by Wang *et al.* using metabonomics [47]. Stress was induced by forced swimming for 5 min, at 40°C for 5 min, water deprivation for 24 h, food deprivation for 24 h, tail squeezing for 1 min, electric shock for 10 s, reversal of day and night, exposure to -10°C for 30 min and 2 h behaviour restriction. Urine samples were collected from the experimental rats and analyzed by GC/MS. The complex GC/MS data obtained were analyzed using multivariate statistical analysis. The results demonstrated that stress affected some of the biochemical pathways which gradually recovered when the stressor was withdrawn. If the stress continued, biological pathways like tyrosine, tryptophan and glutamine pathways were progressively affected leading to depression-like state. Similar experiments with equine plasma samples can also be done using GC/TOFMS. The introduction of exogenous substance could also indicate changes in the biochemical pathways.

As shown in previous human studies, metabonomics can be used to monitor the changes in the endogenous metabolites for indication of diseases and genetic disorders [48-55]. For example in the study of differentiating children with autism from their unaffected siblings done by Wang *et al.* [48]. The

current diagnosis involves observation by a trained clinician and this is subjective. The authors did metabolic profiling using NMR/MS. They found that urinary amino acids glutamate and taurine were perturbed in autistic individuals compared to their controls. Preliminary findings show that urinary metabolites hippurate, N-methyl nicotinic acid and N-methyl nicotinamide and taurine could be possible biomarkers. This shows that even though the children are from the same families as the respective controls, there are still changes in the metabolic profiles. This might also be true in the case of race horses whose genetics is well-conserved but there may still be some metabolic differences.

Metabonomics has also been used to differentiate between the gender [56]. Serum samples were used to investigate sex-specific differences by measuring 131 metabolites from 3,300 independent individuals. LC/MS/MS was used to analyze the samples and linear regression analysis showed significant difference between males and females for 102 metabolites out of 131 metabolites. This shows there is promise in using equine plasma samples for metabonomics and gender can also be used as a discriminating factor.

The main aim of doping is to achieve biological changes in certain metabolic process that will lead to enhanced performance. Anti-doping analyses could detect the different biological changes of the associated metabolic cascade. This approach is currently used in the investigation of disease markers.

Doping in human sports is usually investigated through endogenous steroid profiling. This form of profiling is usually done using GC/MS or isotopic ratio mass spectrometry (IRMS) [45].

The investigation of the metabonomic signature of bike athletes is in-progress through a project funded by World anti-doping agency (WADA) in 2006 [45]. Another group of researchers used a targeted approach to the detection of rhEPO administration [45]. Four urinary metabolites were quantitated by LC/MS. The metabolites were asymmetrical dimethylarginine (ADMA), symmetrical dimethylarginine (SDMA), arginine and citrulline. It was shown that a single dose of rhEPO was sufficient to indicate an increase in all the four metabolites.

Both these human studies showed that the introduction of exogenous substance can cause changes in the level and ratio of endogenous steroids. Therefore metabonomics could be used to study these changes in the biological system.

Previous works have been done using metabonomics as a screening tool in cattle and horse [57, 58]. For example, metabonomics has been used in monitoring the use of AAS in cattle and measuring metabolic changes induced by recombinant equine growth hormone (reGH) in horse. For the analysis of AAS in cattle urine, the authors used pyrolysis/metastable atom bombardment (MAB) and time-of-flight (TOF) analyzer. Linear discriminant analysis (LDA)

was utilized to discriminate controls from treated animals. LDA also correlated to quantitative physiological responses induced by AAS [57]. Work has also been done on horse urine samples using liquid chromatography-electrospray-high resolution mass spectrometry (LC-ESI-HRMS). Their preliminary results indicated significant modifications of the metabolome after reGH treatment. The chemometric model was able to differentiate non-treated and reGH-treated horses [58]. These studies indicate that metabonomics can be used to detect doped animals and it is feasible to use the equine model.

CHAPTER 2

AIMS AND SIGNIFICANCE OF STUDY

2.1 Targeted approach

In-vivo and *in-vitro* metabolic studies of turinabol and mesterolone in horses were reported previously [32, 33]. Turinabol is a synthetic oral AAS which was incubated in horse liver microsomes (HrLM). Five metabolites of turinabol were detected with GC/MS (Figure 8). The *in-vivo* urine samples showed no sign of the parent steroid and nine metabolites were detected [33]. Mesterolone metabolic study was conducted in a similar way with five metabolites detected *in-vitro* and eight metabolites detected *in-vivo* (Figure 9) [32]. As a result of these studies, there is better understanding of these steroids' pharmacokinetics properties. However, metabolic stability studies of other AAS in equine model are lacking. Metabolic stability studies play a vital role in predicting the *in-vivo* half-life of AAS and hence their clearance in equine systems.

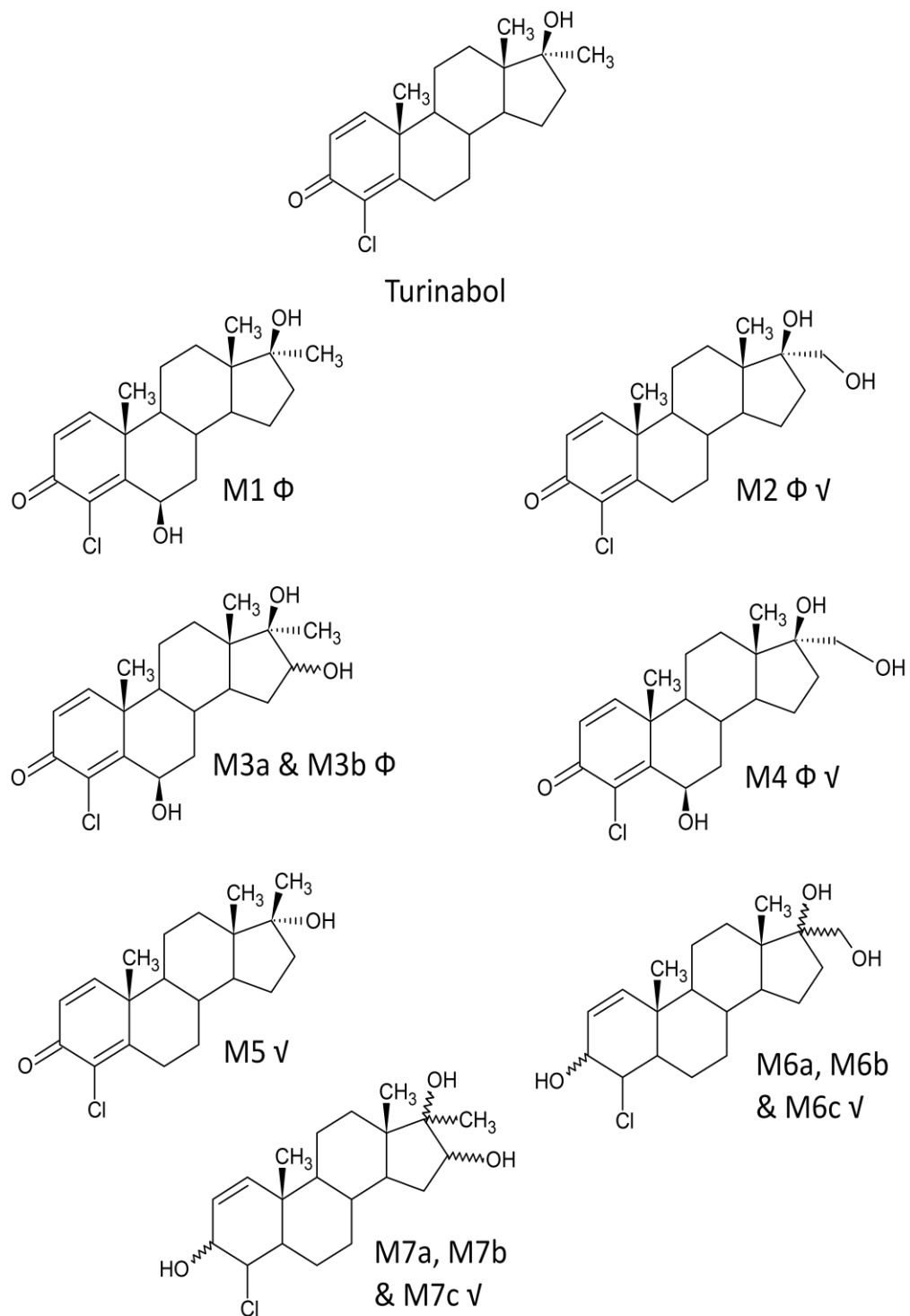


Figure 8: Turinabol and its metabolites. Φ - *in-vitro* metabolites and \vee - urinary metabolites [33].

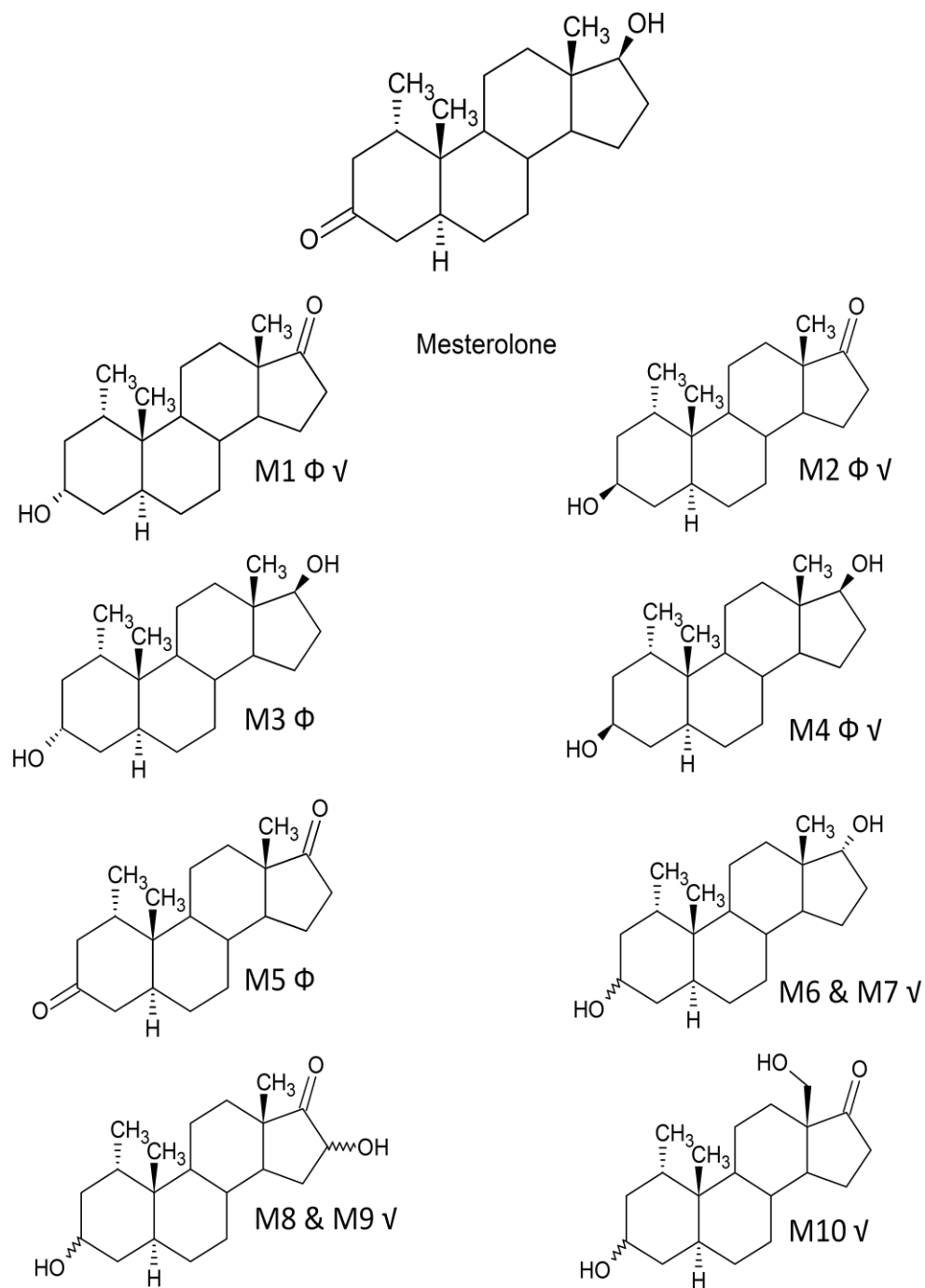


Figure 9: Mesterolone and its metabolites. Φ - *in-vitro* metabolites and \vee -urinary metabolites [32].

Ecdysone and metribolone (Figures 6 and 7) have yet to be studied in equine models. Since they have potential for abuse in equine racing, it becomes imperative to study their metabolic stabilities via *in-vitro* equine models. The information gleaned from such studies can be used to predict their biotransformation in horses and could help identify potential metabolites that could be monitored during routine screening. The *in-vitro* studies could also provide information on the clearance time and half-life of ecdysone and metribolone. These informations could be used for determining sample collection times.

On the other hand, 20-hydroxyecdysone and ethylestrenol (Figures 6 and 7) have been studied in the horse model but lack their respective metabolic stability studies [25, 26, 59]. As a short acting AAS, metabolic stability studies on ethylestrenol can provide useful information on its clearance and half-life. Similarly, 20-hydroxyecdysone, a potentially anabolic arthropod derived ecdysteroid, lacks information on its metabolic stability. These studies could in turn provide the analytical chemist crucial information on the surrogate metabolite to measure so as to detect ethylestrenol and 20-hydroxyecdysone abuse.

The objective of the targeted approach is to investigate the metabolism of ecdysone, 20-hydroxyecdysone, metribolone and ethylestrenol through *in-vitro* metabolic stability and metabolite identification studies.

2.2 Non-targeted approach

Previous studies show that metabonomics can be used to differentiate controls from doped animals [57, 58]. As such, non-targeted metabolic profiling method, like metabonomics, might also be applied to studying the equine metabotypes. With the downstream pharmacologically-induced metabolite perturbation likely to be similar for compounds with the AAS backbone structures, the non-targeted profiling method might be used as screening method for steroid abuse. As biomarkers are hypothesized not to be highly variable and dependent on the exact identity of the AAS doping agent, changes in the endogenous biomarkers could “suggest” the incident of doping without identifying the exact dopant.

Unlike other experimental mammalian models such as rodents, equine plasma is considered relatively easier to obtain than urine due to the difficulty for horses to urinate at stipulated times. Therefore, plasma is the preferred pre-race biological matrix to be collected.

The confounding factors affecting equine plasma samples could be diet, age, genetics and gender. The primary diet of race horses housed in the Singapore Turf Club is controlled. The average lifespan of a horse is forty years and the age of an active race horse typically ranges from two to nine years, which is only twenty percent of its life-span. Therefore the age of a race horse is also well defined. Since only Thoroughbreds are used in racing in Singapore, their

genetic profiles are assumed to be well-conserved. The only possible confounding factor is therefore gender. Thoroughbreds are generally divided into three genders: males (horse and colt), females (mare and filly) and castrated males (geldings). The male horse can be further classified as a rig where his testes are not fully formed outside his body but still have the characteristics of a horse. With one major confounding factor, non-targeted profiling could prove to be an invaluable tool for future monitoring of metabolic perturbations related to doping.

The objective of the non-targeted metabolic profiling of horses in the current thesis is to identify unique plasma biomarkers of the different genders of horses and the unique metabotype related to each gender. Profiling and elucidating the basal metabotype of each gender of horses are important as it forms the basis for future doping studies of novel AAS that are difficult to detect using the targeted screening approach.

2.3 Summary

The summary of this chapter is as follows:

	Specific aims
Targeted approach	To investigate the metabolism of ecdysone, 20-hydroxyecdysone, metribolone and ethylestrenol. This is done through <i>in-vitro</i> metabolic stability studies and metabolite identification studies.
Non-targeted approach	To identify unique plasma biomarkers of different genders and the unique metabotype related to each gender.

Table 1: Summary of the specific aims of this study.

CHAPTER 3

MATERIALS AND METHODS

3.1 Targeted approach

3.1.1 Horse liver microsome (HrLM) preparation

3.1.1.1 Chemicals and reagents

All solvents and reagents were of analytical grade. Ultrapure water (18.2 MΩ cm) was obtained from a Milli-Q water purification system (Millipore, Singapore).

3.1.1.2 Sample preparation

Fresh horse livers were harvested from horses that were euthanized. The livers were immediately frozen in liquid nitrogen and stored subsequently at -80°C. The livers were homogenized with 12 mL of homogenising buffer (0.1 M Tris-Cl, 10 mM EDTA and 150 mM potassium chloride). The homogenate was centrifuged at 12,000 g at 4°C for 15 min. The supernatant was decanted and further centrifuged at 105,000 g at 4°C for 70 min. The supernatant was discarded and the pellet was re-suspended in 8 mL ice-cold pyrophosphate

buffer (0.1 M sodium pyrophosphate and 10 mM EDTA). The suspension was centrifuged at 105,000 g for 45 min. The supernatant was discarded and 6 mL of microsome buffer (0.05 M Tris-Cl, 10 mM EDTA and 20% glycerol) was added [60].

Protein concentration was determined using the Bradford protein assay kit. HrLM was diluted to 1 mg/mL protein in 0.2 M phosphate buffer for cytochrome P450 and P420 quantification. A few crystals of sodium hydrosulfite was added and mixed until dissolved. Carbon monoxide was bubbled for 30 sec and the mixture was scanned from 400 to 500 nm. The remainder of the liver microsomes was aliquoted and stored at -80°C.

3.1.2 Metabolite identification (Met ID) studies

3.1.2.1 Chemicals and reagents

NADPH was obtained from BD Gentest (MA, U.S.A.). All solvents were of analytical grade. Acetonitrile, pyridinium chlorochromate, tetrahydrofuran, dichloromethane and lithium aluminium hydride were purchased from Sigma Adrich (MO, U.S.A.). Sodium dihydrogen phosphate monohydrate (NaH_2PO_4) and sodium-di hydrogen phosphate (Na_2PO_4) were obtained from Merck (Singapore). Standards for ecdysone, ethylestrenol and norethandrolone were purchased from Steraloids (RI, U.S.A.). 20-hydroxyecdysone and caffeine

were obtained from Sigma (Singapore) and metribolone was from AK Scientific (CA, U.S.A.). 17α -ethyl- 5α -estrane- $3\alpha,17\beta$ -diol and 17α -ethyl- 5β -estrane- $3\alpha,17\beta$ -diol were purchased from the National Measurement Institute (NSW, AUS). Prednisolone was purchased from Sigma Aldrich (U.S.A.). Trimethylsilyl imidazole (TMSI) and N-methyl-N-trimethylsilyltrifluoroacetamide (MSTFA) were obtained from Thermo Scientific (U.S.A.). Methoxyamine hydrochloride (MOX) was from Sigma Fluka (Singapore).

3.1.2.2 Synthesis of putative 17α -ethyl- 5α -estrane- $3\beta,17\beta$ -diol and 17α -ethyl- 5β -estrane- $3\beta,17\beta$ -diol standards

1.6 mmol of 17α -ethyl- 5α -estrane- $3\alpha,17\beta$ -diol was added to 3 mL to dichloromethane containing pyridinium chlorochromate (PCC) (2 mg/mL). 10 mg of anhydrous sodium acetate was added to the mixture and was incubated subsequently at 80°C for 2 hr with stirring. The resultant mixture is cooled to room temperature and passed through a 3.5 cm Celite column packed in a Pasteur pipette. The column was eluted with 5 mL 10% acetone in dichloromethane. The resultant solution was dried down and re-constituted with 10 mL of tetrahydrofuran (THF). This solution was added dropwise over 1 hr to a stirring solution of 0.8 mmol of lithium aluminium hydride (LiAlH_4) in 0.8 mL of THF at 0°C . This solution was stirred further for another 6 hr under nitrogen. This reaction was quenched with the addition of 0.2 N sodium

hydroxide. After filtering and drying under nitrogen, the residue was re-constituted in hexane and passed through the Celite column. The column was eluted with 5 mL ethyl acetate/hexane (1:2) [61, 62]. The ethyl acetate/hexane mixture was dried and derivatized with 50 μ L of MOX in pyridine for 30 min at 60^oC followed by 50 μ L of TMSI at 60^oC for 2 h [25]. This experiment was repeated with 17 α -ethyl-5 β -estrane-3 α ,17 β -diol for the synthesis of 17 α -ethyl-5 β -estrane-3 β ,17 β -diol.

3.1.2.3 HrLM incubation and sample derivatization

3 μ L of 10 mM ethylestrenol was incubated in 11 μ L HrLM together with 15 μ L NADPH A, 3 μ L NADPH B and 268 μ L of 100 mM potassium phosphate buffer for 1 h at 37^oC. The final reaction mixture contained 1% (v/v) of methanol that was used to dissolve the substrate. 150 μ L aliquots of the incubation mixture were quenched with 300 μ L ice-cold acetonitrile at time intervals of 0 and 60 min. The experiment was repeated in the absence of either NADPH or substrate to yield the negative controls. The quenched aliquots were subjected to solid-phase extraction (SPE) and derivatized with 50 μ L of MOX in pyridine for 30 min at 60^oC followed by 50 μ L of TMSI at 60^oC for 2 h [25]. The same experiment was repeated for ecdysone, 20-hydroxyecdysone and metribolone using different derivatisation reagents. Ecdysone and 20-hydroxyecdysone were derivatized with 100 μ L of MSTFA/2% TMSI mixture at 80^oC for 24 h [24]. Metribolone was derivatized

with 50 μ L MOX in pyridine followed by 50 μ L of MSTFA/2% TMSI for 30 min [63].

3.1.2.4 Chromatographic condition

The GC/TOFMS system (Agilent HP-6890 GC coupled to Waters GCT Premier) was used to analyze the derivatized samples. A DB 1MS (30 m x 0.25 mm x 0.25 μ m, Agilent J&W Scientific Folsom, CA, U.S.A.) chemically bonded column with 100% dimethylpolysiloxane cross-linked stationary phase was used. The carrier gas was helium with the flow rate of 1.0 mL/min and the injector was operated in the splitless mode. The injector and source temperatures were set at 250⁰C. The oven temperature was kept at 185⁰C at 0 min and increased at 25⁰C/min to 260⁰C followed by another increase at 40⁰C/min to 300⁰C where it remained for 16 min. The mass spectrometer was operated in electron ionization (EI) mode (70 eV). Data acquisition was performed in full scan mode from m/z 100 to 700 with scan time of 1.0 sec.

Metribolone metabolites were further analyzed using the Thermo Discovery LTQ-Obitrap linked to Agilent 1200 LC pump. Chromatography was carried out using reverse-phase Sunfire C₁₈ column (5 μ m, 2.1 x 150 mm, Waters) held at 4⁰C. Mobile phases A and B were 0.15% formic acid in Millipore water and acetonitrile, respectively. Gradient chromatography was performed at 0.35 mL/min with 80% solvent A and 20% solvent B at the start ($t = 0$ min), decreasing to 0% solvent A and 100% solvent B at $t = 11$ min and hold for 3

min (until $t = 14$ min). The gradient was then increased to 80% solvent A and 20% solvent B at $t = 14.5$ min and held for 1.5 min. Injection volume was 10 μL each. Ionization was carried out in the positive mode using the electrospray source at a capillary temperature of 225°C , a sheath gas flow of 30 units, an auxiliary gas flow of 5 units and an electrospray voltage of 5 kV. MS/MS precursor ion was first isolated in the LTQ and then fragmented at a normalized collision energy of 35 V. The full-scan analysis was performed over a range from 80 to 350 amu. All data were acquired and processed using the Xcalibur version 2.4 software.

3.1.3 Metabolic stability studies

3.1.3.1 Chemicals and reagents

Tris (trimethylol aminomethane) was purchased from Merck (Singapore). UGT (uridinediphosphate-glucuronosyltransferase) solutions A and B were obtained from BD Gentest (MA, U.S.A.). Saccharolactone and hydrochloric acid were purchased from Sigma Aldrich (Singapore) and Fisher Scientific (Singapore), respectively.

3.1.3.2 Sample preparation for Phase I metabolism experiment

10 μL of 50 μM ethylestrenol was incubated in 18 μL HrLM together with 25 μL NADPH A, 5 μL NADPH B and 442 μL of 100 mM phosphate for 1 h at 37°C. The final reaction mixture contained 1% (v/v) of methanol that was used to dissolve the substrate. 75 μL aliquots of the incubation mixture were quenched with 150 μL ice-cold acetonitrile at time intervals of 0, 5, 15, 30, 45 and 60 min. The experiment was repeated without HrLM, as a control. The experiment was repeated for ecdysone, 20-hydroxyecdysone and metribolone. Prednisolone was used as internal standard (ISTD). The quenched aliquots were dried and re-constituted with 50 μL Millipore water.

3.1.3.3 Sample preparation for Phase II metabolism experiment (for ecdysone and 20-hydroxy ecdysone)

100 μL of 250 mM Tris-HCl buffer was mixed with 18 μL HrLM, 182 μL Millipore water and 100 μL UGT B and kept on ice for 15 min. 50 μL of 50 mM saccharolactone and 10 μL of 50 μM of ecdysone or 20-hydroxy ecdysone was added and pre-incubated at 37°C for 3 min. Finally, 40 μL UGT A was added and the mixture was incubated for 1 h at 37°C [64]. The final reaction mixture contained 1% (v/v) of methanol that was used to dissolve the substrate. 75 μL aliquots of the incubation mixture were quenched with 150 μL ice-cold acetonitrile at time intervals of 0, 5, 15, 30, 45 and 60 min. The

experiment was repeated without HrLM, as a control. Prednisolone was used as ISTD. The quenched aliquots were dried and re-constituted with 50 μ L Millipore water.

3.1.3.4 Chromatographic condition

Metabolic stability analysis was carried using the Agilent 1290 Infinity LC interfaced with Agilent 6430 QQQ MS (Agilent Technologies, CA, U.S.A.). The analytical column was reverse-phase Acquity UPLC BEH C₁₈ (1.7 μ m, 2.1 x 50 mm, Waters). The mobile phase was composed of 0.1% formic acid in Millipore water as solvent A and 0.1% formic acid in acetonitrile as solvent B. Gradient chromatography was performed at 0.6 mL/min with 80% solvent A and 20% solvent B at the start ($t = 0$ min), decreasing to 5% solvent A and 95% solvent B at $t = 1.4$ min and hold for 0.5 min (until $t = 1.9$ min). The gradient was then increased to 95% solvent A and 5% solvent B at $t = 1.95$ min and held for 0.55 min. This solvent gradient program was used for ecdysone, 20-hydroxyecdysone and metribolone. Injection volume was 5 μ L each. The source was operated in positive electrospray ionisation (ESI) mode. The gas temperature was set at 350⁰C. The gas flow and capillary voltage were set at 12 mL/min and 3500 V, respectively. Detection of the drugs was performed in the multiple reaction monitoring (MRM) mode with single time segment. The dwell time was set at 20 msec per scan. The collision energies

range from 4 to 20 V and fragmentor voltage ranges from 104 to 140 V. Results were processed using Agilent MassHunter quantitative analysis.

GraphPad Prism software (version 5, CA, U.S.A.) was used to analyze the data and plot the metabolic stability profile. The equation used for one-phase exponential decay is $Y = \text{Span}(e^{-KX}) + \text{plateau}$ where X is time and Y is the percentage of substrate remaining with respect to 0 min. The non-linear regression results were presented in a semi-log scale to provide a linear relationship with respect to incubation time. This helps to visualise data that changes with an exponential relationship. This linear relationship would be represented by $\ln Y = -KX + \ln \text{Span}$ where K is the rate elimination constant and can be obtained from the gradient of the graph. The half-life of the decay was calculated based on $\ln 2/K$. Since the equation is based on the metabolic degradation of the parent drug, it was used to analyze the kinetics of the Phase II experiments.

3.2 Non-targeted approach

3.2.1 Method validation

3.2.1.1 Intra-day and inter-day precision

Intra-day precision was analyzed with seven replicates of pooled plasma samples that were processed independently. The inter-day precision was determined by analysing the pooled samples on three consecutive days. The criteria for acceptability of the precision data were within 20% relative standard deviation (RSD).

3.2.1.2 Autosampler stability

Autosampler stability, defined as the stability of the derivatized metabolites when stored in the autosampler of the analytical instrument, was also evaluated. The stability of the TMS-derivatised metabolites, kept in the autosampler at ambient temperature ($25 \pm 2^\circ\text{C}$), was determined periodically by injecting replicates of the processed samples up to 24 h. The peak areas of the selected analytes (leucine, proline, ribose, serine, threonine and valine) obtained at the initial run were used as the reference to determine the relative stability of each analyte at subsequent time-points. The analytes were selected

based on the availability of their standards and the spread of their retention time (RT) over the entire run. The criteria for acceptability of the stability data were within 20% RSD.

3.2.1.3 Freezer stability study

Freezer stability of the metabolites in the equine plasma was assessed by processing and analysing pooled plasma samples stored at -80°C (for up to 6 months) and 4°C (for 2 weeks). These temperatures were chosen with relation to the workflow of sample analysis at the Singapore Turf Club laboratory. Samples stored at -80°C were analyzed on 0, 1, 2, 4, 12 and 24 weeks. Samples stored at 4°C were analyzed on 0, 1, 3, 7, 11, 14 days.

3.2.2 Plasma profiling

3.2.2.1 Sample preparation

Prior to sample preparation and GC/TOFMS analysis, all the plasma samples were randomized. Equine plasma samples were collected from horse (H, > 3 year male), rig (R), mare (M, > 3 year female), filly (F, < 3 year female), colt (C, < 3 year male) and gelding (G) (n = 25). The collected plasma samples were stored at -80°C until ready to use. 10 µg/mL of caffeine was added as

ISTD. Acetonitrile (1200 μ L) was added to 400 μ L of plasma to precipitate the proteins. The mixture was vortex-mixed at high speed for 2 min and subsequently centrifuged for 20 min at 14000 g. The supernatant was separated and evaporated to dryness at 50⁰C under a gentle stream of nitrogen gas. The dried extract was derivatized with 60 μ L of MSTFA for 45 min at 60⁰C. Each derivatized extract was transferred to a GC/MS vial.

All the samples were pooled to form the quality control (QC) samples and they were also prepared in the same way for GC/TOFMS analysis.

3.2.2.2 Chromatographic condition

The GC/TOFMS system (Agilent HP-6890 GC coupled to Waters GCT Premier) was used for the validation of the non-targeted metabolic profiling method. A DB 1MS (30 m x 0.25 mm x 0.25 μ m, Agilent J&W Scientific Folsom, CA, U.S.A.) chemically bonded column with 100% dimethylpolysiloxane cross-linked stationary phase was used. The carrier gas was helium with the flow rate of 1.0 mL/min and the injector was operated in the splitless mode. The injector and source temperatures were set at 250⁰C. The oven temperature was kept at 70⁰C for 0.20 min and increased at 20⁰C/min to 300⁰C where it remained for 5 min. The mass spectrometer was operated in EI mode (70 eV). Data acquisition was performed in full scan mode from m/z 50 to 600 with scan time of 0.9 sec.

3.2.2.3 Chemometrics analysis

RT correction of peaks was performed using the WATERS MarkerLynx™ software with respect to caffeine as ISTD. The total area normalized for each sample was performed by dividing the area of each peak by the area of the ISTD. The normalization aided in correcting variations due to sample preparation and analysis.

All processed data were mean centred and univariate (UV) scaled during chemometric data analysis. Normalised samples were exported to SIMCA-P (Version 12.0, Umetrics, Umea, Sweden) to perform principal component analysis (PCA). PCA is an unsupervised multivariate data analysis technique that was used to observe grouping trends and outliers in the data. After PCA analysis, the data was subjected to a supervised partial least-squares discriminant analysis (PLS-DA) followed by orthogonal partial least-squares discriminant analysis (OPLS-DA). This model was used to identify marker metabolites to differentiate the different genders of horses. The Q^2 value is the predictive ability of the model and R^2X value determines the overall correlation.

Permutation test with 100 iterations were performed using SIMCA-P software to investigate the predictability of the PLS-DA plot.

CHAPTER 4

RESULTS AND DISCUSSION

4.1 Targeted approach

4.1.1 Results of metabolite identification studies

4.1.1.1 Ethylestrenol

Ethylestrenol was detected at 5.28 min in assays containing HrLM with and without cofactors (Figure 10A-D). As expected, the parent drug was absent in the controls without substrate (Figure 10E-F). This confirmed the selectivity of our method in detecting ethylestrenol. The HrLM mixtures were compared with the standards (Figure 11A-D) and found to match the retention times (RT) of norethandrolone (RT = 7.31 min) and ethylestrenol (RT = 5.29 min) respectively (Figure 11A and D). The peak (*) at 6.47 min was clearly absent in the 0 min incubation sample (Figure 11E) demonstrating that the compound was generated during incubation (Figure 11F). A closer look at the time range from 5.80 to 7.50 min, revealed that the RT for neither 17α -ethyl- 5β -estrane- $3\alpha,17\beta$ -diol (Figure 12A) nor 17α -ethyl- 5α -estrane- $3\alpha,17\beta$ -diol (Figure 12B) standards matched the peak (*) at 6.47 min in the 60 min HrLM assay (Figure 12C). When the mass spectra of 17α -ethyl- 5α -estrane- $3\alpha,17\beta$ -diol and 17α -

ethyl-5 β -estrane-3 α ,17 β -diol standards (Figure 13A and B) were compared with the unknown peak at 6.47 min (Figure 13C), the former standard mass spectrum (Figure 13A) matched better with the unknown peak mass spectrum (Figure 13C). The spectra of 17 α -ethyl-5 α -estrane-3 α ,17 β -diol and 17 α -ethyl-5 β -estrane-3 α ,17 β -diol differed by the presence of the ion at m/z 331 in the latter and absence in the former standard (Figure 13A and B). The absence of this ion in both the spectra of 17 α -ethyl-5 α -estrane-3 α ,17 β -diol and the unknown metabolite detected in HrLM (Figure 13A and C) further confirmed the similarity of their spectra. This indicated that the unknown metabolite (*) at 6.47 min was potentially generated via metabolism of ethylestrenol by the HrLM as it shares the same chemical backbones as the other known metabolites of ethylestrenol.

The chromatograms indicated the RT of the putative chemically-synthesized 17 α -ethyl-5 β -estrane-3 β ,17 β -diol and 17 α -ethyl-5 α -estrane-3 β ,17 β -diol standards were 6.12 and 6.35 min, respectively (Figure 14A and B). The RT of the 5 α -isomer was closer to the unknown peak of interest in the HrLM (Figure 14C). The mass spectrum of the chemically-synthesised 17 α -ethyl-5 α -estrane-3 β ,17 β -diol (Figure 15A) was a better match to the unknown compound (Figure 15 B).

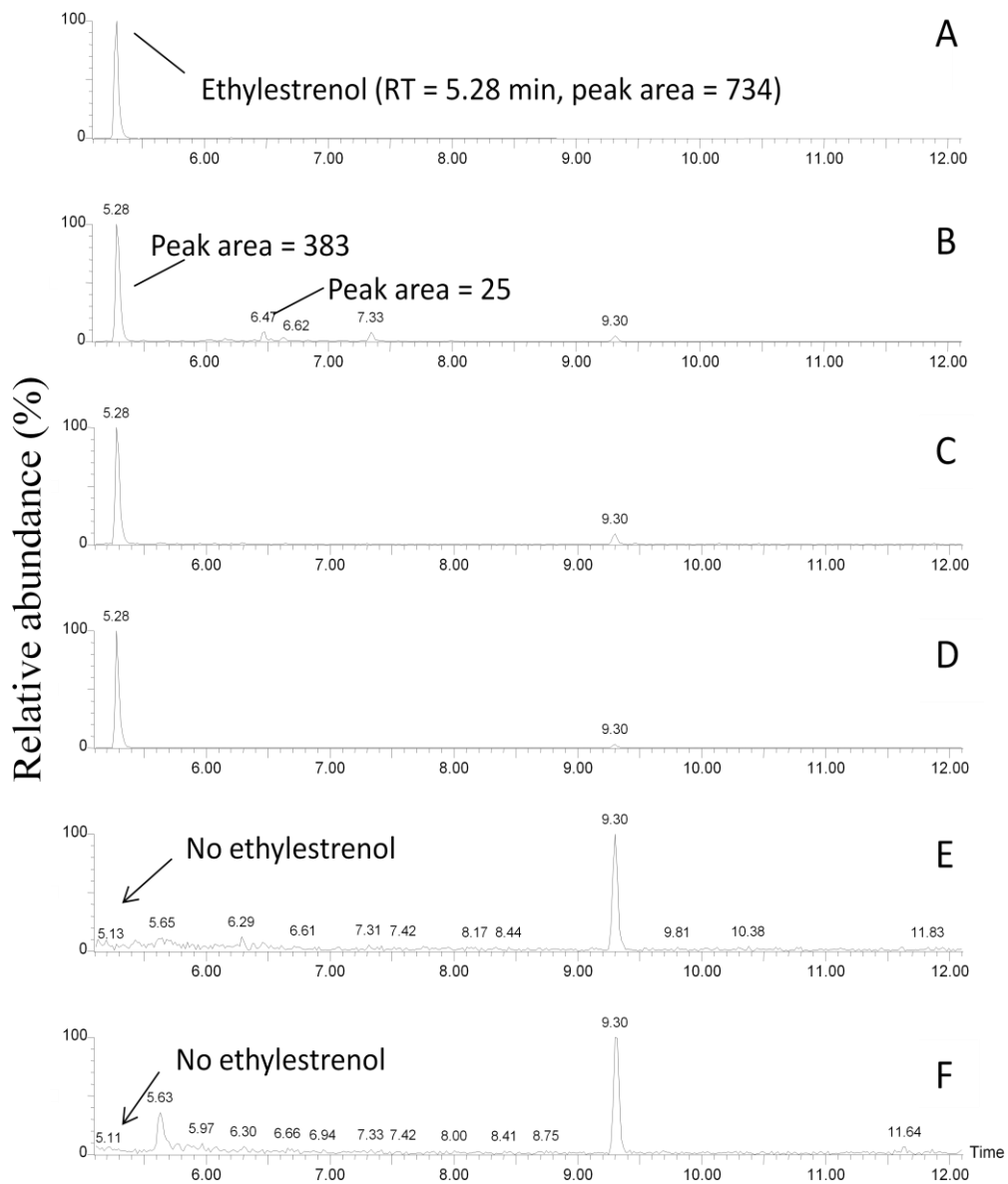


Figure 10: Chromatograms of ethylestrenol incubated with (A) HrLM at 0 min, (B) HrLM at 60 min, (C) HrLM mixture without cofactor at 0 min, (D) HrLM mixture without cofactor at 60 min, (E) HrLM mixture without substrate at 0 min and (F) HrLM mixture without substrate at 60 min. The analytes were derivatized with their respective derivatizing agents.

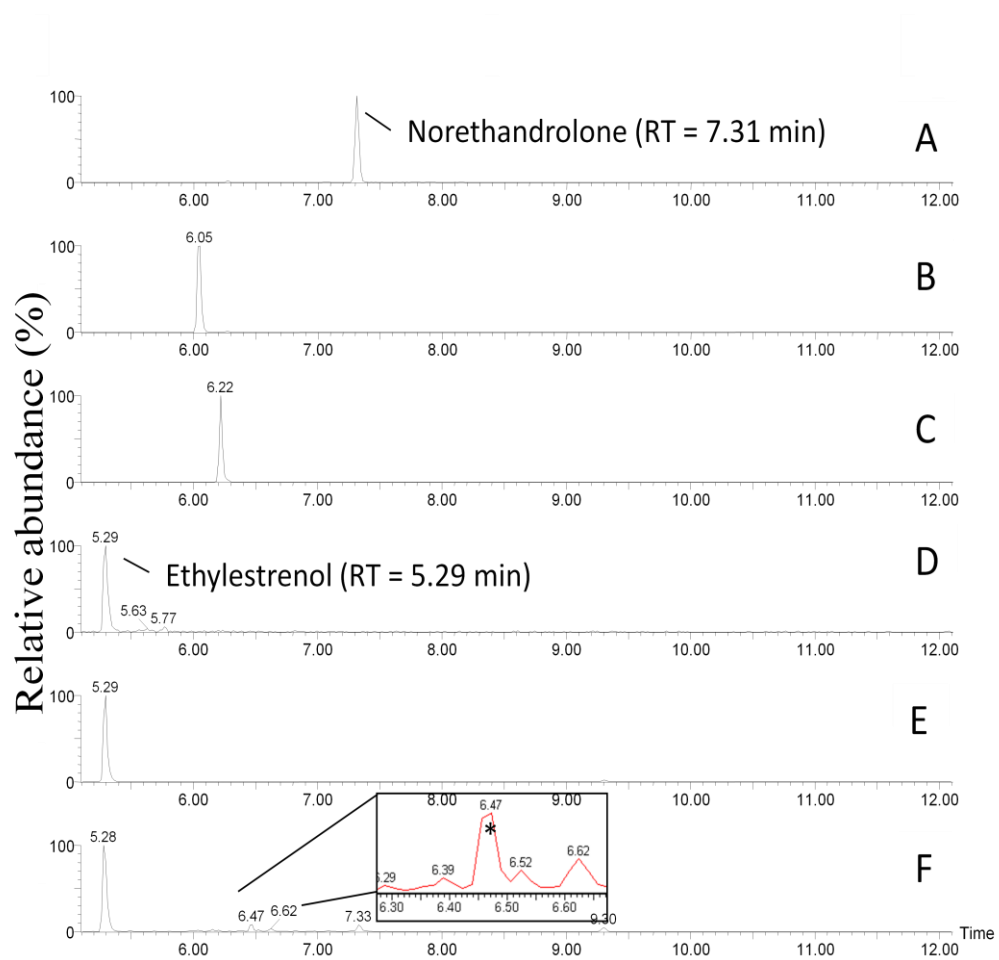


Figure 11: Chromatograms of standards and HrLM mixture. (A) norethandrolone standard (B) 17α -ethyl- 5α -estrane- 3α , 17β -diol standard (C) 17α -ethyl- 5β -estrane- 3α , 17β -diol standard (D) ethylestrenol standard (E) HrLM mixture at 0 min and (F) HrLM mixture at 60 min. The analytes were derivatized with their respective derivatizing agents.

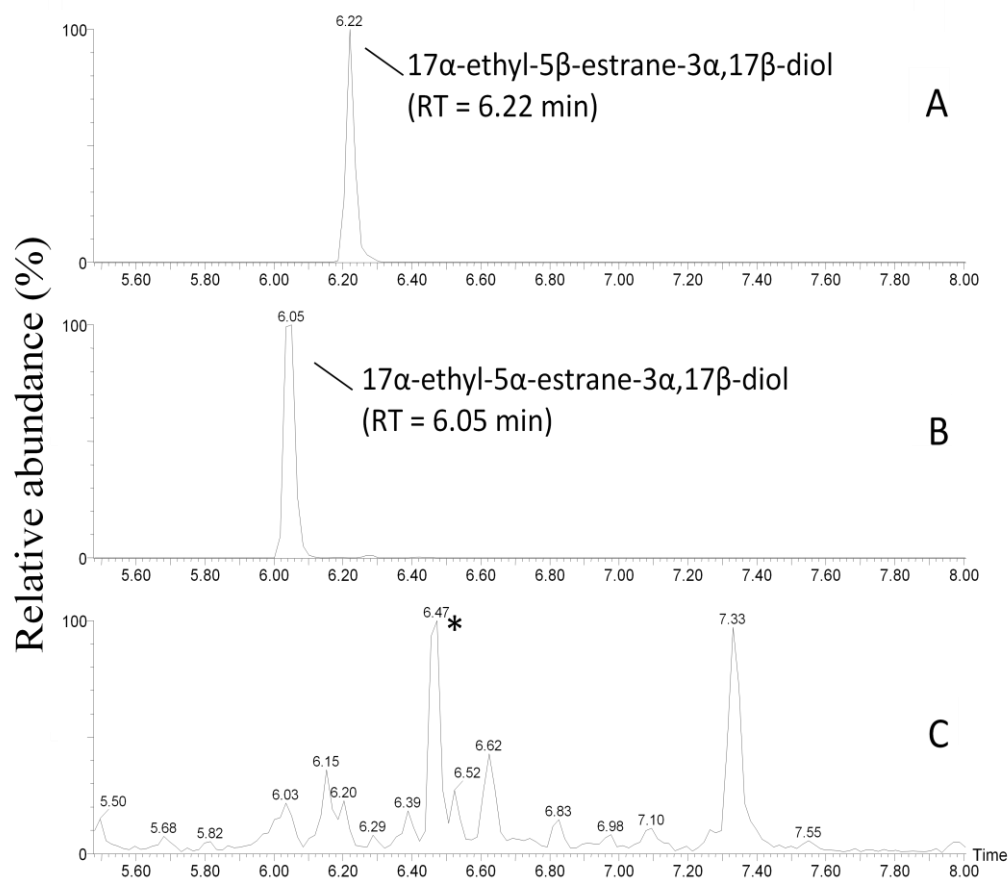


Figure 12: Chromatograms of standards and HrLM mixture. (A) 17 α -ethyl-5 β -estrane-3 α ,17 β -diol standard, (B) 17 α -ethyl-5 α -estrane-3 α ,17 β -diol standard and (C) HrLM mixture at 60 min. The analytes were derivatized with their respective derivatizing agents.

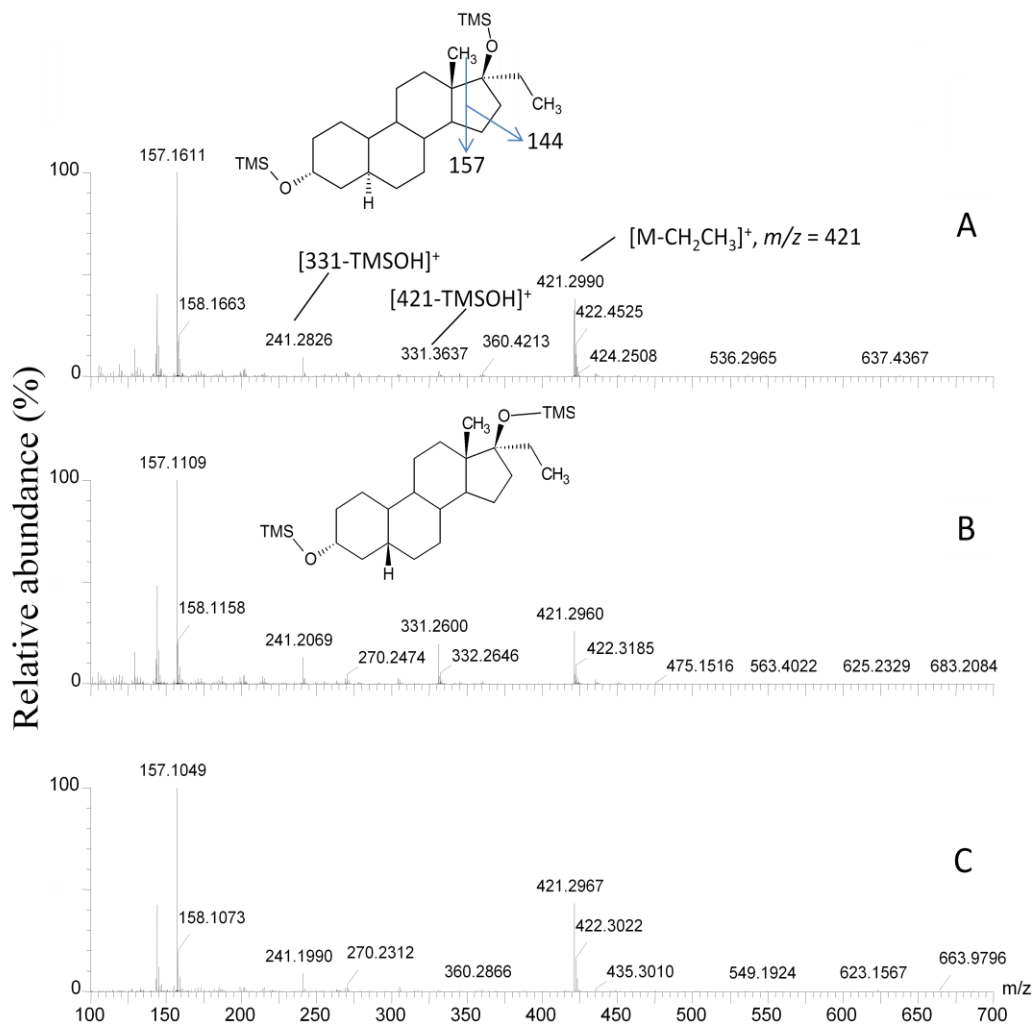


Figure 13: Mass spectra of (A) 17 α -ethyl-5 α -estrane-3 α ,17 β -diol standard (B) 17 α -ethyl-5 β -estrane-3 α ,17 β -diol standard and (C) unknown metabolite (peak at 6.47 min) in HrLM mixture at 60 min.

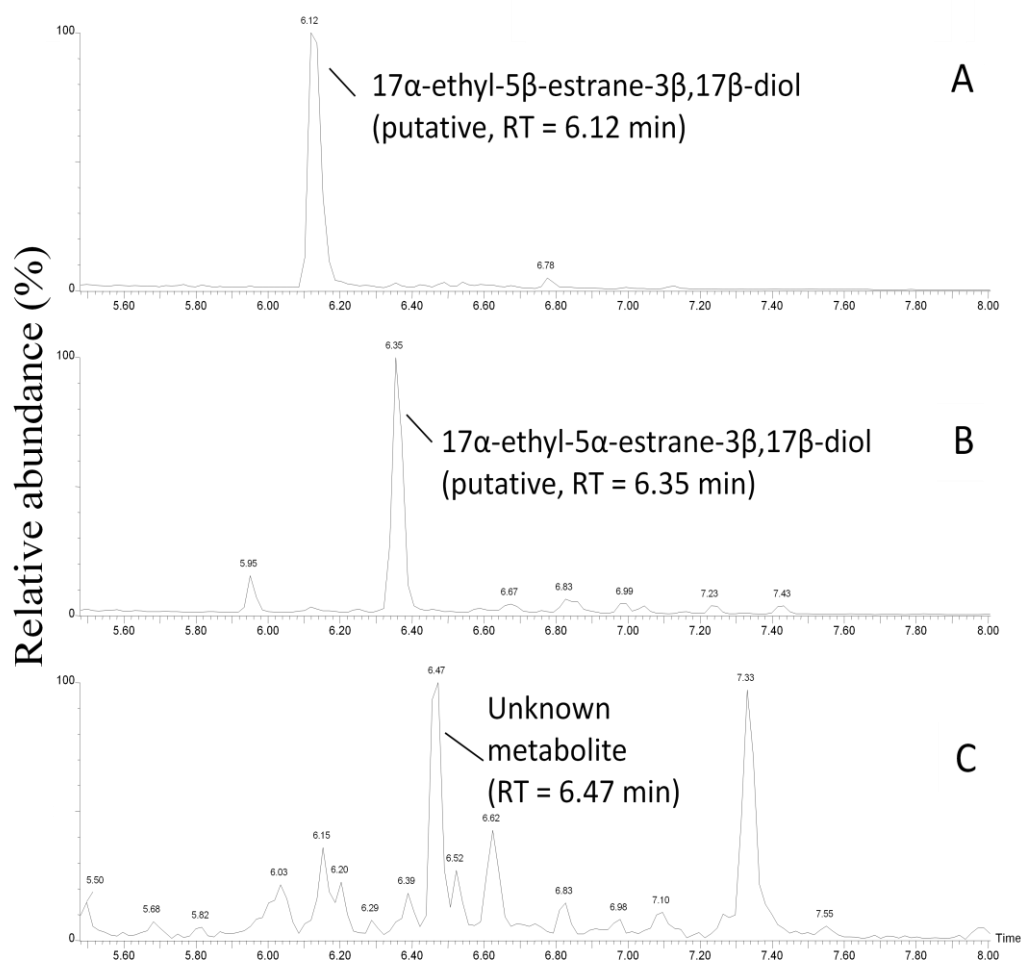


Figure 14: Chromatograms of HrLM mixture with synthesized standards. (A) 17 α -ethyl-5 β -estrane-3 β ,17 β -diol (putative) standard (B) 17 α -ethyl-5 α -estrane-3 β ,17 β -diol (putative) standard and (C) unknown metabolite (peak at 6.47 min) in HrLM mixture at 60 min. The analytes were derivatized with their respective derivatizing agents.

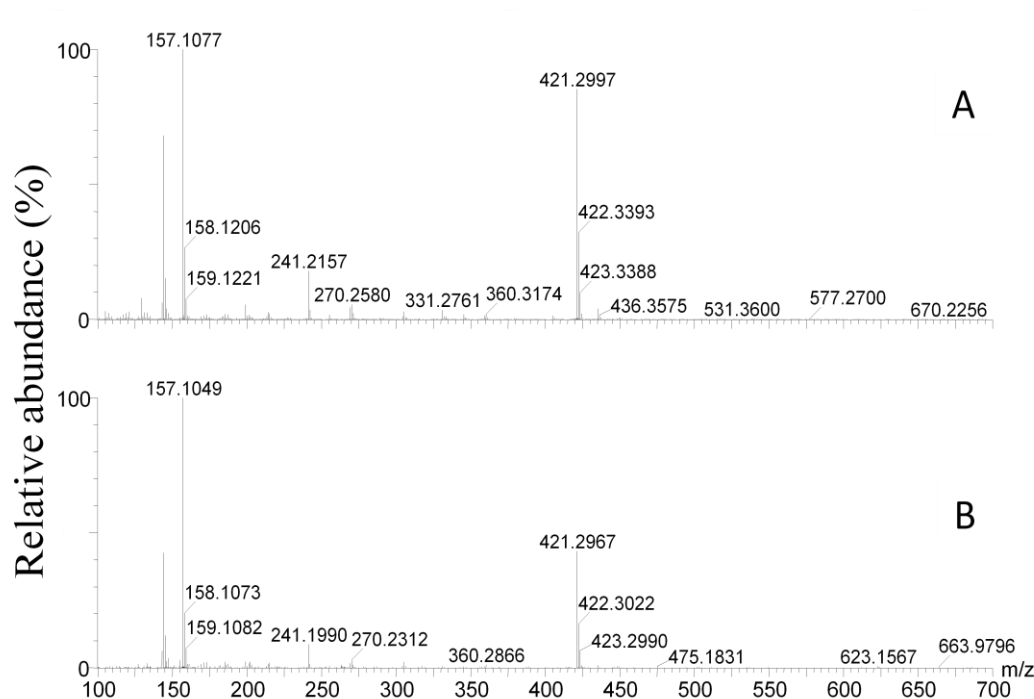


Figure 15: Mass spectra of (A) 17α -ethyl- 5α -estrane- 3β , 17β -diol (putative) standard and (B) unknown metabolite (peak at 6.47 min) in HrLM mixture at 60 min.

4.1.1.2 Ecdysone

The metabolism of ecdysone had been well characterized in *Pieris* larvae (Figure 16) [65]. 20-hydroxy ecdysone and ecdysone standards were detected at RT 21.96 and 19.25 min, respectively (Figure 17A and B). The parent drug, ecdysone, was detected in the HrLM assays in the presence and absence of cofactors (Figure 17C-F). On the other hand, the parent drug was absent in the negative controls (Figure 17G-H). The RT of the parent drug matched that of the ecdysone standard (RT = 19.25 min, Figure 17B). In HrLM, the major

metabolite of ecdysone, 20-hydroxy ecdysone (RT = 21.96 min, Figure 17A) was absent (Figure 17D). Furthermore, the intensity of the parent drug was found to be consistent throughout the 60 min incubation period (Figure 17C-D).

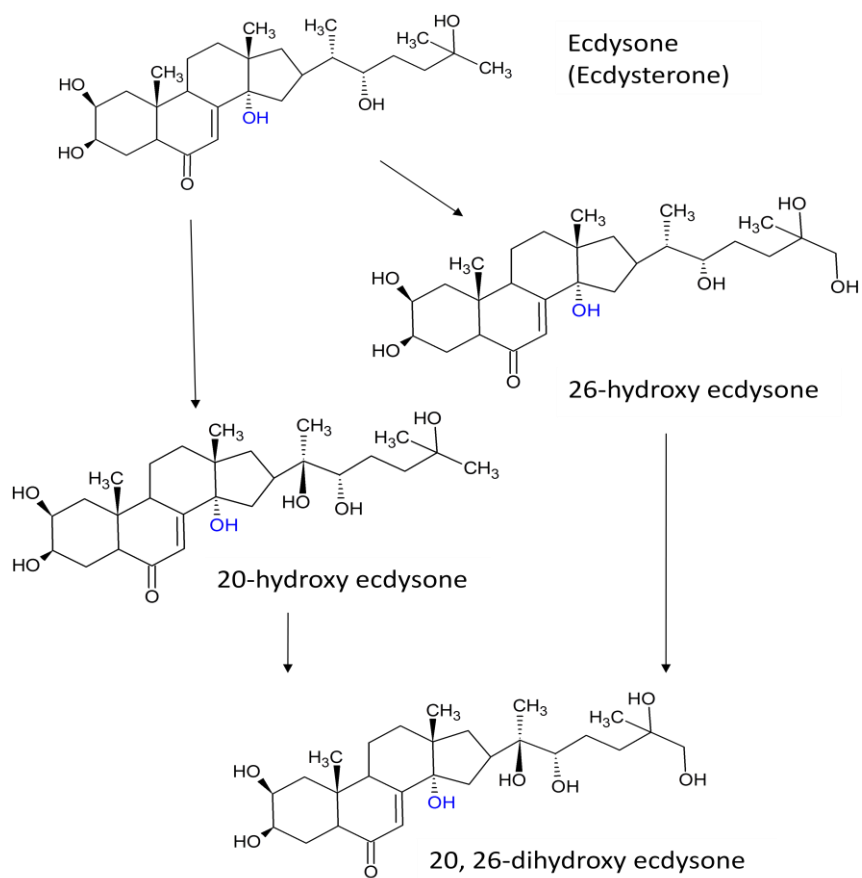


Figure 16: Ecdysone and its metabolites in *Pieris* larvae.

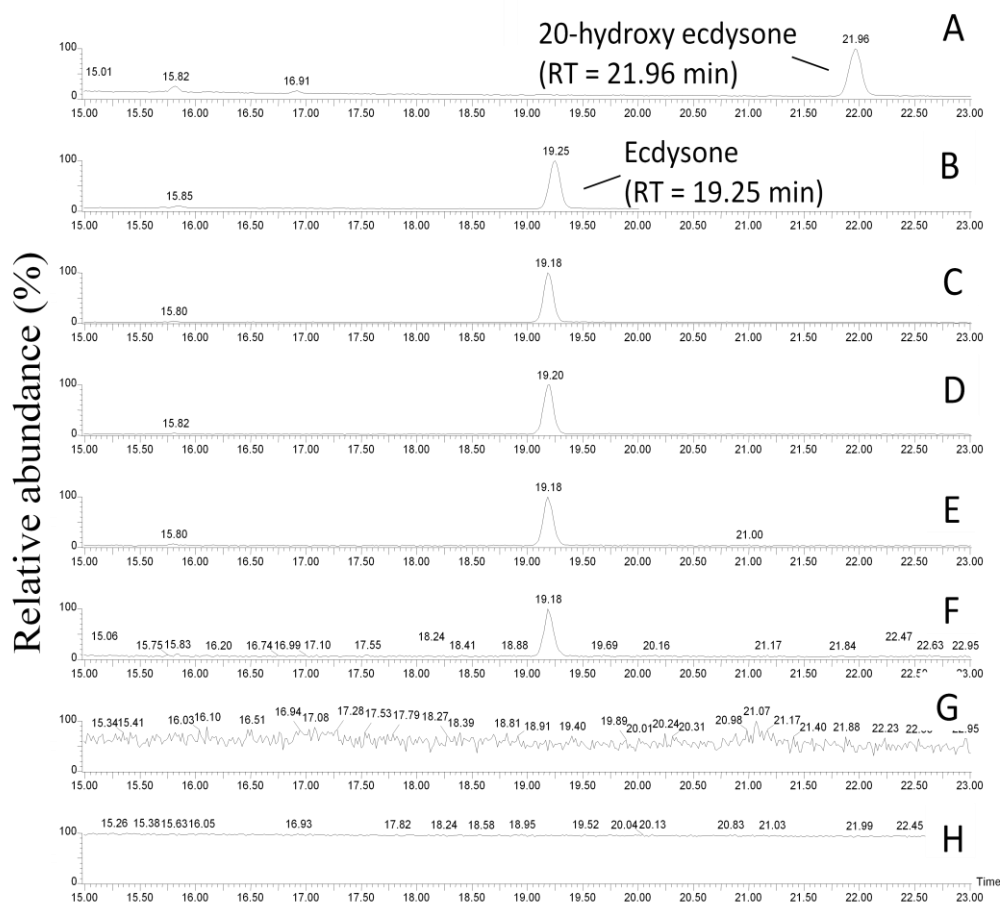


Figure 17: Chromatograms of (A) 20-hydroxy ecdysone standard, (B) ecdysone standard, (C) HrLM mixture at 0 min, (D) HrLM mixture at 60 min, (E) HrLM mixture without cofactor at 0 min, (F) HrLM mixture without cofactor at 60 min, (G) HrLM mixture without substrate at 0 min and (H) HrLM mixture without substrate at 60 min. The analytes were derivatized with their respective derivatizing agents.

The fragmentation pattern of derivatized ecdysone standard (Figure 18A) comprised product ions at m/z 131 and 171 that corresponded to mass losses from the C_{17} side chain. The molecular ion of the fully silylated ecdysone (M^+ , m/z 824) was absent in the mass spectrum but the ion m/z 567 is characteristic

of a fully silylated ecdysone [66]. Figure 18B shows the mass spectrum of ecdysone as detected in the HrLM mixture at 60 min.

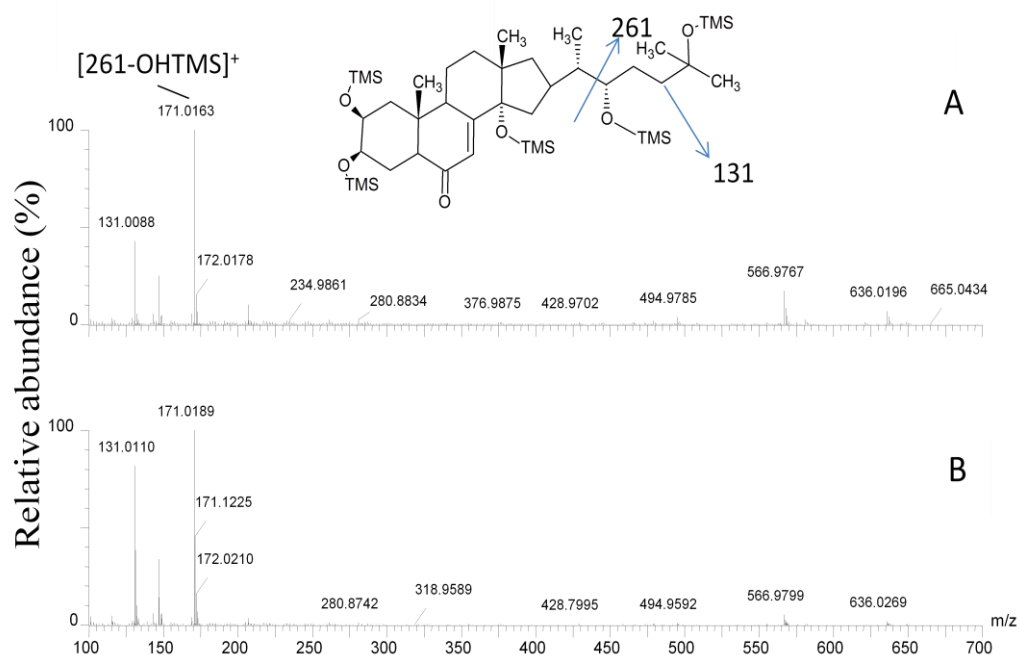
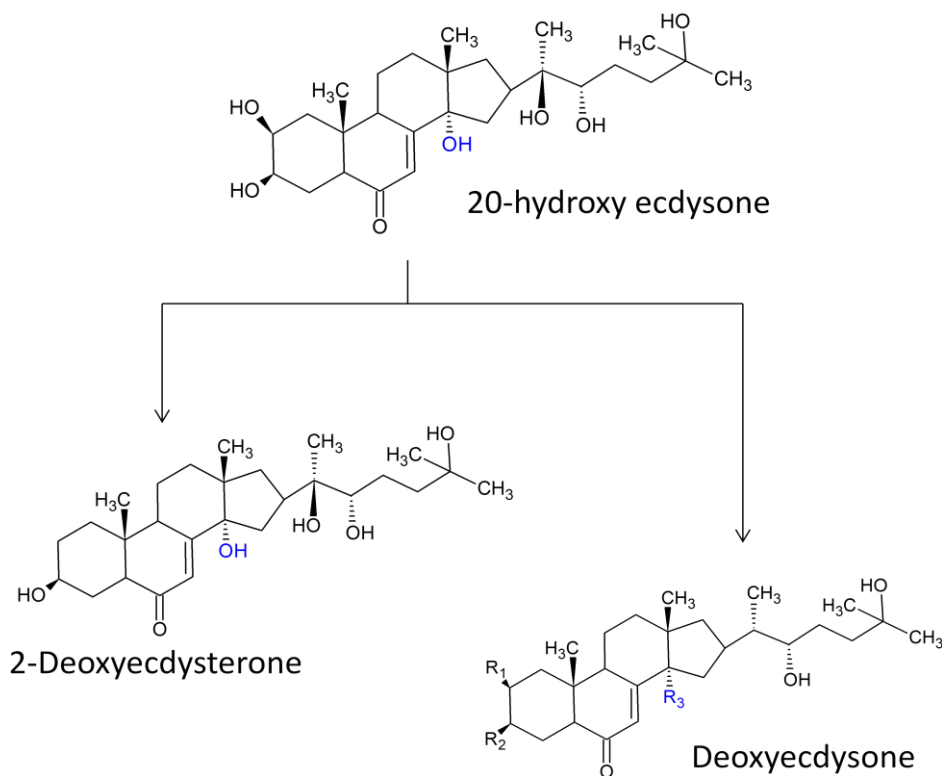


Figure 18: Mass spectra of (A) derivatized ecdysone standard and (B) derivatized ecdysone (peak at 19.20 min) in HrLM mixture at 60 min.

4.1.1.3 20-hydroxy ecdysone

The metabolites of 20-hydroxy ecdysone in humans were reported to be 2-deoxyecdysterone and deoxyecdysone (Figure 19) [24].



where $R_1=R_2=OH$, $R_3=H$ or $R_1=R_3=OH$, $R_2=H$ or $R_2=R_3=OH$, $R_1=H$

Figure 19: 20-hydroxy ecdysone and its metabolites in humans.

20-hydroxy ecdysone standard was detected at RT 21.96 min (Figure 20A). The parent drug was detected in the HrLM mixtures with and without cofactor (Figure 20B-E). As expected, 20-hydroxy ecdysone was absent in the negative controls (Figure 20F-G). The RT of the parent drug, 20-hydroxy ecdysone, matched with the standard (RT = 21.96 min, Figure 20A). The intensity of the parent drug was consistent throughout the 60 min incubation period (Figure 20B and C).

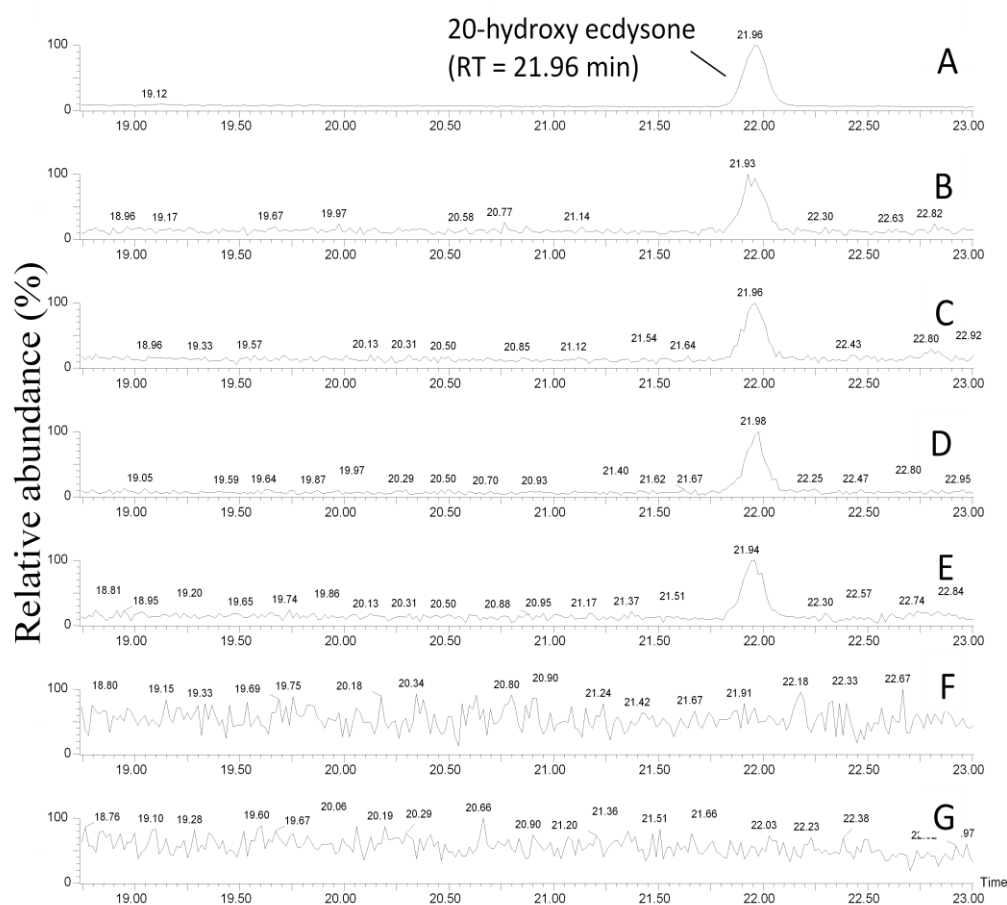


Figure 20: Chromatograms of (A) 20-hydroxy ecdysone standard, (B) HrLM mixture at 0 min, (C) HrLM mixture at 60 min, (D) HrLM mixture without cofactor at 0 min, (E) HrLM mixture without cofactor at 60 min, (F) HrLM mixture without substrate at 0 min and (G) HrLM mixture without substrate at 60 min. The analytes were derivatized with their respective derivatizing agents.

20-Hydroxy ecdysone also needs long reaction times similar to ecdysone for GC/MS analysis. The fragmentation pattern (Figure 21) is also similar to ecdysone with product ions detected at m/z 131, 147 and 171. The ion m/z 561 arises from cleavage of the side chain between C_{20} and C_{22} followed by the loss of 90 Da which corresponds to $(CH_3)_3SiOH$ (Figure 21A and B). The m/z

ion at 561 has been previously reported to be a suitable screening ion [24]. Standards of 2-deoxyecdysterone and deoxyecdysone are not available commercially.

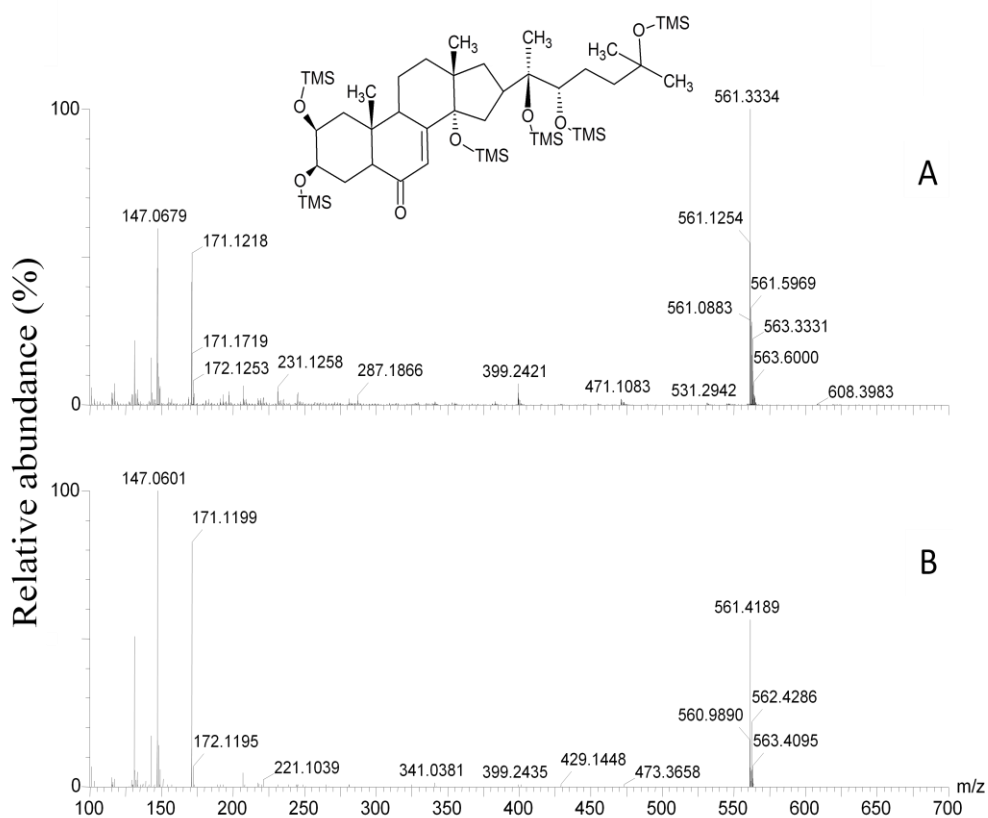


Figure 21: Mass spectra of (A) 20-hydroxy ecdysone standard and (B) parent drug (peak at 21.96 min) in HrLM mixture at 60 min.

4.1.1.4 Metribolone

There is no reported metabolite of metribolone [67]. The RT of metribolone standard was 6.98 min (Figure 22A). The parent drug, metribolone, was detected in the HrLM mixture in the presence and absence of cofactors (Figure 22B-E). The RT of the parent drug in the HrLM mixtures matched the RT of metribolone standard (RT = 6.98 min, Figure 22A). The parent drug was not detected in the negative controls (Figure 22F-G). In the 60 min HrLM incubation mixture, the peak intensity of the parent drug decreased significantly over time indicating that the metabolism of metribolone had taken place (Figure 22B-C).

A closer look of the chromatogram showed that metribolone had been metabolized within the 60 min incubation period (Figure 23B-C). In the 0 min HrLM incubation mixture, metribolone peak area was 880 units whereas after 60 min, the peak area decreased significantly to 97 units. The mass spectrum of the 60 min HrLM mixture also suggested the presence of the parent drug (Figure 24). The ion at m/z 385 is characteristic of a fully silylated metribolone.

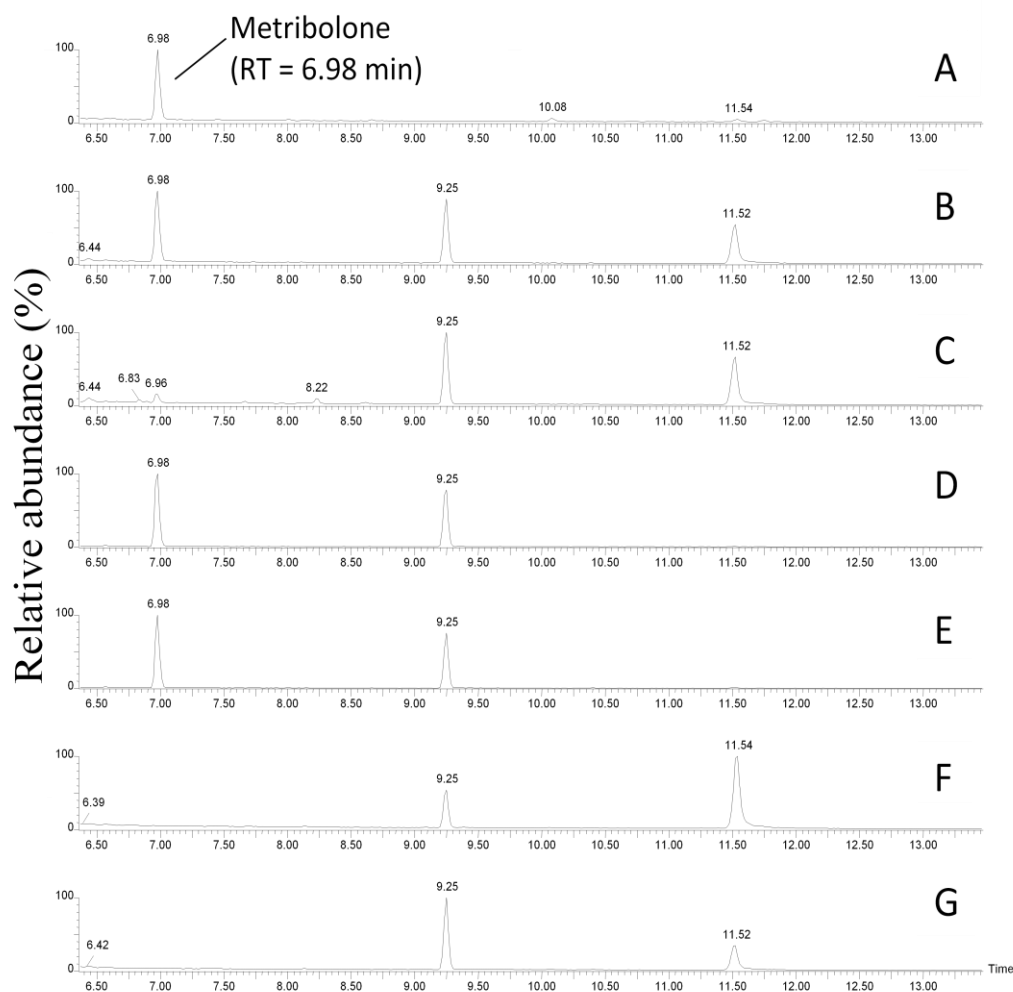


Figure 22: Chromatograms of (A) metribolone standard, (B) HrLM mixture at 0 min, (C) HrLM mixture at 60 min, (D) HrLM mixture without cofactor at 0 min, (E) HrLM mixture without cofactor at 60 min, (F) HrLM mixture without substrate at 0 min and (G) HrLM mixture without substrate at 60 min. The analytes were derivatized with their respective derivatizing agents.

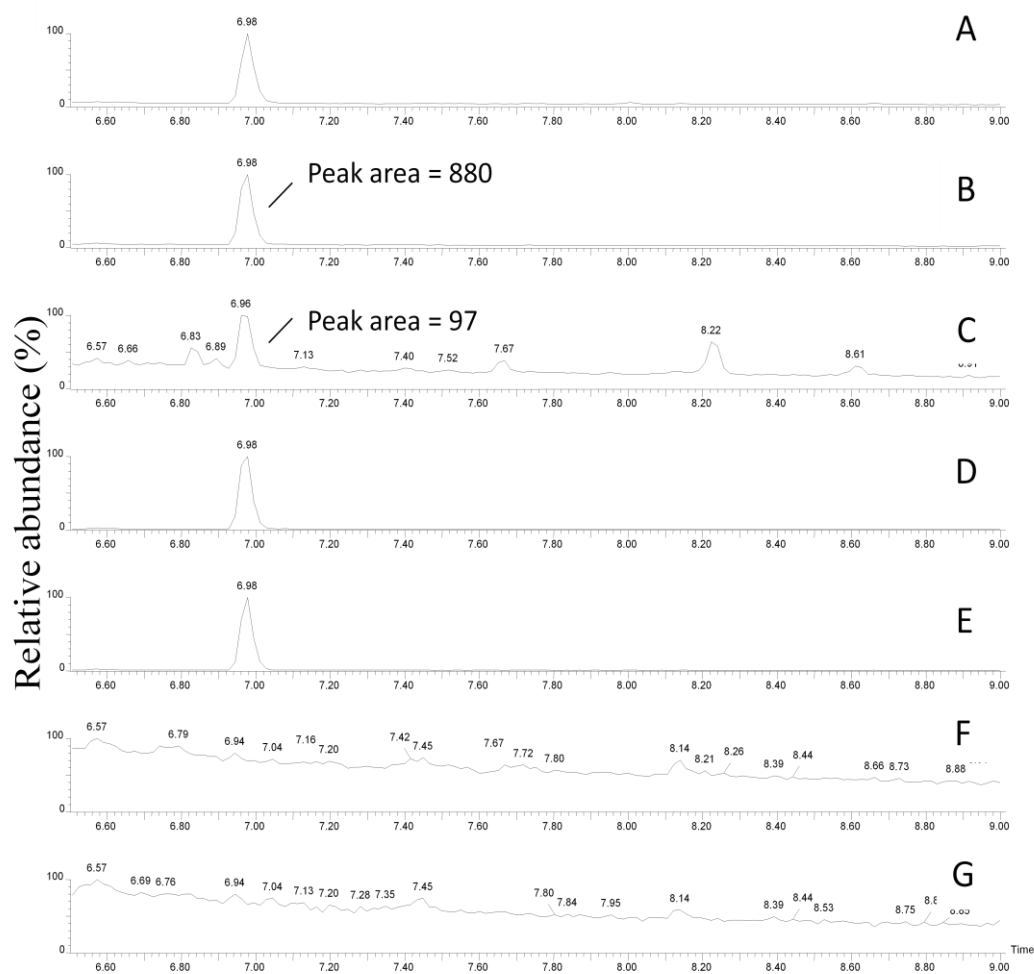


Figure 23: Expanded view of the chromatograms (A) metribolone standard, (B) HrLM mixture at 0 min, (C) HrLM mixture at 60 min, (D) HrLM mixture without cofactor at 0 min, (E) HrLM mixture without cofactor at 60 min, (F) HrLM mixture without substrate at 0 min and (G) HrLM mixture without substrate at 60 min.

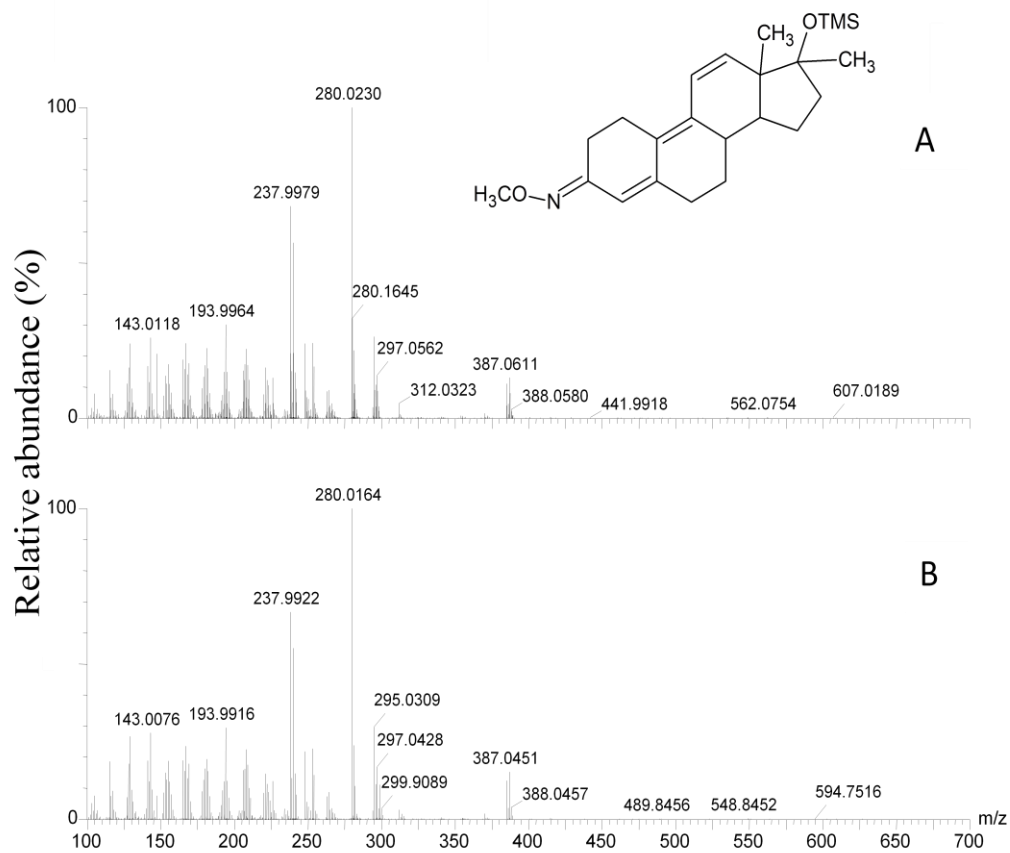


Figure 24: Mass spectra of (A) metribolone and (B) parent drug (peak at 6.98 min) in HrLM mixture at 60 min.

The 60 min HrLM mixture was further analyzed for possible metabolites using the Thermo Orbitrap. It was observed from the data that there were multiple possible metabolites. Due to the poor intensities of most of the peaks, only the peak of highest intensity was further investigated (Figure 25).

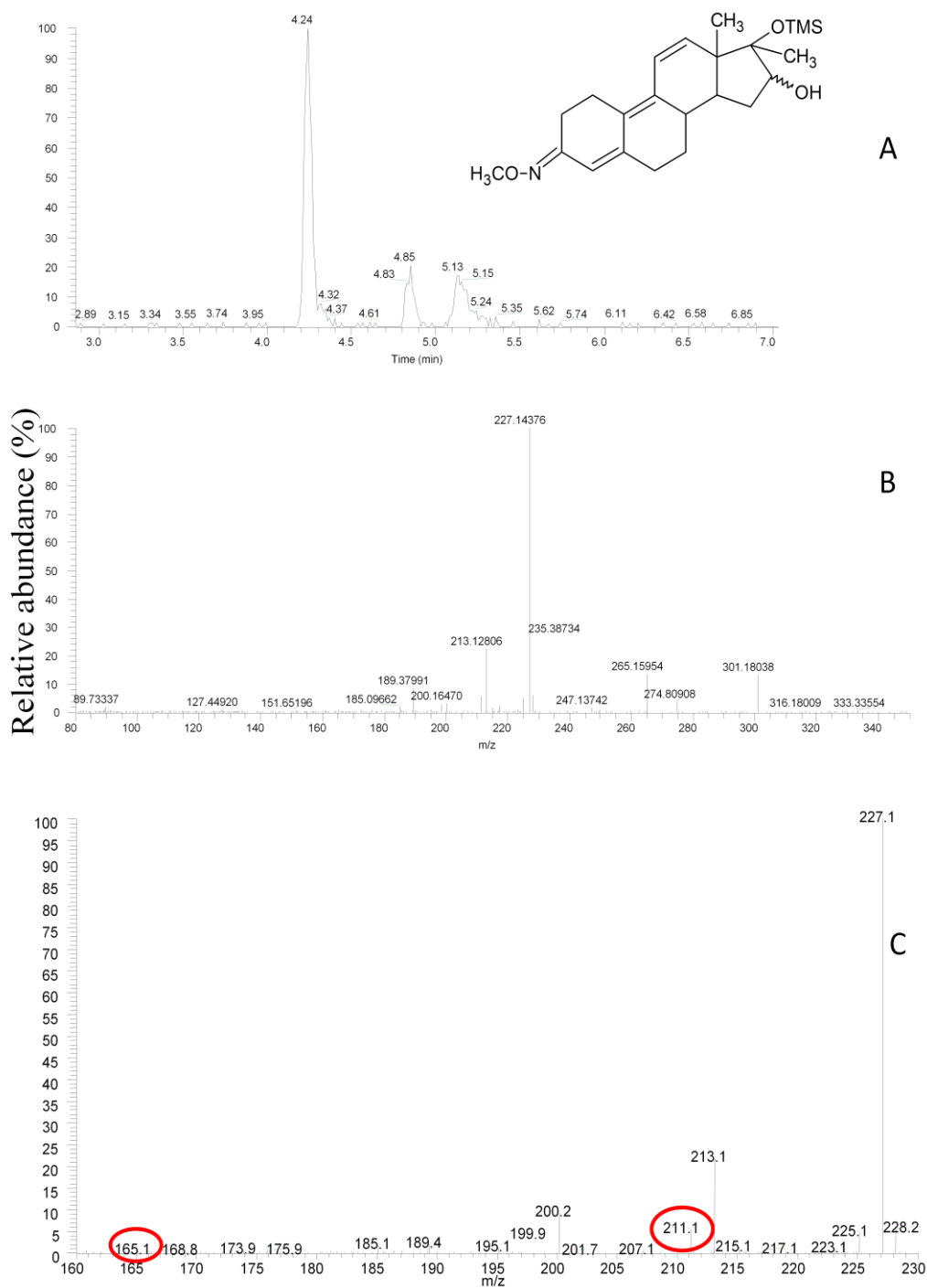


Figure 25: (A) Chromatogram of possible metribolone metabolites (B) mass spectrum of unknown compound at RT 4.24 min and (C) expanded mass spectrum (m/z 160 to 230) of unknown compound at RT 4.24 min. The analytes were derivatized with their respective derivatizing agents.

The unknown compound at RT 4.24 min has the highest intensity compared to the rest of the analytes at 4.85 min and 5.13 min, respectively (Figure 25A). The m/z of 227 ion was extracted from the chromatogram as it was diagnostic of the 4,9,11- triene structure (Figure 25B). Similarly, the ions at m/z 165.2 and 211.1 are diagnostic of the 4,9,11-triene family (Figure 25C) [68].

	Formula	Calculated mass (amu)	Experimental mass (amu)	Mass Error (ppm)
Metribolone	$C_{19}H_{24}O_2$	285.18491	285.18546	1.9
16-hydroxy metribolone	$C_{19}H_{24}O_3$	301.17982	301.18030	1.6

Table 2: Accurate mass measurement of metribolone and metabolite B, 16-hydroxy metribolone

The elemental compositions of the postulated metabolite B was further confirmed using accurate mass measurement. The comparison of the experimental masses with the calculated values is summarized in Table 1.

4.1.2 Results of metabolic stability studies

4.1.2.1 Testosterone (positive control)

Testosterone was chosen as positive control for both Phase I and II metabolic stability experiments to validate the enzymatic activity of HrLM and the suitability of the assay. In experiments conducted with Phase I cofactors, NADPH, the metabolic half-life was calculated to be 0.43 min. The elimination rate constant, K , was calculated to be 1.60 min^{-1} . The percentage of testosterone in the control remained consistent throughout the 5 min incubation period while it decreased gradually in the HrLM mixture (Figure 26).

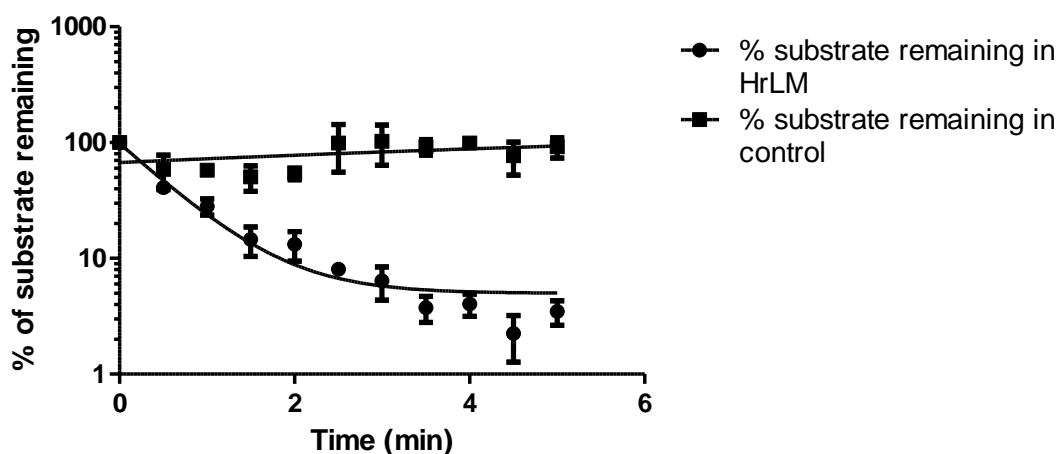


Figure 26: Phase I metabolic profile of testosterone (positive control).

In Phase II metabolic stability experiments with UGT as cofactors, the half-life of testosterone was calculated to be 9.10 min. The elimination rate constant was calculated to be 0.077 min^{-1} , suggesting that conjugation metabolism had taken place (Figure 27).

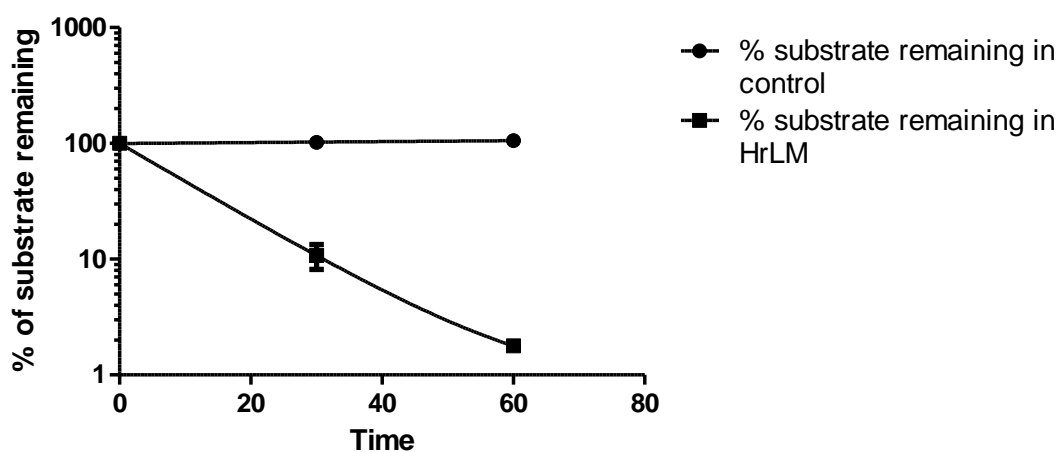


Figure 27: Phase II metabolic profile of testosterone (positive control).

4.1.2.2 Ethylestrenol

Ethylestrenol was not functionally amenable for ionisation via LC/MS/MS as it did not have any ionisable sites. Therefore metabolic stability assay was not performed for ethylestrenol using the LC/MS/MS.

4.1.2.3 Ecdysone

Ecdysone metabolic stability samples were analyzed in triplicates. The results showed that ecdysone was metabolically stable over the 60 min incubation period (Figure 28). Increasing trends were observed for both the controls and HrLM samples. The reasons of the increasing trends were unknown but they were reproducible when the experiments were repeated. The percentage substrate remaining was above 100% over the 60 min incubation **period**. This was consistent with the metabolite identification studies where metabolite of the parent drug was also not observed. Further experiments with UGT were carried out to evaluate the potential Phase II metabolism of ecdysone.

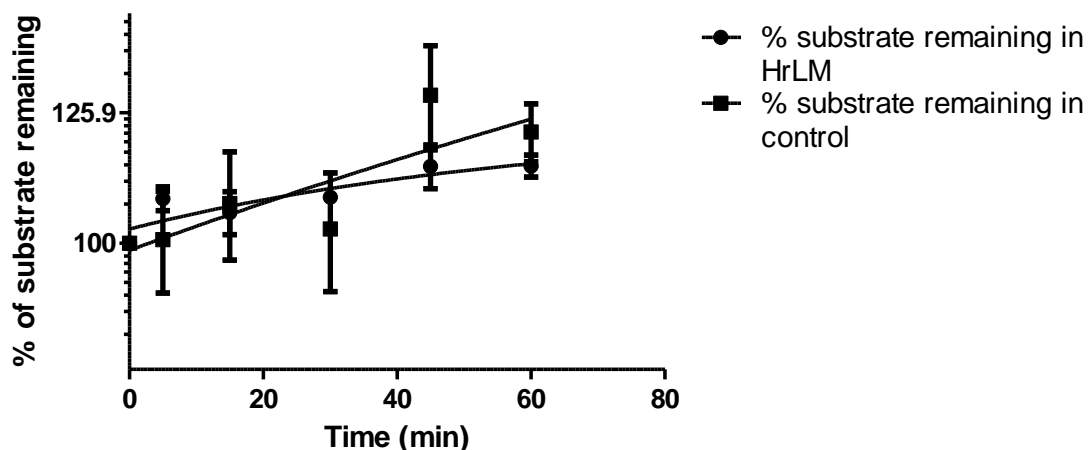


Figure 28: Phase I metabolic stability profile of ecdysone.

Ecdysone was also found to be metabolically stable in the Phase II UGT metabolism assays (Figure 29). The profile was found to be similar to the Phase I metabolic stability profile. Increasing trends in terms of percentage

substrate remaining were also observed in both control and HrLM assays. While the trend was reproducible, the reason accounting for it remained unknown.

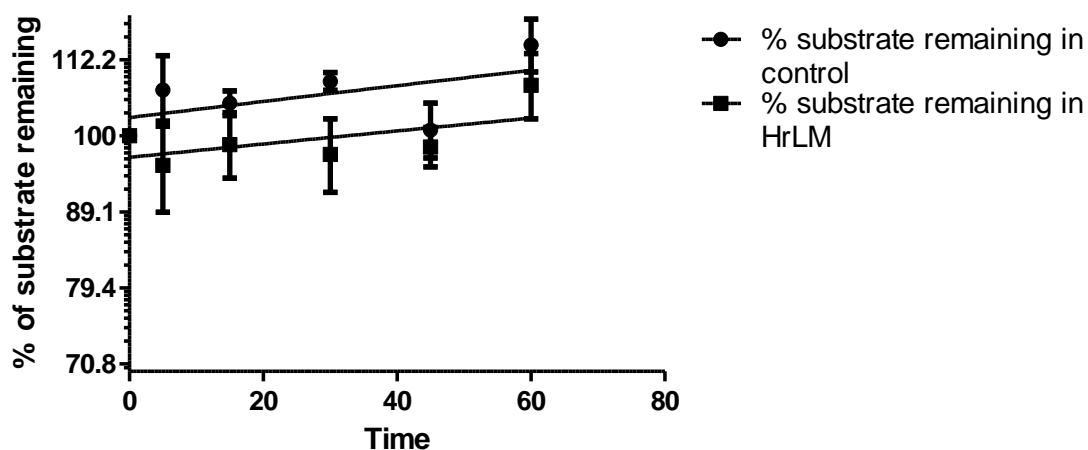


Figure 29: Phase II metabolic stability profile of ecdysone.

4.1.2.4 20-Hydroxy ecdysone

Metabolic stability assay samples of 20-hydroxy ecdysone demonstrated first order metabolic degradation profile (Figure 30). Although the substrate in the control was increasing over the 60 min incubation period, the substrate in the HrLM mixture was decreasing over time. This suggested that 20-hydroxy ecdysone underwent metabolism. The elimination rate constant, K , and half-life were calculated to be $2.2 \times 10^{-7} \text{ min}^{-1}$ and $3.2 \times 10^6 \text{ min}$, respectively. This was inconsistent with the metabolite identification results where metabolite of 20-hydroxy ecdysone was not observed. Therefore, further experiments to

evaluate Phase II metabolism of 20-hydroxy ecdysone via UGT conjugation were carried out.

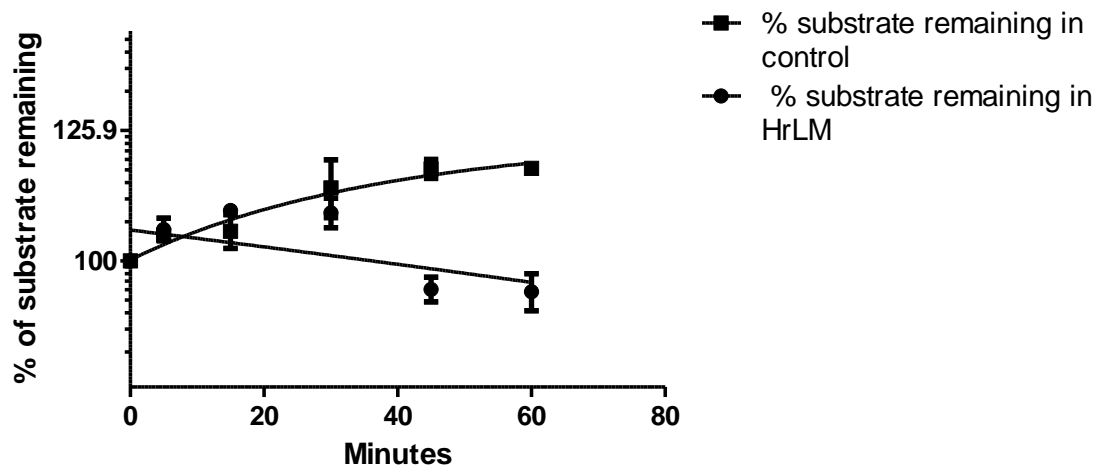


Figure 30: Phase I metabolic stability profile of 20-hydroxy ecdysone.

Phase II experiments demonstrated that 20-hydroxy ecdysone was metabolically stable (Figure 31). The percentage of substrate remaining in the control and HrLM incubation mixtures remained consistent over the 60 min incubation period.

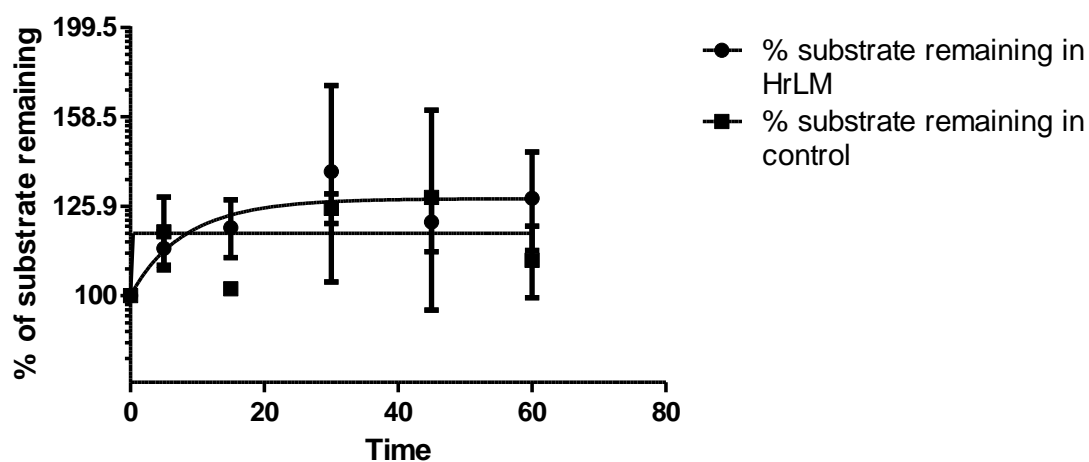


Figure 31: Phase II metabolic stability profile of 20-hydroxy ecdysone.

4.1.2.5 Metribolone

The result of metabolic stability assay of metribolone was consistent with that of its metabolite identification assay. The metabolic stability assay of metribolone demonstrated its first order metabolic degradation profile (Figure 32) [69]. The percentage of substrate remaining in the control was consistent throughout the 60 min incubation. The percentage substrate remaining in the HrLM assay decreased gradually over the 60 min incubation period. The value for K was calculated to be 0.032 min^{-1} . The half-life was calculated to be 21.74 min.

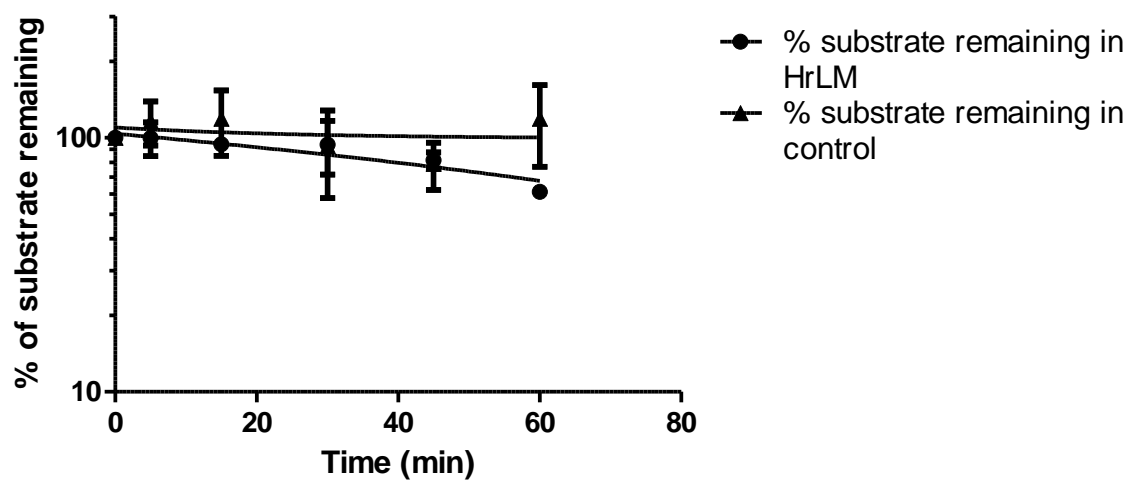


Figure 32: Phase I metabolic stability profile of metribolone.

4.1.3 Discussion

4.1.3.1 Metabolite identification studies

4.1.3.1.1 Ethylestrenol

The metabolites of ethylestrenol postulated in the current study seemed similar to those reported in previous studies (Figure 33) [26].

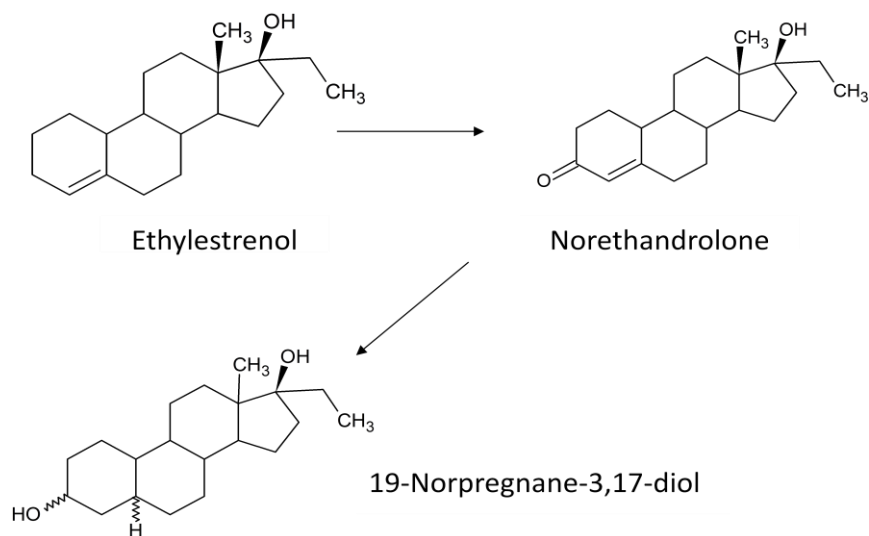


Figure 33: Ethylestrenol and its metabolites [26].

The differences in the ion intensities of ethylestrenol at 0 and 60 min (RT = 5.2 min, Figure 11E and F) and the development of new peaks at 6.47 and 7.33 min after incubation indicated that metabolism of ethylestrenol had taken place. The analyte at RT 7.33 min matched the RT of norethandrolone standard at 7.31 min (Figure 11A and F). The analyte at 6.47 min in the 60 min HrLM incubation mixture could not be identified chromatographically using the standards (17 α -ethyl-5 α -estrane-3 α ,17 β -diol and 17 α -ethyl-5 β -estrane-3 α ,17 β -diol) available in the laboratory (Figure 12). This prompted the further investigation of this unknown metabolite. The mass spectrum of the unknown metabolite was compared subsequently with the mass spectra of the standards to get a better idea of the possible structure of this metabolite (Figure 13).

In Figure 13, the data suggested that the cleavages between C₁₄ and C₁₅, and C₁₃ and C₁₇ produced ion at m/z 157 which is specific to the D-ring fragmentation. The fragmentation of the D-ring with TMS ether at C₁₇ is extensive due to a destabilizing bond between the C₁₃ and C₁₇ [70]. The ions at m/z 157, 144 and 241 corresponded to the loss of TMS and ethyl group from the molecular ion ($m/z = 450$). While the RT of the unknown metabolite did not match putative standards (Figure 14), the spectrum was a closer match to the putative 17 α -ethyl-5 α -estrane-3 β ,17 β -diol standard. It was postulated that the unknown metabolite could be associated with the 5 α -isomer with variations of the hydroxyl group in the C₃ position.

A further attempt was made to identify 19-norpregnane-3,17-diol. Hence, 17 α -ethyl-5 α -estrane-3 α ,17 β -diol and 17 α -ethyl-5 β -estrane-3 α ,17 β -diol were oxidized with pyridinium chlorochromate (PCC) and reduced with tetrahydrofuran (THF) to synthesize a mixture of the corresponding 3 α and 3 β isomers (Figure 34) [61, 62].

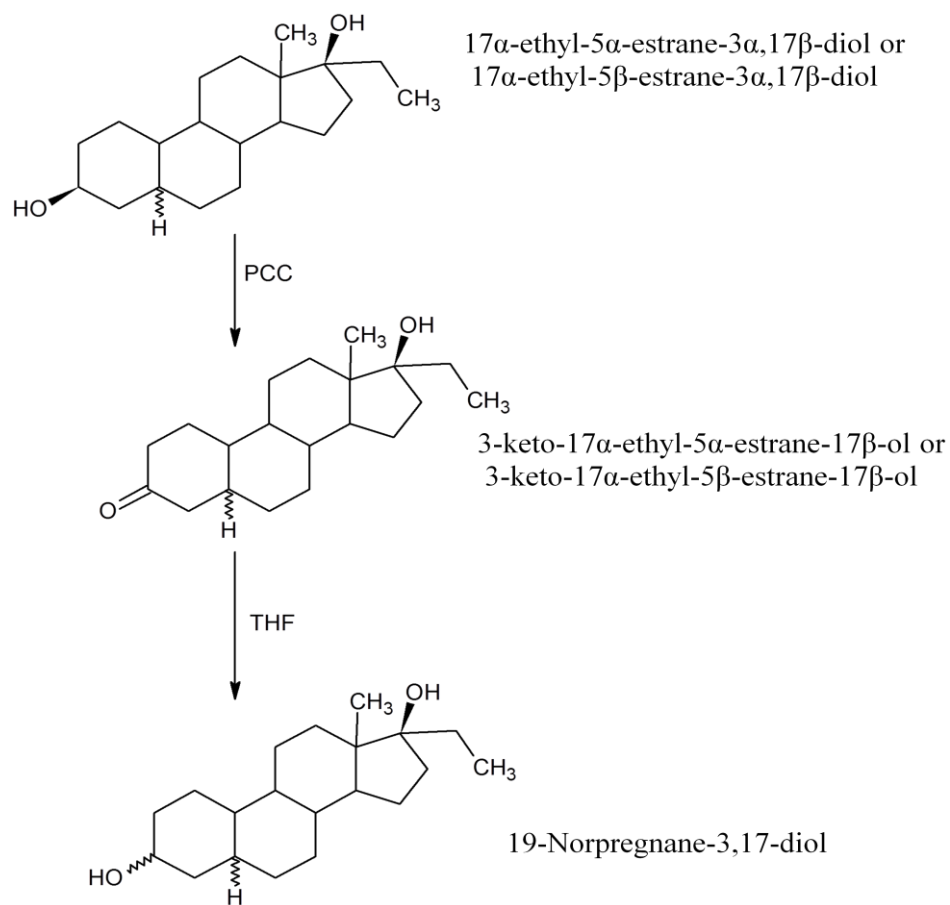


Figure 34: Schematic flow of synthesis.

Since the 3 α -isomers standards did not match the RT of the unknown metabolite (RT = 6.47 min), we proceeded to compare the putative 3 β -isomer standards (Figure 14). The unknown metabolite shared a closer RT with the 5 α ,3 β - isomer standard (RT = 6.35 min) than 5 β ,3 β - isomer standard (RT = 6.12 min). While the mass spectra of the unknown metabolite and the putative 5 α ,3 β - isomer correlated well with each other, we still could not confirm the identity of the unknown metabolite in the current study.

The mass spectrum of the unknown metabolite is comparable to those *in-vitro* studies on cattle and rat (Figure 35) [27, 28]. This shows that horses may metabolize ethylestrenol in a similar way as cattle and rat. As the synthesized standard was not adopted in the previous studies, our current results provided a better understanding of the possible structure of the metabolite.

4.1.3.1.2 Ecdysone and 20-hydroxy ecdysone

The analysis of ecdysteroids in GC-MS was problematic due to their complex structures. Long derivatisation times were required (24 h) as the C₁₄ and C₂₀ hydroxyl groups were found to be silylated with difficulty. When MSTFA/2% TMSI was used, the keto-TMS derivatives were produced. As there is a lack of information of ecdysone in mammals, it is assumed that the metabolism maybe similar to arthropods. Studies done on larvae (Figure 16) indicated that

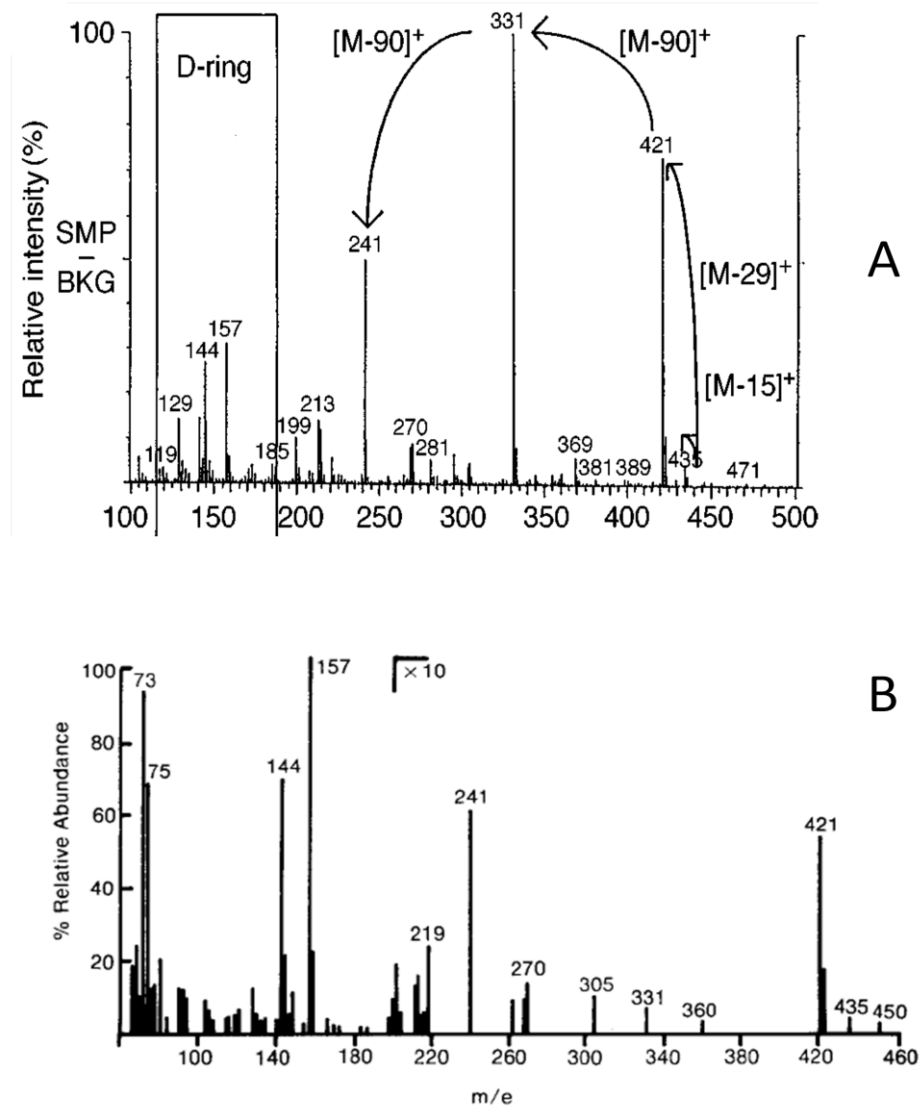


Figure 35: Mass spectra of ethylestrenol metabolite in (A) cattle and (B) rat [27, 28].

20-hydroxy ecdysone is the major metabolite of ecdysone. This metabolite was not observed in the current experiment due to the lack of Phase I metabolism. This was also evident from the lack of change in the peak intensity of ecdysone over the 60 min incubation period (Figure 17C-D).

20-hydroxy ecdysone has been reported to be further metabolized differently in different species [71]. In humans, 20-hydroxy ecdysone metabolizes into deoxygenated metabolites (Figure 19) and does not yield 20,26-dihydroxylated product as indicated in Figure 16 [24]. The 20,26-dihydroxylated product has only been reported in decapods crustaceans [72]. Therefore 20,26-dihydroxy ecdysone was not expected in this experiment.

The trend observed in the Phase I metabolism of 20-hydroxy ecdysone in our study was inconsistent with met ID study. In the met ID study of 20-hydroxy ecdysone, no metabolites were observed. The lack of Phase I metabolism of 20-hydroxy ecdysone was supported in a recently published literature [59]. In this paper, Phase I experiments of 20-hydroxy ecdysone was conducted in equine liver microsomes and S9 fraction. None of the 20-hydroxy ecdysone metabolites were detected in LC- or GC-MS. Although the study was done in triplicate, the trend observed was consistent. Therefore the observed trend could not be explained.

The lack of Phase I metabolism of ecdysone and 20-hydroxy ecdysone indicated that HrLM did not hydroxylate neither ecdysone nor 20-hydroxy ecdysone. One possible explanation for the lack of Phase I metabolism could be that ecdysone and 20-hydroxy ecdysone undergo Phase II metabolism that was not tested in the current HrLM assay. However, due to the hydrophilic nature of ecdysone and 20-hydroxy ecdysone, it is also reasonable to assume that a large amount of each parent drug would be excreted unchanged in urine

via the kidney. In addition, in an earlier study performed in calves [73], 20-hydroxy ecdysone was also measured in its native form for the monitoring of its fraudulent doping in the animals. Together with our findings, we confirmed that it would be more relevant to monitor the parent drug of ecdysone and 20-hydroxy ecdysone in horse racing rather than their metabolites.

4.1.3.1.3 Metribolone

With metribolone indicating Phase I metabolism, possible metabolites were predicted based on similar 4,9,11-triene AAS and THG structures (Figure 36) [67, 68]. To identify the possible metabolites, further structural elucidations of the metabolite were performed using the Orbitrap mass analyzer.

The ion at m/z 301.2 was the parent ion while the product ion at m/z 265.2 was derived from the loss of two water molecules from the parent ion (Figure 25). Since the 4,9,11-triene structure was found to be intact without any modifications, it was postulated that the loss of water would probably be due to the loss of hydroxyl group at positions C₁₆ and C₁₇. This suggested that the possible metabolite in the microsome assay could be metabolite B (Figure 36). The comparison of the experimental masses with the calculated values did not deviate significantly (< 2 ppm), confirming the identity of metabolite B to be 16-hydroxy metribolone (Table 1).

testosterone formation using human hepatocytes and liver microsomes. These experiments were the study of 6 β -hydroxy testosterone formation whereas this study was on the decay of testosterone. Moreover, the parameters indicated in the literature were K_m and V_{max} . These parameters were not comparable to the half-life calculation used in this study. Therefore we were unable to extrapolate this data to the current study.

The increasing trend observed in Figure 28 for ecdysone was consistently observed in three independent assays and was unexpected. Nevertheless, it was obvious that Phase I metabolism had not taken place. This result was consistent with the respective metabolic identification results where metabolite of ecdysone was absent.

Similar results were observed for 20-hydroxy ecdysone. The diverging trends (Figure 30) observed in the metabolic stability study of 20-hydroxy ecdysone were unexpected. These trends were initially postulated to be attributed to the instability of the parent substrate in the autosampler. In the initial experiment, the 60 min assay samples were injected first to prevent carry-over followed by samples of other time-points. It was speculated that the analytes belonging to the later injections could have degraded while stored in the autosampler leading to the observed trend. This was further investigated with a reverse-order analysis but the outcome remained unchanged. In our study, testosterone was used as positive control and subjected to the same HrLM study. The result of the experiment on testosterone showed first order metabolic degradation

profile (Figure 26). Therefore, the non-degrading Phase I trends observed for ecdysone and 20-hydroxy ecdysone could be unique for these compounds in HrLM. Further experiments including UGT cofactors were performed to investigate if ecdysone is susceptible to Phase II metabolism.

The trends observed in both the control and HrLM assay, indicated the lack of Phase II metabolism of ecdysone (Figure 29). Three independent sets of assays were analyzed and similar trends were observed. The Phase II metabolic stability profile of 20-hydroxy ecdysone showed diverging trend (Figure 31). The experiment was repeated but the same trend was observed. As positive controls demonstrated that the HrLM was metabolically active (Figure 27), these trends observed could be unique to this family of steroids. One possible reason for the lack of Phase II activities in ecdysteroids could be due to the innate nature of HrLM. Ecdysteroids studies in insects have been reported to have phosphate esters as the major metabolite in Phase II metabolic reactions [76]. Such phosphorylation conjugation reaction of 20-hydroxy ecdysone should be tested in future study.

With first-order degradation profile (Figure 32), metribolone demonstrated Phase I metabolism. The half-life of metribolone was slower compared to testosterone in HrLM under similar conditions ($K = 1.60 \text{ min}^{-1}$ and half-life = 0.43 min). This indicated that metribolone took a longer time to decrease by half its original value. The elimination rate constant also suggested that metribolone was metabolized by Phase I metabolism in the equine system at a

slower rate. In order to understand the implication of the metabolism of metribolone in the detection of horse doping, further *in-vitro* to *in-vivo* scaling or *in-vivo* pharmacokinetics studies in horses need to be performed. In the near future, the monitoring of both metribolone and its metabolite may be essential to detect its doping in horse racing.

4.1.3.3 Summary

The summary of the targeted approach results is as follows:

	Ethylestrenol	Ecdysone	20-hydroxy ecdysone	Metribolone
Met ID	Metabolites norethandrolone and 19-norpregnane-3,17-diol detected	No metabolism was observed		6-hydroxy metribolone identified as possible major metabolite
Metabolic stability	Not applicable	Phase I and Phase II metabolism absent	Phase I metabolism trend could not be explained and Phase II metabolism was not observed.	Phase I metabolism was observed with half-life = 0.43 min and $K = 1.60 \text{ min}^{-1}$

Table 3: Summary of the met ID and metabolic stability studies.

4.2 Non-targeted approach

4.2.1 Method validation

4.2.1.1 Results of intra-day and inter-day precision

Seven injections were done on the same day for intra-day precision. Inter-day precision was determined by analyzing injections (seven each day) carried out over three consecutive days. The different values of the internal standard and six selected endogenous metabolites in the TMS derivatized plasma samples are shown in Figure 37 and 38.

The RSDs for the intra-day precision were below 20% (Figure 37). The RSDs for caffeine (ISTD), L-valine, L-isoleucine, proline, L-serine, threonine and ribose were 4.9, 8.1, 12.2, 13.0, 6.5, 6.0 and 14.2%, respectively.

The inter-day precision for the selected metabolites and ISTD were also below 20% (Figure 38). The RSDs for caffeine (ISTD), L-valine, L-isoleucine, proline, L-serine, threonine and ribose were 8.3, 12.7, 9.3, 7.2, 5.3, 11.2 and 18.0%, respectively.

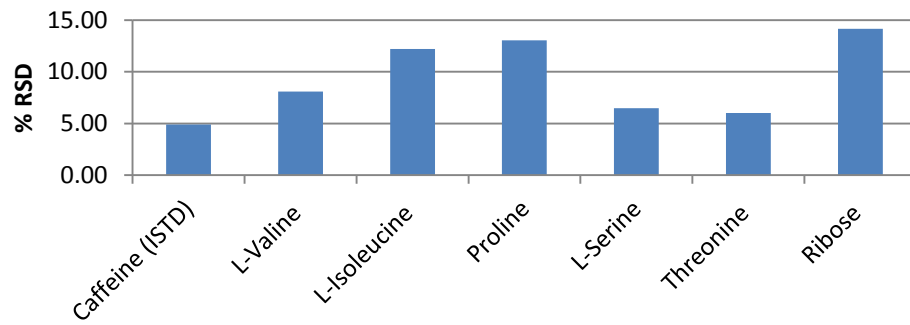


Figure 37: Relative standard deviation of intra-day precision of ISTD and six endogenous metabolites in equine plasma.

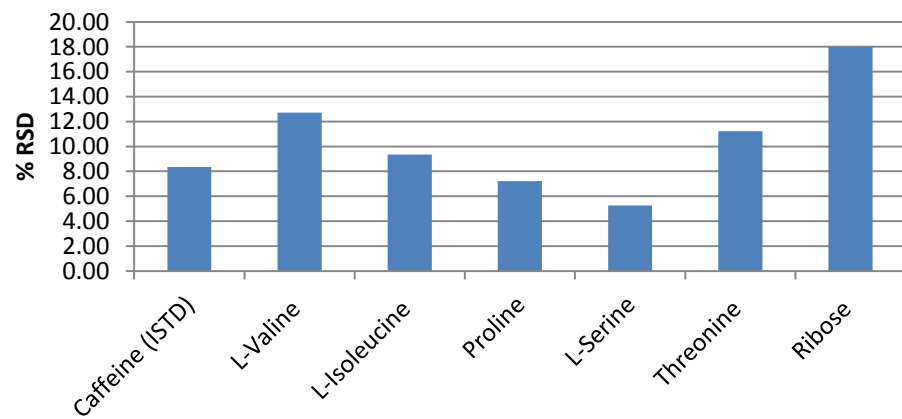


Figure 38: Relative standard deviation of inter-day precision of ISTD and six endogenous metabolites in equine plasma.

4.2.1.2 Results of autosampler stability

Autosampler stability of the derivatized plasma samples was evaluated for 24 h. RSDs of ribose and L-serine were slightly higher than 20% at 24.6 and 22.3%, respectively (Figure 39).

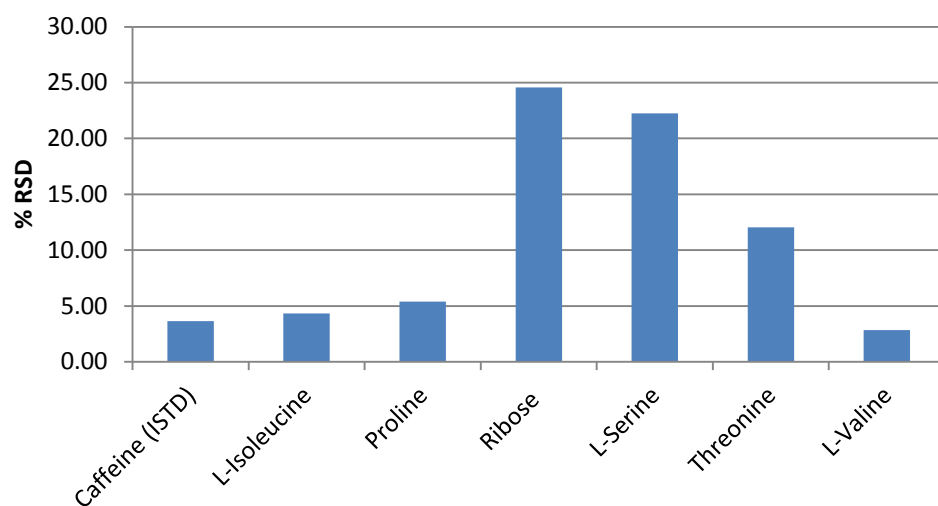


Figure 39: Relative standard deviation of autosampler stability of ISTD and six endogenous metabolites in equine plasma.

4.2.1.3 Results of freezer stability

The metabolites were relatively stable over the two weeks except for L-isoleucine, ribose and L-serine when plasma samples were stored at 4°C (Figure 40).

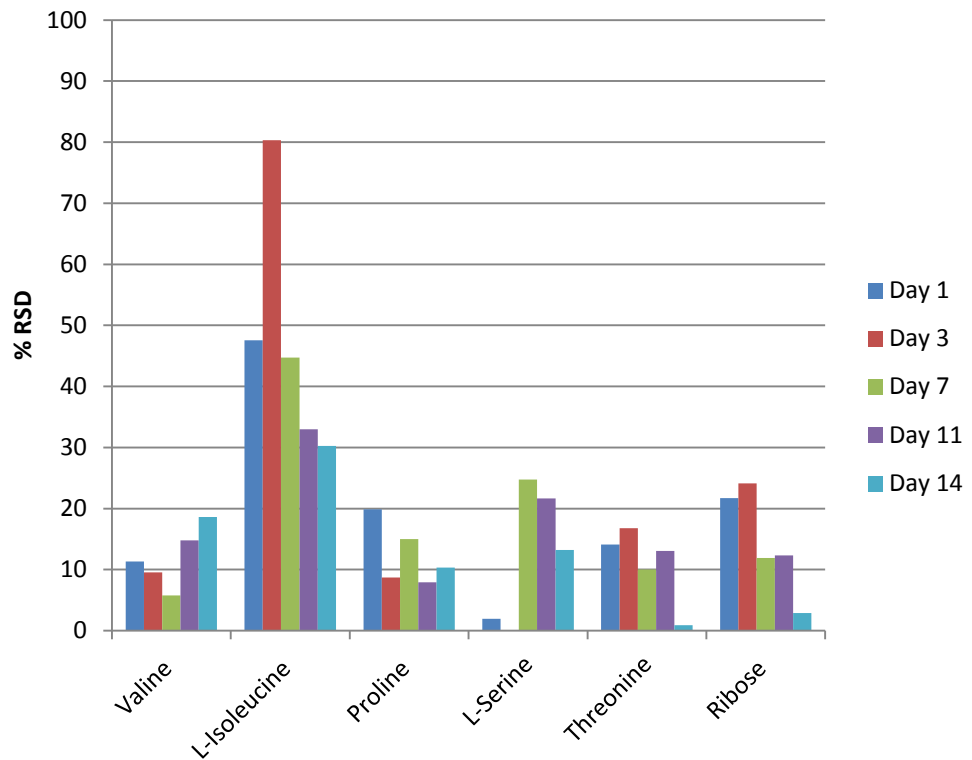


Figure 40: Stability of ISTD and six endogenous metabolites over two weeks stored at 4°C with respect to day 0.

Plasma samples stored at -80°C were analyzed over a six month period. L-isoleucine and ribose RSDs varied between week 1 and week 24 indicating their instability, similar to storage at 4°C (Figure 41). Valine metabolite appeared to be unstable after week 12 at -80°C.

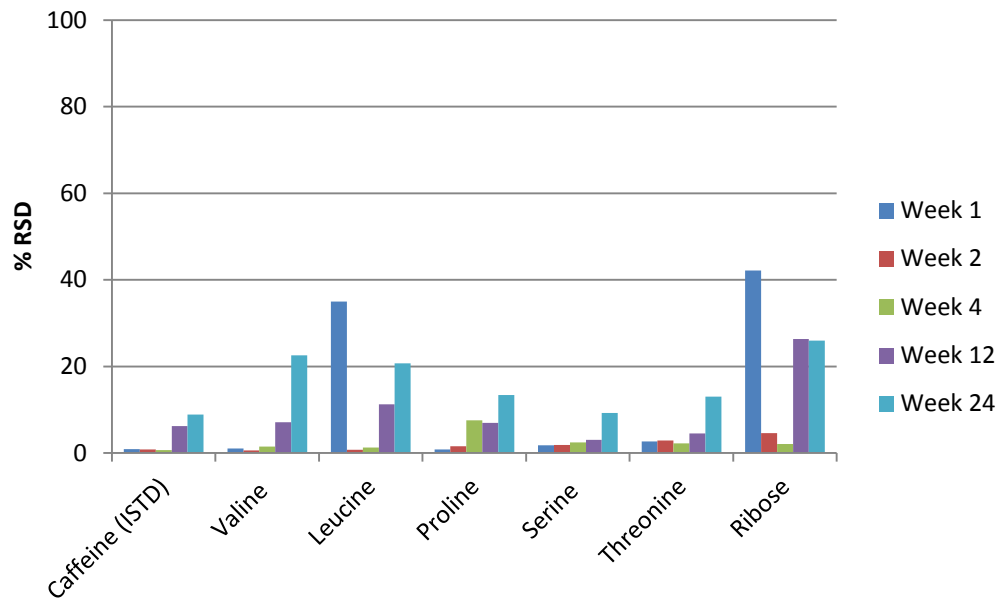


Figure 41: Stability of ISTD and six endogenous metabolites over six months stored at -80°C with respect to week 0.

4.2.2 Chemometrics

The randomized equine plasma samples were analyzed using the SIMCA-P software. The PCA was plotted with the different genders of horses and six QCs (Figure 42). One of the colt plasma samples was a severe outlier. The six QC samples were clustered loosely around the centre of the eclipse. The Q^2 value for this plot was 0.115 and the R^2X value was 0.461.

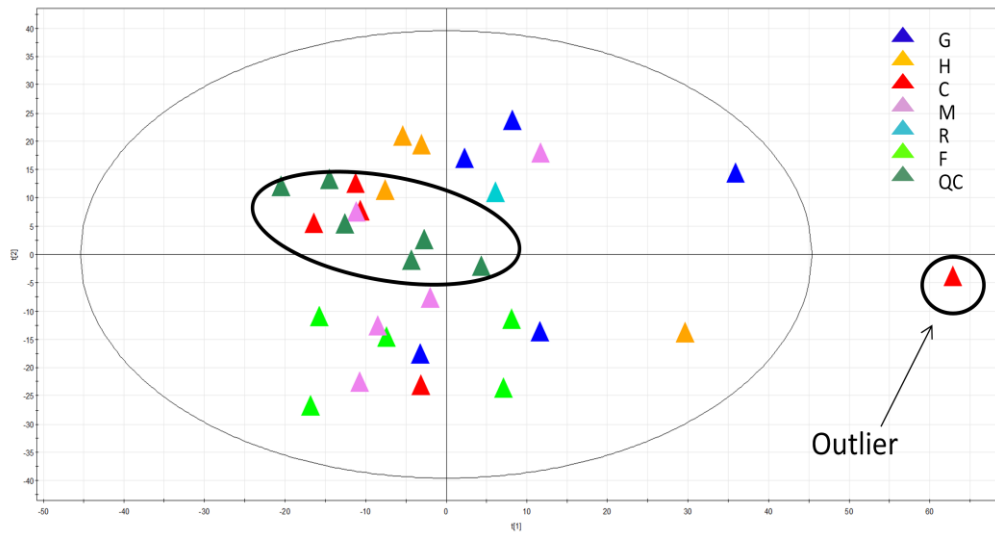


Figure 42: PCA plot obtained from equine plasma samples of different genders of horses with QC samples. H = horse, G = gelding, M = mare, R = rig, F = filly, C = colt and QC = quality control samples.

For a better comparison of the clustering, the QC samples and outlier were removed from the plot (Figure 43). There was obvious clustering between the males (H and C) and the females (F and M). The Q^2 value was 0.0919 and the R^2X value was 0.376.

The OPLS-DA plot obtained from the male horse (horse, colt and rig) and female horses (mare and filly) indicated that each gender was indeed clustered (Figure 44). The Q^2 value was 0.368, R^2X value was 0.347 and R^2Y was 0.98.

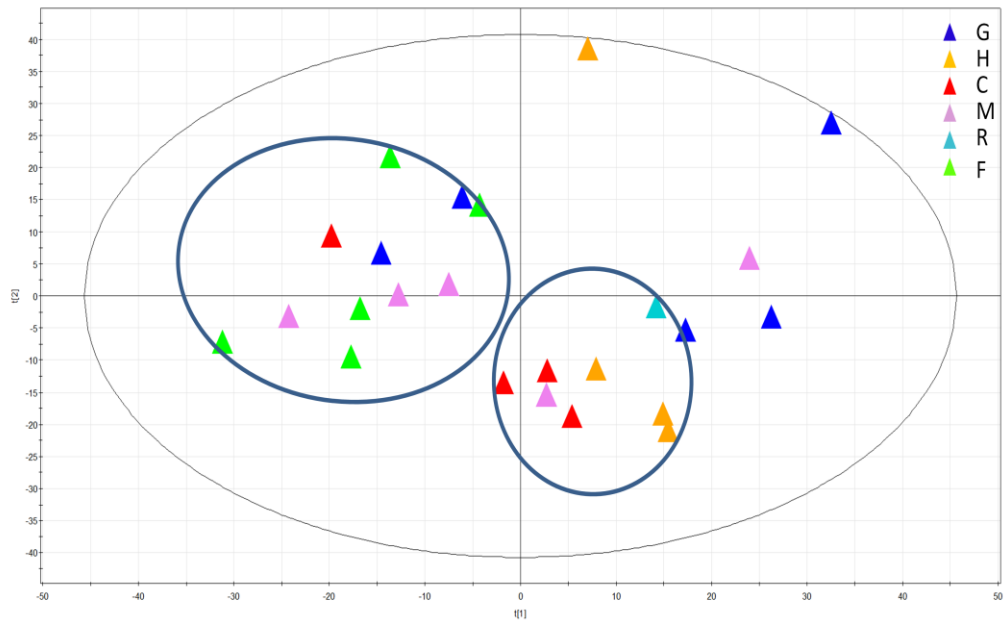


Figure 43: PCA plot obtained from all equine plasma samples, without QC samples and outlier. H = horse, G = gelding, M = mare, R = rig, F = filly and C = colt.

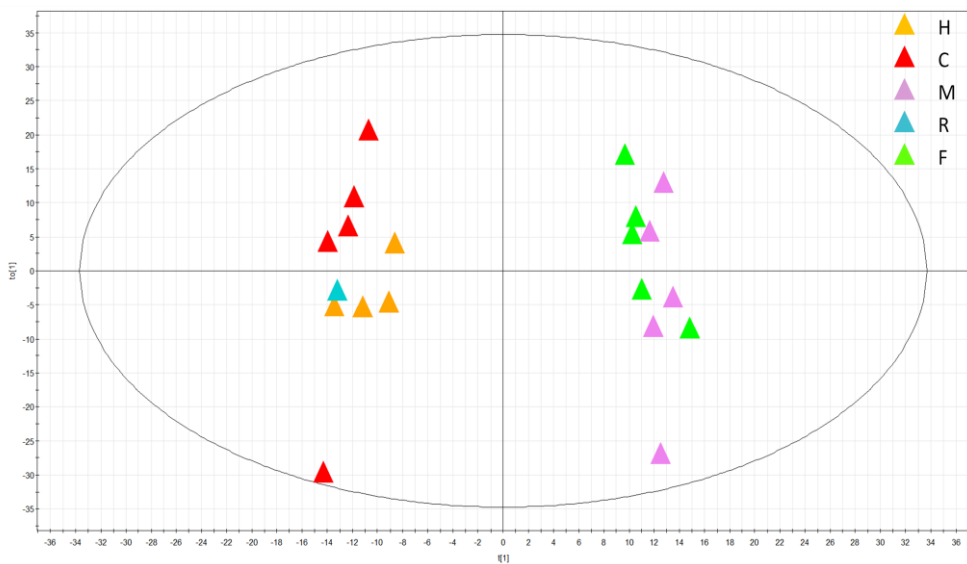


Figure 44: OPLS-DA plot obtained from male horses and female horses. H = horse, M = mare, R = rig, F = filly and C = colt.

Male horses (horse, colt and rig) were compared with gelding horses in the OPLS-DA plot (Figure 45). The male horses were clearly discriminated from the gelding horses. It was obvious that the male horses had some similar characteristics within the group as they clustered together regardless of their age and different development stages. The Q^2 value was 0.0696, R^2X value was 0.293 and R^2Y was 0.906.

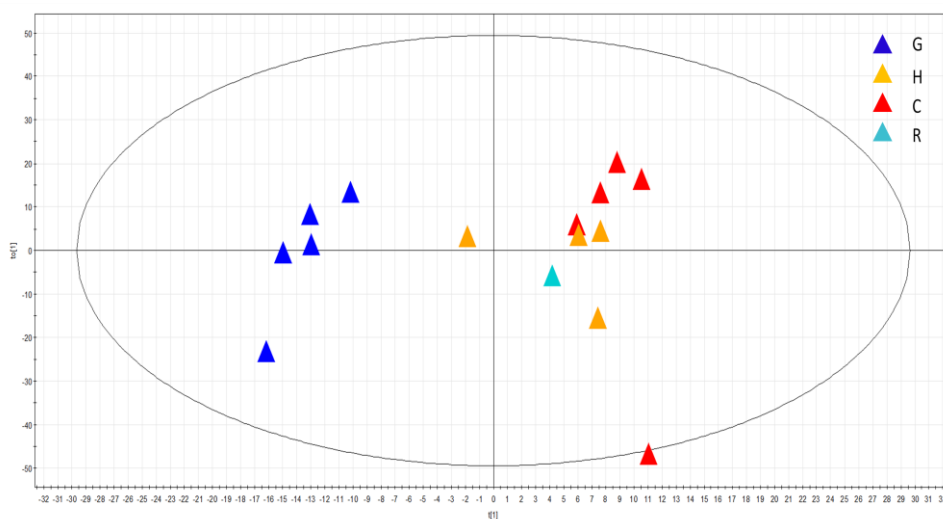


Figure 45: OPLS-DA plot obtained from male horses and gelding horses. H = horse, G = gelding, R = rig and C = colt.

Female horses (mare and filly) were compared with gelding horses in the OPLS-DA plot (Figure 46). The female horses were well discriminated from the gelding horses. The Q^2 value was 0.175, R^2X value was 0.378 and R^2Y was 0.996.

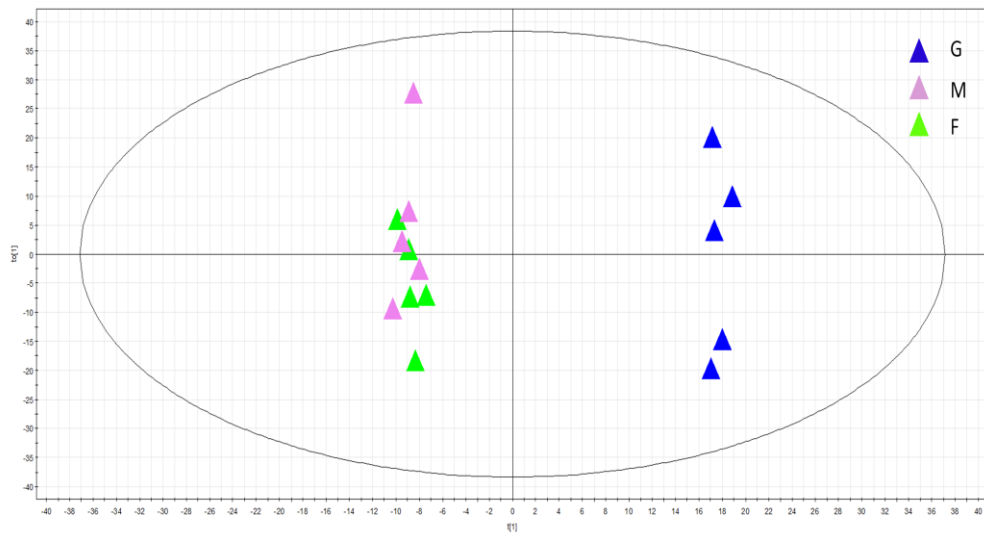


Figure 46: OPLS-DA plot obtained from female horses and gelding horses. G = gelding, M = mare and F = filly.

Permutation test is the comparison of the goodness of fit (R^2 and Q^2) between the original data and the permuted data. The OPLS-DA models were validated (Figure 47). The R^2 and Q^2 values of the validated OPLS-DA model for the male and female horses were 0.931 and 0.191, respectively (Figure 47A). The validated OPLS-DA model for the male and gelding horses had R^2 and Q^2 values of 0.944 and 0.200, respectively (Figure 47B). The validation of the female and gelding horses had R^2 and Q^2 values of 0.948 and 0.311, respectively (Figure 47C). For the three validation plots (Figure 47A-C), the lines joining the original and permuted Q^2 values cut the y-axis within the positive regions. In addition, some permuted Q^2 values were clearly greater than the original Q^2 values (far right) of the three plots.

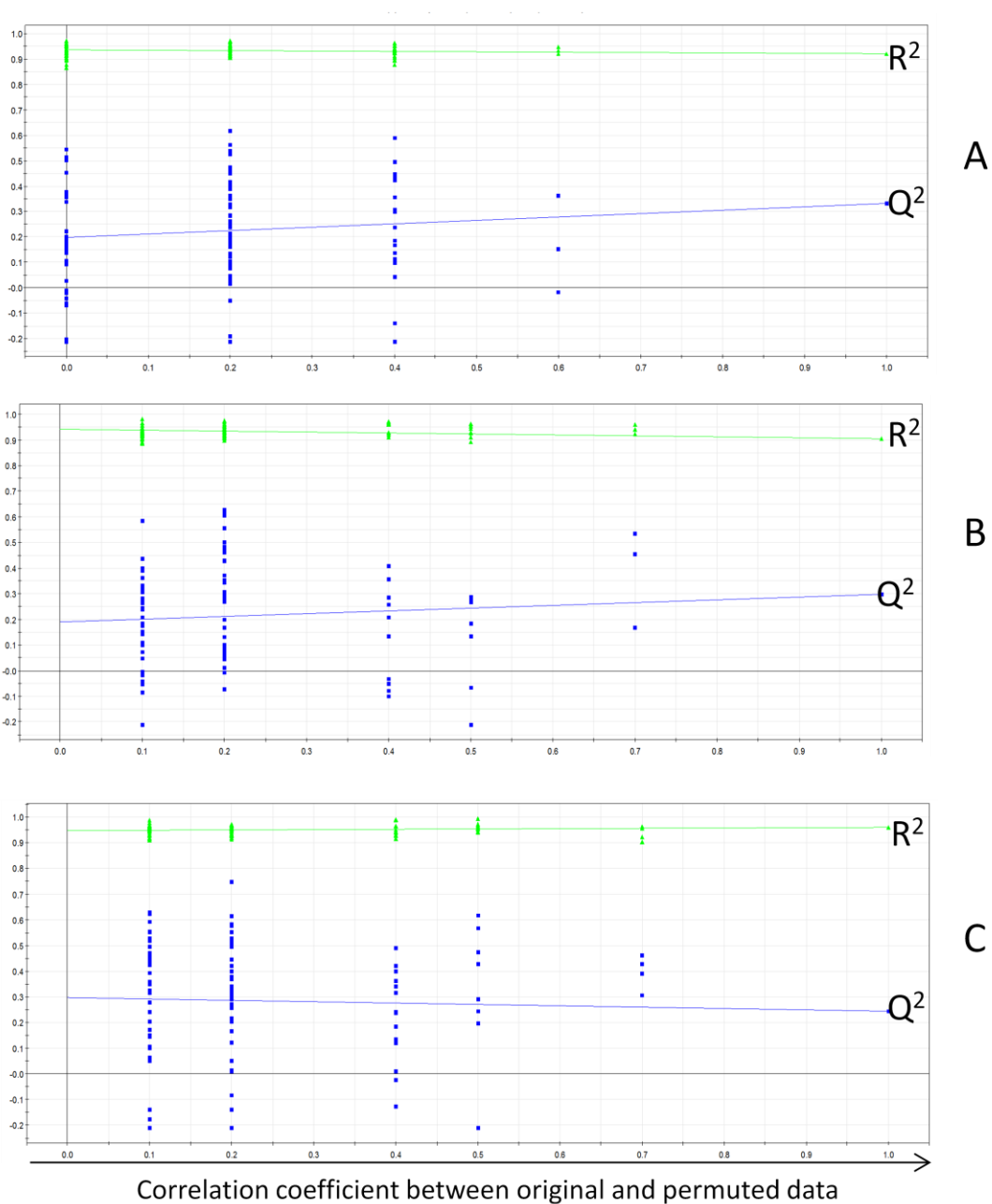


Figure 47: Validation plot of OPLS plots. A = OPLS for male horses and female horses, B = OPLS for male horses and gelding horses and C = OPLS for female horses and gelding horses.

4.2.3 Discussion

The storage of the plasma samples in the Singapore Turf Club is regulated by the release of the final analytical report to the stipendiary stewards. Samples are usually stored at 4⁰C for two weeks while the analysis is in-progress. After two weeks, the final analytical results are released and negative samples are discarded. Longer term storage is done at -80⁰C.

The six endogenous metabolites were chosen based on the availability of their standards and the spread of their retention times over the entire analytical runtime. These endogenous metabolites were chosen for the purpose of validating the analytical method and may not be used as biomarkers in actual samples.

The precision data for the intra-day and inter-day pooled plasma samples demonstrated RSD within 20% and were found to be satisfactory. Ribose and L-serine were suspected to be unstable as their RSDs were slightly higher than 20% (Figure 37 and 38). Therefore the plasma samples were analyzed within 24 h of derivatisation.

Ribose, L-isoleucine and L-serine were suspected to be unstable at 4⁰C as their RSDs were higher than 20% (Figure 40). The variations of ribose seemed to stabilize after three days, the possible reason could be that some of the

multiple peaks of ribose have degraded. RSD of L-isoleucine remained above 20% throughout the 14-day period. L-serine RSD varied on the seventh and eleventh day indicating its instability. Therefore the metabolites found to be unstable when stored at 4°C for 14-day period (ribose, L-isoleucine and L-serine) should be interpreted prudently in the subsequent metabonomics study.

Plasma samples stored at -80°C showed variations in some of the endogenous metabolites (Figure 41). L-isoleucine had a high variation (RSD = 34.99%) in the first week but it decreased significantly in the second week to less than 1%. However, it gradually increased over the next twenty weeks. Similarly, ribose had the same trend. This indicated the instability of L-isoleucine and ribose over 24 weeks. Valine degraded after 12 weeks. L-serine metabolite was more stable when the plasma samples were stored at -80°C (Figure 41) with their RSD was below 20%. The plasma samples were more stable when stored at -80°C than at 4°C. Therefore plasma samples should preferably be stored at -80°C for metabonomics studies. Ribose and L-isoleucine should be interpreted prudently in the subsequent metabonomics study due to their instability. The samples should be processed and analyzed within 12 weeks of storage.

PCA is an unsupervised mathematical procedure that uses an orthogonal transformation to convert a set of observations of possibly correlated variables into a set of values of uncorrelated variables called principal components.

Partial least-squares (PLS) method is used when a qualitative relationship between two data tables X and Y is desired. X mainly consists of spectral or chromatographic data and Y contains quantitative values like concentration of endogenous metabolites. When PLS is used for discriminant analysis, it is known as PLS-DA, where the Y matrix contains qualitative values like gender. OPLS is a modification of supervised PLS analysis. In OPLS, the systematic variations of X are separated into two parts. The two parts consist of one part linearly related to Y and the other orthogonally related to Y [77, 78]. These different chemometric analyses are necessary to generate interpretable models for the collected data.

This analysis had 31 observations and 2214 variables. PCA plots are used to observe the trends and outliers in the variables being analyzed. PCA is a form of unsupervised technique that was used to check the validity of the data in metabonomics analysis. Figure 42 showed the QC samples were loosely clustered indicating probable inconsistency in the preparation of the samples and the analytical method. The PCA indicated some clustering between the genders, hence the QCs were removed to investigate if it was true (Figure 43). The female horses (mare and filly) were clustered away from the male horses (horse, colt and rig). There seem to be separated by the second component ($t[2]$). Unsupervised PCA was followed by a supervised technique, OPLS-DA.

Figure 44 shows the discrimination between the male and the female horses. The groups were clustered and discriminated by the first latent variable, $t[1]$.

The separation within the cluster indicates within-class variation. To demonstrate the differences between the male horses and the gelding horses, the samples were subjected to OPLS-DA analysis (Figure 45). The male and the gelding horses were differentiated by the first latent variable, $t[1]$. Similarly, the female horses were differentiated from the gelding horses by the first latent variable (Figure 46).

Although, the PCA plot indicated clustering of the different genders, the Q^2 values were less than 0.5. The validation plots (Figure 47) indicated the failure of the model as the Q^2 regression line did not have a negative intercept and all the permuted Q^2 values on the left were of the same level as the original point to the right. Therefore OPLS-DA models (Figure 44 - 46) were not robust and validated.

The overlays of the QC samples and their ISTD indicated the consistency of the analytical method (Figure 48 and 49). Hence, the low Q^2 values and poor robustness of the OPLS-DA models could be attributed to the complexity of

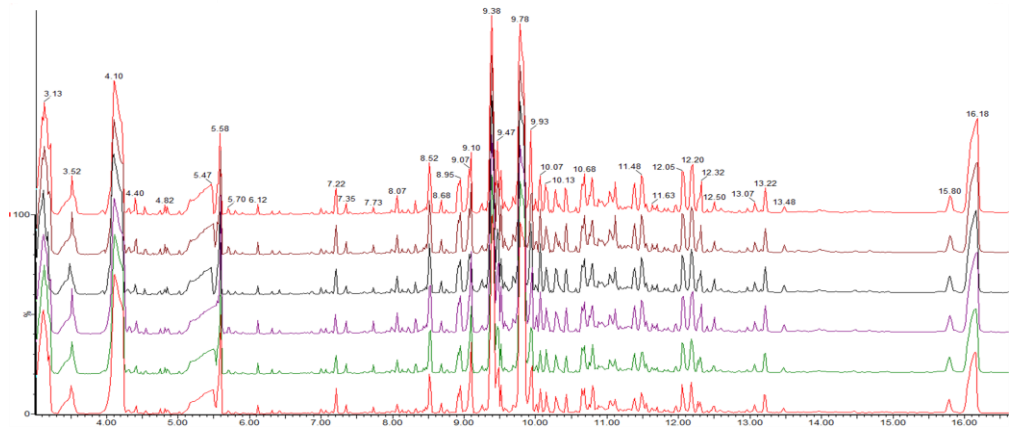


Figure 48: An overlay of GC/MS chromatograms of the six QC samples.

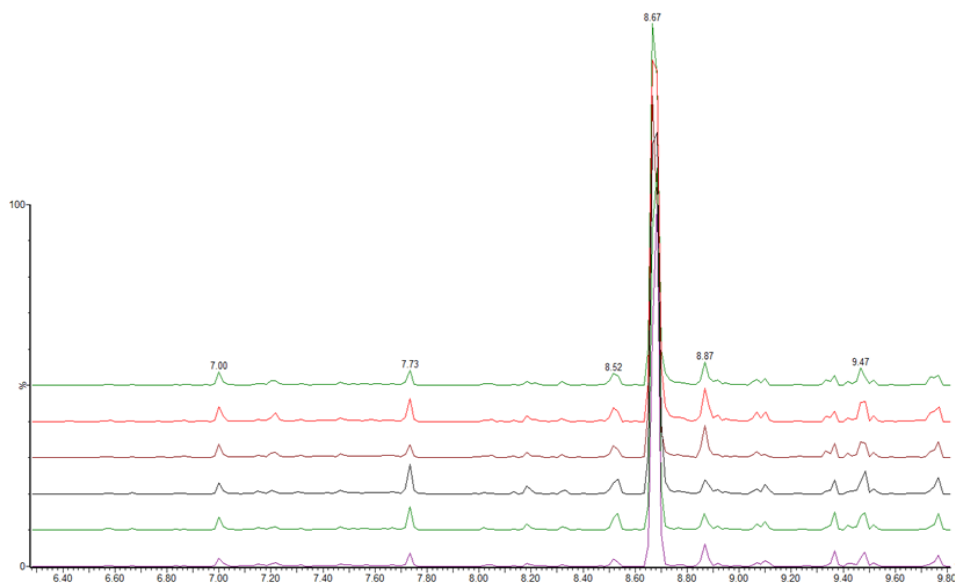


Figure 49: An overlay of GC/MS extracted chromatograms of caffeine (ISTD at RT = 8.67 min) in the six QC samples.

the raw data since re-processing of the data and chemometrics analysis did not yield any improvement. Therefore the current analytical method may not be robust to differentiate the different genders.

CHAPTER 5

CONCLUSION AND FUTURE WORK

5.1 Conclusion

5.1.1 Targeted approach

Ethylestrenol metabolite identification experiment confirmed that local horses in Singapore metabolize ethylestrenol in a similar way to other race horses, cattles and rats [25, 27, 28]. From the small-scale synthesis experiment, it is also clearer that the unknown metabolite could possibly be associated with 17α -ethyl- 5α -estrane- $3\beta,17\beta$ diol. The met ID experiment could be extended longer than 60 min to observe more metabolites.

Liver microsomes was found to be a suitable enzymatic system to study Phase I and II metabolism of ecdysone and 20-hydroxyecdysone in horses due to the stability of the enzymes and availability of horse livers. The use of different cofactors also facilitated our investigation of the Phase I and II metabolism of the substrate. Our study confirmed that it would be more appropriate to monitor the parent drug of ecdysone and 20-hydroxy ecdysone in dope testing, due to the hydrophilic nature of ecdysteroids.

In-vitro metabolism study on metribolone in our study yielded novel results. Metribolone showed Phase I metabolism and first order metabolic degradation profile. Further experiments suggested that 16-hydroxy metribolone could be the major metabolite of metribolone. Further *in-vitro* and *in-vivo* pharmacokinetics studies need to be performed to determine whether it is more accurate to screen for doped metribolone or its metabolite in horse racing.

In conclusion, our study demonstrated that metabolic stability studies and met ID studies provide valuable information in the fight against doping through elucidating the biotransformation of the doped drugs to their metabolites from a kinetic perspective. While it is not a common practice to perform *in-vitro* metabolism studies in horse racing laboratory currently such studies should be incorporated as a core research and development effort in the future to determine the optimal analyte (parent drug or metabolite) for routine screening.

5.1.2 Non-targeted approach

To our best knowledge, there had been no reports on non-targeted profiling of equine plasma. However metabolic profiling of human biological fluids showed no indication of instability for these metabolites [79]. Therefore further work needs to be done to understand metabonomics of horses.

The global plasma profiling of equine plasma was unsuccessful as the developed prediction models are not robust and validated. However the broad observed trends indicate the potential of the chemometric models in differentiating the different genders of horses. Therefore with better analytical methods and larger sample size, this model could still be used to identify unique plasma biomarkers of the horse genders. Identifying the unique baseline metabotype of each gender is an important preliminary step before metabonomic can be further explored to detect perturbations of the metabotype related to doping.

5.2 Future work

5.2.1 Targeted approach

The predicted metabolite 17α -ethyl- 5α -estrane- $3\beta,17\beta$ diol could be synthesised in a larger scale. The unknown metabolites could be synthesized in larger quantities, purified and crystallized. Elemental analysis could be performed to confirm the elemental composition. NMR could also be used to elucidate the structure of the metabolites. The product could also be further structurally characterized and analyzed with *in-vivo* samples derived from ethylestrenol administration. The identity of the putative metabolite could give the analytical chemist more analytes to monitor during the screening of equine

samples. As such, this could aid the chemist to deduce confidently ethylestrenol abuse.

The metabolic stability assay of testosterone could be studied using human and mouse liver microsomes in order to better understand the metabolic capacity of HrLM.

Ecdysone and 20-hydroxy ecdysone could be studied in horse hepatocytes to have a better understanding of their Phase II activities. This could be used to investigate the possibility of phosphorylation of ecdysone and 20-hydroxy ecdysone in equine as reported in insects. These Phase II activities could be further verified with *in-vivo* studies.

With the calculated half-life of metribolone, the clearance could be further studied *in-vivo* where its biological half-life can be investigated. The identity of the postulated metabolite, 16-hydroxy metribolone, could be further elucidated using commercially available standards.

5.2.2 Non-targeted approach

The limitations of the current global equine plasma profiling model might be potentially overcome by increasing the sample size and exploring other analytical methods such as comprehensive two-dimensional GC (GC x GC)

coupled to TOFMS, LC/MS, CE/MS or NMR. The samples could be analyzed using instruments like GC x GC/TOFMS to provide a higher metabolic space coverage with enhanced detection limit. This analytical method could increase the number of detectable peaks with high spectral purity.

REFERENCES

1. Pittinger, J.L.F.a.B., *Pharmacology, doping and sports*, ed. J.L. Fourcroy. 2009: Routledge. 1-9.
2. Tobin, T., *Drugs and the performance horse*. 1981: Charles C Thomas.
3. *British Horseracing Authority: The 1st place for British Horseracing (Internet)* 2004; Available from: www.britishhorseracing.com/resources/equine-science-and-welfare/dope-testing.
4. Sparkman, J.T.W.a.O.D., *Introduction to mass spectrometry: instrumentation, application and strategies fro data interpretation*. Fourth edition ed. 2008: John Wiley & Sons, Ltd.
5. Fang, M., *Mass spectrometry for microbial proteomics*, ed. S.a.S.E.G. Haroun N. 2010: WILEY.
6. Sussman, K.G.K.a.M.R., *Protein quantitation using isotope-assisited mass spectrometry*. Annual Reviews of Biophysics, 2010. **39**: p. 291-308.
7. F. Guan, C.U., L. Soma, A. Hess and Y. Luo. *Screening and confirmation of select anabolic steroids in equine plasma by LC/TSQ-MS/MS*. in *15th International Conference of Racing Analysts and Veterinarians*. 2004. Dubai, United Arab Emirates.
8. C.E. Uboh, M.C.K., L.R. Soma, Y. Luo, F. Guan, J.A. Rudy, E. Birks, D. Teleis and D. Tsang. *Separation and indentification of beta-andrenoceptor agents in equine samples by CE/MS/MS*. in *15th International Conference of Racing Analysts and Veterinarians*. 2004. Dubai, United Arab Emirates.
9. M. Yamada, S.A., T. Hosoe, M. Kurosawa, I. Kijima-Suda, K. Saito and H. Nakazawa, *Characterization and quantitation of fluoxymesterone metabolite in horse urine by gas chromatography/mass sepectrometry*. Analytical Sciences, 2008. **24**: p. 911-914.
10. N. H. Yu, E.N.M.H., T. S. M. Wan and A. S. Y. Wong, *Doping control analysis of recombinant human erythropoietin, darbepotin alfa and methoxy polyethylene glycol-epoetin beta in equine plasma by nano-liquid chromatography-tandem mass spectrometry*. Analytical and Bioanalytical Chemistry, 2010. **396**: p. 2513-2521.
11. Clark, R.V., *Pharmacology, doping and sports*, ed. J.L. Fourcroy. 2009: Routledge. 23-37.
12. Murlin, C.D.K.a.J.R., *The effect of male hormone on the protein and energy metabolism of castrate dogs*. Journal of Nutrition, 1935. **10**(4): p. 437-459.
13. Fieser, L.F.F.a.M., *Steroids*. 1959: Reinhold Publishing Corporation.
14. K. F. Austen, S.J.B., F. S. Rosen and T. B. Strom, *Therapeutic Immunology*. Second Edition ed. 2001: Blackwell Science Inc.
15. Kuipers, H. *Anabolic steroids and sport performance*. in *10th International Conference of Racing Analysts and Veterinarians* 1994. Stockholm, Sweden.
16. Taylor, W.N., *Anabolic Steroids and The Athletes*. 2nd Edition ed. 2001: MacFarland & Company, Inc.

17. Anthony W. Norman, M.T.M.D.P.G.N., *Steroid-homone rapid actions, membrane receptors and a conformational ensemble model*. Nature Reviews Drug Discovery, 2004. **3**(1): p. 27-41.
18. Yue Chen, J.D.Z.a.H.E.M., *Androgen regulation of satellite cell function*. Journal of Endocrinology, 2005. **186**: p. 21-31.
19. NT, S., *A review of the chemistry, biological action and clinical applications of anabolic-androgenic steroids*. Clinical Therapeutics, 2001. **23**(9): p. 1355-1390.
20. Finley, B., *Horse racing officials move toward steroid ban*, in *The New York Times*. 2007.
21. Bowers, L.D., *Pharmacology, doping and sports*, ed. J.L. Fourcroy. 2009: Routledge. 55-60.
22. Catlin DH, A.B., Kucherova Y, *Detection of norbolethone, an anabolic steroid never marketed, in athletes' urine*. Rapid Communications in Mass Spectrometry, 2002. **16**: p. 1273-1275.
23. Tuttle, D., *User's guide to sports nutrients*, ed. J. Challem. 2002: Basic Health Publications Inc.
24. Christina Tsitsimpikou, G.D.T., Panayotis A. Siskos, Maria-Helen E. Spyridaki and Costas G. Georgakopoulos, *Study of excretion of ecdysterone in human urine*. Rapid Communications in Mass Spectrometry, 2001. **15**: p. 1796-1801.
25. Beresford, T.A.G.a.G.D. *The detection of ethylestrenol and its metabolites in the horse*. in *Proceedings of the 10th International Conference of Racing Analysts and Veterinarians*. 1994. Stockholm, Sweden.
26. C S Kim, T.W.a.G.D.B. *Detection of ethylestrenol in equine urine and plasma*. in *Proceedings of the 11th International Conference of Racing Analysts and Veterinarians*. 1996. Queensland, Australia.
27. J. W. Steele, L.J.B.a.R.C.S.A., *Anabolic steroids. Part 3: metabolism of ethylestrenol in rat liver preparations in vitro*. Xenobiotica, 1981. **11**(2): p. 117-121.
28. M. Van Puymbroeck, M.E.M.K., R. F. M. Maas, R. F. Witkamp, L. Leysens, D. Vanderzande, J. Gelan and J. Raus, *In vitro liver models are important tools to monitor the abuse of anabolic steroids in cattle*. The Analyst, 1998. **123**: p. 2453-2456.
29. JP, B.C.a.R., *Methyltrienolone, a specific ligand for cellular androgen receptors*. Steroids, 1975. **26**: p. 227-232.
30. JP, B.C.a.R., *Assay of androgen binding sites by exchange with methyltrienolone (R1881)*. Steroids, 1976. **27**: p. 497-507.
31. G, K.H.a.N., *Liver toxicity of a new anabolic agent methyltrienolone (17-alpha-methyl-4,9,11-estratriene-17-beta-ol-3-one)*. Steroids, 1966. **8**: p. 13-24.
32. Emmie N.M. Ho, D.K.K.L., Gary N.W. Leung, Terence S.M. Wan, Henry N.C. Wong, Xiaohua Xu, John H.K. Yeung, *Metabolic studies of mesterolone in horses*. Analytica Chimica Acta, 2007. **569**(1): p. 149-155.
33. E.N.M. Ho, W.H.K., D.K.K. Leung, T.S.M. Wan, A.S.Y. Wong, *Metabolic studies of turinabol in horses*. Analytica Chimica Acta, 2007. **586**(1-2): p. 208-216.

34. W H Kwok, D.K.K.L., G N W Leung, T S M Wan, C H F Wong and J K Y Wong. *Detection of some designer steroids in horse urine.* in *Proceedings of the 16th International Conference of Racing Analysts and Veterinarians.* 2006. Tokyo, Japan.
35. John C. Lindon, J.K.N.a.E.H., ed. *The handbook of metabonomics and metabolomics.* 2007, Elsevier.
36. J. C. Lindon, H.C.K., T. MD. Ebbels, J. MT. Pearce, E. Holmes and J. K. Nicholson, *The Consortium for Metabonomic Toxicology (COMET): aims, activities and achievements.* *Pharmacogenomics*, 2005. **6**(7): p. 691-699.
37. J. F. Xia, Q.L.L., P. Hu, Y. M. Wang, G. A. Luo, *Recent trends in strategies and methodologies for metabonomics.* *Chinese Journal of Analytical Chemistry*, 2009. **37**(1): p. 136-143.
38. Rochfort, S., *Metabolomics reviewed: A new "Omics" platform technology for systems biology and implications for natural products research.* *Journal of Natural Products*, 2005. **68**(12): p. 1813-1820.
39. M. Chen, L.Z.a.W.J., *Metabonomic study on the biochemical profiles of a hydrocortisone-induced animal model.* *Journal of Proteome Research*, 2005. **4**(6): p. 2391-2396.
40. Wang, R.E.G.a.T.J., *The search for new cardiovascular biomarkers.* *Nature*, 2008. **451**: p. 949-952.
41. M. Chen, M.S., L. Zhao, J. Jiang, P.Liu, J. Cheng, Y. Lai, Y. Liu and W. Jia, *Metabonomics study of aristolochic acid-induced nephrotoxicity in rats.* *Journal of Proteome Research*, 2006. **5**(4): p. 995-1002.
42. H. Idborg, P.E.a.S.P.J., *Multivariate approaches for efficient detection of potential metabolites from liquid chromatography/ mass spectrometry data.* *Rapid Communications in Mass Spectrometry*, 2004. **18**(9): p. 944-954.
43. Z. Lei, D.V.H.a.L.W.S., *Mass spectrometry strategies in metabolomics.* *Journal of Biological Chemistry*, 2011. **286**(29): p. 25435-42.
44. D. R. Robertson, M.D.R.a.J.D.B., *Metabonomics in pharmaceutical discovery and development.* *Journal of Proteome Research*, 2007. **6**: p. 526-539.
45. Reichel, C., *OMICs-strategies and methods in the fight against doping.* *Forensic Science International*, 2011. **213**: p. 20-34.
46. D. I. Ellis, W.B.D., J. L. Griffin, J. W. Allwood and R. Goodacre, *Metabolic fingerprinting as a diagnostic tool.* *Pharmacogenomics*, 2007. **8**(9): p. 1243-1266.
47. X. Wang, T.Z., Y. Qiu, M. Su, T. Jiang, M. Zhou, A. Zhao and W. Jia, *Metabonomics approach to understanding acute and chronic stress in rat models.* *Journal of Proteome Research*, 2009. **8**: p. 2511-2518.
48. I. K. S. Yap, M.A., K. A. Veselkov, E. Holmes, J. C. Lindon and J. K. Nicholson, *Urinary metabolic phenotyping differentiates children with autism from their unaffected sibilings and age-matched controls.* *Journal of Proteome Research*, 2010. **9**: p. 2996-3004.
49. Lucroy, M.D., *Clinical Biochemistry of Domestic Animals.* 6th Edition ed. 2008: Academic Press.
50. Elaine R. Garvican, A.V.-T., Peter D. Clegg, John F. Innes, *Biomarkers of cartilage turnover. Part 2: Non-collagenous markers* *The Veterinary Journals*, 2010. **185**(1): p. 43-49.

51. J. Yang, X.Z., X. Liu, C. Wang, P. Gao, J. Wang, L. Li, J. Gu, S. Yang and G. Xu, *High performance liquid chromatography-mass spectrometry for metabonomics: Potential biomarkers for acute deterioration of liver function in chronic hepatitis B*. Journal of Proteome Research, 2006. **5**: p. 554-561.
52. K. K. Pasikanti, K.E., P. C. Ho, R. Mahendran, R. Kamaraj, Q. H. Wu, E. Chiong and E. C. Y. Chan, *Noninvasive urinary metabonomics diagnosis of human bladder cancer*. Journal of Proteome Research, 2010. **9**: p. 2988-2995.
53. Y. Qiu, G.C., M. Su, T. Chen, Y. Liu, Y. Xu, Y. Ni, A. Zhao, S. Cai, L. X. Xu and W. Jia, *Urinary metabonomics study on colorectal cancer*. Journal of Proteome Research, 2010. **9**: p. 1627-1634.
54. J. Carrola, C.M.R., A. S. Barros, A. M. Gil, B. J. Goodfellow, I. M. Carreira, J. Bernardo, A. Gomes, V. Sousa, L. Carvalho and I. F. Duarte, *Metabolic signatures of lung cancer in biofluids: NMR-based metabonomics of urine*. Journal of Proteome Research, 2011. **10**: p. 221-230.
55. S. O. Diaz, J.P., G. Graca, I. F. Duarte, A. S. Barros, E. Galhano, C. Pita, Maria do Ceu Almeida, B. J. Goodfellow, I. M. Carreira and A. M. Gil, *Metabolic biomarkers of prenatal disorders: An exploratory NMR metabonomics study of second trimester maternal urine and blood plasma*. Journal of Proteome Research, 2011. **10**(8): p. 3732-3742.
56. K. Mittelstrass, J.S.R., Z. Yu, J. Krumsiek, C. Gieger, C. Prehn, W. Roemisch-Margi, A. Polonikov, A. Peters, F.J. Theis, T. Meitinger, F. Kronenberg, S. Weidinger, H.E. Wichmann, K. Suhre, R. Wang-Sattler, J. Adamski and T. Illig, *Discovery of sexual dimorphisms in metabolic and genetic biomarkers*. PLoS Genetics, 2011. **7**(8): p. 1-12.
57. Marc-Emmanuel Dumas, L.D., Loic Beyet, Denis Lesage, Francois Andre, Alain Paris and Jean-Claude Tabet, *Analyzing the physiological signature of anabolic steroids in cattle urine using pyrolysis/metastable atom bombardment mass spectrometry and pattern recognition*. Analytical Chemistry, 2002. **74**(20): p. 5393-5404.
58. Fanny Kieken, G.P., Jean-Phillippe Antignac, Fabrice Monteau, Anne Christelle Paris, Marie-Agnes Popot, Yves Bonnaire and Bruno Le Bizec, *Development of a metabonomic approach based on LC-ESI-HRMS measurements for profiling of metabolic changes induced by recombinant equine growth hormone in horse urine*. Analytical and Bioanalytical Chemistry, 2009. **394**: p. 2119-2128.
59. Adam Clarke, J.S., Phil Teale, Clive Pearce and Lynn Hillyer, *The use of in vitro technologies and high-resolution/accurate-mass LC-MS to screen for metabolites of 'designer' steroids in the equine*. Drug testing and analysis, 2011. **3**: p. 74-87.
60. Hill, J.R., *In vitro drug metabolism using liver microsomes*. Current protocols in pharmacology, 2003: p. 7.8.1 - 7.8.11.
61. Rodgers, S.M.R.S.a.J.P. *Use of immunoaffinity chromatography with HPLC-particle beam/MS and GC/MS for the confirmatory analysis of corticosteroids in equine urine*. in *Proceeding of the 10th International Conference of Racing Analysts and Veterinarians*. 1994. Stockholm, Sweden.
62. P. Smid, H.K.A.C.C., H. G. Keizer, R. van Hes, J. P. de Moes, A. P. den Hartog, B. Stork, R. H. Plekkenpol, L. C. Niemann, C. N. J. Stroomer, M. Th.

- M. Tulp, H. H. van Stuivenberg, A. C. McCreary, M. B. Hesselink, A. H. J. Herremans and C. G. Kruse, *Synthesis, structure-activity relationships, and biological properties of 1-heteroaryl-4-[(1H-indol-3-yl)alkyl]piperazines, novel potential antipsychotics combining potent dopamine D₂ receptor antagonism with potent serotonin reuptake inhibition*. Journal of medicinal chemistry, 2005. **48**: p. 6855-6869.
63. Marlice Aparecida Sipoli Marques, H.M.G.P., Monica Costa Padilha, Francisco Radler de Aquino Neto, *Analysis of synthetic 19-norsteroids trenbolone, tetrahydrogestrinone and gestrinone by gas chromatography-mass spectrometry* Journal of Chromatography A, 2007. **1150**: p. 215-225.
64. M. B. Fisher, K.C., B. L. Ackermann, M. Vandenbranden and S. A. Wrighton, *In vitro glucuronidation using human liver microsomes and the pore-forming peptide alamethicin*. Drug metabolism and disposition, 2000. **28**(5): p. 560-566.
65. Rene Lafont, P.B., Ghislaine Somme-Martin and Catherine Blais, *High-performance liquid chromatography of ecdysone metabolites applied to the cabbage butterfly, Pieris Brassicae L*. Steroids, 1980. **36**(2): p. 185-207.
66. R. P. Evershed, J.G.M.a.H.H.R., *Capillary gas chromatography-mass spectrometry of ecdysteroids*. Journal of Chromatography, 1987. **390**: p. 357-369.
67. A.G. Fragkaki, Y.S.A., A. Tsantili-Kakolidou, M. Koupparis and C. Georgakopoulos, *Schemes of metabolic patterns of anabolic androgenic steroids for the estimation of metabolites of designer steroids in human urine*. Journal of Steroid Biochemistry and Molecular Biology, 2009. **115**: p. 44-61.
68. E. M. Brun, R.P.a.A.M., *Analytical methods for anti-doping control in sport: anabolic steroids with 4,9,11-triene structure in urine*. Trends in analytical chemistry, 2011. **30**(5): p. 771-783.
69. RS, O., *Prediction of human clearance of twenty-nine drugs from hepatic microsomal intrinsic clearance data: an examination of in vitro half-life approach and nonspecific binding to microsomes* Drug metabolism and disposition, 1999. **27**: p. 1350-1359.
70. R. J. Ward, A.M.L.a.C.H.L.S., *Metabolism of anabolic steroid drugs in man and the marmoset monkey (callithrix jacchus)- I. Nilevar and obabolin*. Journal of steroid Biochemistry, 1977. **8**: p. 1057-1063.
71. R. Lafont, P.B., C. Blais, M. Garcia, F. Lachaise, F. Riera, G. Somme and J. P. Girault, *Ecdysteroid metabolism*. Insect biochemistry, 1986. **16**(1): p. 11-16.
72. Mykles, D.L., *Ecdysteroid metabolism in crustaceans*. Journal of Steroid Biochemistry and Molecular Biology, 2010. **In Press, Corrected proof**.
73. B. Destrez, G.P., F. Monteau, R. Lafont, B. Le Bizec, *Detection and identification of 20-hydroxy ecdysone metabolites in calf urine by liquid chromatography-high resolution or tandem mass spectrometry measurements and establishment of their kinetics of elimination after 20-hydroxy ecdysone administration*. Analytica Chimica Acta, 2009. **637**: p. 178-184.
74. J. L. Fayer, D.M.P., B. J. Ring, S. A. Wrighton and K. J. Ruterbories, *A novel testosterone 6-beta hydroxylase activity assay for the study of CYP3A-mediated metabolism, inhibition, and induction in vitro*. Journal of Pharmaceutical and Toxicological Methods, 2002. **46**: p. 117-123.

75. J. Maenpaa, O.P., T. Cresteil and A. Rane, *The role of cytochrome P450 3A (CYP3A) isoforms in oxidation metabolism of testosterone and benzphetamine in human adult and fetal liver* The Journal of Steroid Biochemistry and Molecular Biology, 1993. **44**(1): p. 61-67.
76. H. Sonobe, T.O., K. Ieki, S. Maeda, Y. Ito, M. Ajimura, K. Mita, H. Matsumoto and M. N. Wilder, *Purification, kinetic characterization and molecular cloning of a novel enzyme, ecdysteroid 22-kinase*. The journal of biological chemistry, 2006. **281**(40): p. 29513-29524.
77. J. Trygg, E.H.a.T.L., *Chemometrics in metabonomics*. Journal of Proteome Research, 2007. **6**: p. 469-479.
78. E. C. Y. Chan, K.K.P.a.J.K.N., *Global urinary metabolic profiling procedures using gas chromatography-mass spectrometry*. Nature Protocol, 2011. **6**(10): p. 1483-1499.
79. K. K. Pasikanti, P.C.H.a.E.C.Y.C., *Development and validation of a gas chromatography/ mass spectrometry metabonomic platform for the global profiling of urinary metabolites*. Rapid Communications in Mass Spectrometry, 2008. **22**: p. 2984-2992.